

# Tumor necrosis factor stimulates fibroblast growth factor 23 levels in chronic kidney disease and non-renal inflammation

**Citation for published version (APA):**

Egli-Spichtig, D., Imenez Silva, P. H., Glaudemans, B., Gehring, N., Bettoni, C., Zhang, M. Y. H., Pastor-Arroyo, E. M., Schönenberger, D., Rajski, M., Hoogewijs, D., Knauf, F., Misselwitz, B., Frey-Wagner, I., Rogler, G., Ackermann, D., Ponte, B., Pruijm, M., Leichtle, A., Fiedler, G-M., ... Wagner, C. A. (2019). Tumor necrosis factor stimulates fibroblast growth factor 23 levels in chronic kidney disease and non-renal inflammation. *Kidney International*, 96(4), 890-905. Advance online publication. <https://doi.org/10.1016/j.kint.2019.04.009>

**DOI:**

[10.1016/j.kint.2019.04.009](https://doi.org/10.1016/j.kint.2019.04.009)

**Document status and date:**

Published: 01/10/2019

**Document Version:**

Accepted manuscript including changes made at the peer-review stage

**Please check the document version of this publication:**

- A submitted manuscript is the version of the article upon submission and before peer-review. There can be important differences between the submitted version and the official published version of record. People interested in the research are advised to contact the author for the final version of the publication, or visit the DOI to the publisher's website.
- The final author version and the galley proof are versions of the publication after peer review.
- The final published version features the final layout of the paper including the volume, issue and page numbers.

[Link to publication](#)

**General rights**

Copyright and moral rights for the publications made accessible in the public portal are retained by the authors and/or other copyright owners and it is a condition of accessing publications that users recognise and abide by the legal requirements associated with these rights.

- Users may download and print one copy of any publication from the public portal for the purpose of private study or research.
- You may not further distribute the material or use it for any profit-making activity or commercial gain
- You may freely distribute the URL identifying the publication in the public portal.

If the publication is distributed under the terms of Article 25fa of the Dutch Copyright Act, indicated by the "Taverne" license above, please follow below link for the End User Agreement:

[www.tue.nl/taverne](http://www.tue.nl/taverne)

**Take down policy**

If you believe that this document breaches copyright please contact us at:

[openaccess@tue.nl](mailto:openaccess@tue.nl)

providing details and we will investigate your claim.



## TNF stimulates FGF23 levels in chronic kidney disease and non-renal inflammation

Journal:	<i>Kidney International</i>
Manuscript ID	KI-07-18-1031.R1
Article Type:	Basic Research
Date Submitted by the Author:	n/a
Complete List of Authors:	<p>Egli-Spichtig, Daniela; University of Zurich, Physiology  Imenez Silva, Pedro; University of Zurich, Physiology  Glaudemans, Bob; University of Zurich, Institute of Physiology  Gehring, Nicole; University of Zurich, Physiology  Bettoni, Carla; University of Zurich, Physiology  Zhang, Martin; University of California at San Francisco, Department of Pediatrics, Division of Nephrology  Pastor-Arroyo, Eva-Maria; University of Zurich, Physiology  Schönenberger, Desiree; University of Zurich, Physiology  Rajski, Michal; University of Zurich, Institute of Physiology  Hoogewijs, David; University of Fribourg, Physiology  Knauf, Felix; Charite Universitaetsmedizin Berlin, Department of Nephrology and Medical Intensive Care  Misselwitz, Benjamin; University Hospital Zurich, Department of Gastroenterology  Frey-Wagner, Isabelle; University Hospital Zurich, Department of Gastroenterology  Rogler, Gerhard; University Hospital Zurich, Department of Gastroenterology  Ackermann, Daniel; University Clinic for Nephrology and Hypertension, Ponte, Bélen; University Hospital of Geneva (HUG), Nephrology  Pruijm, Menno; University Hospital of Lausanne (CHUV), Service of Nephrology and Hypertension  Leichtle, Alexander; Inselspital, University Hospital Bern, Laboratory Medicine  Fiedler, Georg; Inselspital, University of Bern, Laboratory Medicine  Bochud, Murielle; University Institute for Social and Preventive Medicine, Community Prevention Unit  Ballotta, Virginia; Eindhoven University of Technology Faculty of Biomedical Engineering  Hofmann Boss, Sandra; Eindhoven University of Technology Faculty of Biomedical Engineering  Perward, Farzana; University of California at San Francisco, Department of Pediatrics, Division of Nephrology  Föllner, Michael; University of Hohenheim, Physiology  Lang, Florian; Eberhard-Karls-Universität of Tuebingen, Department of Physiology  Wenger, Roland; University of Zürich, Institute of Physiology  Frew, Ian; University of Zurich, Physiology; University of Freiburg,</p>

1  
2  
3  
4  
5  
6  
7  
8  
9  
10  
11  
12  
13  
14  
15  
16  
17  
18  
19  
20  
21  
22  
23  
24  
25  
26  
27  
28  
29  
30  
31  
32  
33  
34  
35  
36  
37  
38  
39  
40  
41  
42  
43  
44  
45  
46  
47  
48  
49  
50  
51  
52  
53  
54  
55  
56  
57  
58  
59  
60

	Internal Medicine Wagner, Carsten; University of Zurich, Physiology
Subject Area:	Mineral and Bone Disorders
Keywords:	bone, cell signaling, chronic kidney disease, FGF23, cytokines

SCHOLARONE™  
Manuscripts

1  
2  
3  
4  
5 **1 Antibody mediated TNF neutralization decreases FGF23 levels**  
6  
7 **2 in animal models of chronic kidney disease and non-renal**  
8  
9 **3 inflammation**

4 Daniela Egli-Spichtig<sup>1,2#</sup>, Pedro Henrique Imenez Silva<sup>1#</sup>, Bob Glaudemans<sup>1</sup>, Nicole  
5 Gehring<sup>1</sup>, Carla Bettoni<sup>1</sup>, Martin Zhang<sup>2</sup>, Eva Pastor Arroyo<sup>1</sup>, Désirée Schönenberger<sup>1</sup>,  
6 Michal Rajski<sup>1</sup>, David Hoogewijis<sup>1</sup>, Felix Knauf<sup>3</sup>, Benjamin Misselwitz<sup>4</sup>, Isabelle Frey-  
7 Wagner<sup>4</sup>, Gerhard Rogler<sup>4</sup>, Daniel Ackermann<sup>5</sup>, Belen Ponte<sup>6</sup>, Menno Pruijm<sup>7</sup>, Alexander  
8 Leichtle<sup>8</sup>, Georg-Martin Fiedler<sup>8</sup>, Murielle Bochud<sup>9</sup>, Virginia Ballotta<sup>10</sup>, Sandra Hofmann<sup>10</sup>,  
9 Farzana Perwad<sup>2</sup>, Michael Föller<sup>10</sup>, Florian Lang<sup>11</sup>, Roland H. Wenger<sup>1</sup>, Ian Frew<sup>1</sup>,  
10 Carsten A. Wagner<sup>1\*</sup>

11  
12 # contributed equally to the manuscript

13  
14 <sup>1</sup>Institute of Physiology, University of Zurich, Zurich, Switzerland and National Center of  
15 Competence in Research NCCR Kidney.CH, Switzerland

16 <sup>2</sup>Department of Pediatrics, Division of Nephrology, University of California San Francisco,  
17 San Francisco, California, United States of America

18 <sup>3</sup>Division of Nephrology, Charité - Universitätsmedizin Berlin, Berlin, Germany

19 <sup>4</sup>University Hospital Zurich, Clinic for Gastroenterology and Hepatology, Zürich,  
20 Switzerland

21 <sup>5</sup>Department of Nephrology and Hypertension, Inselspital, Bern University Hospital and  
22 University of Bern, Switzerland

23 <sup>6</sup>Department of Nephrology, University Hospital of Geneva (HUG), Switzerland

24 <sup>7</sup>Department of Nephrology, Lausanne University Hospital (CHUV), Switzerland

25 <sup>8</sup>Institute of Clinical Chemistry, Inselspital, Bern University Hospital, University of Bern,  
26 Switzerland.

27 <sup>9</sup>Institute of Social and Preventive Medicine (IUMSP), Lausanne University Hospital  
28 (CHUV), Switzerland

29 <sup>10</sup>Department of Biomedical Engineering and Institute for Complex Molecular Systems,  
30 Eindhoven University of Technology, P.O. Box 513, 5600 MB Eindhoven, The  
31 Netherlands

32 <sup>11</sup>Institute of Physiology, University of Hohenheim, 70599 Stuttgart, Germany.

33  
34 <sup>12</sup>Institute of Physiology I, University of Tübingen, Germany

1  
2  
3  
4  
5  
6  
7  
8  
9  
10  
11  
12  
13  
14  
15  
16  
17  
18  
19  
20  
21  
22  
23  
24  
25  
26  
27  
28  
29  
30  
31  
32  
33  
34  
35  
36  
37  
38  
39  
40  
41  
42  
43  
44  
45  
46  
47  
48  
49  
50  
51  
52  
53  
54  
55  
56  
57  
58  
59  
60

36 \* **Corresponding author**  
37  
38 Carsten A. Wagner  
39 Institute of Physiology  
40 University of Zurich  
41 Winterthurerstrasse 190  
42 CH-8057 Zurich  
43 Switzerland  
44 Phone: +41-44-63 55023  
45 Fax: +41-44-63 56814  
46 Email: [Wagnerca@access.uzh.ch](mailto:Wagnerca@access.uzh.ch)  
47

For Peer Review Only

## 48 Abstract

49 Fibroblast growth factor 23 (FGF23) regulates phosphate homeostasis and its early rise  
50 in patients with chronic kidney disease (CKD) is independently associated with all-cause  
51 mortality. Since inflammation is characteristic for CKD and has been associated with  
52 plasma FGF23 we examined whether inflammation directly stimulates FGF23. In a  
53 population-based cohort, plasma tumor necrosis factor (TNF) was the only inflammatory  
54 cytokine that independently and positively correlated with plasma FGF23. Mouse models  
55 of CKD showed signs of renal inflammation, renal FGF23 expression and elevated  
56 systemic FGF23. Renal FGF23 expression coincided with expression of the orphan  
57 nuclear receptor Nurr1 regulating FGF23 in other organs. Antibody-mediated  
58 neutralization of TNF normalized plasma FGF23 and ectopic renal *Fgf23* expression.  
59 Conversely, TNF administration to control mice increased plasma FGF23 without altering  
60 plasma phosphate. Similarly, in *Il10* deficient mice with inflammatory bowel disease and  
61 normal kidney function, FGF23 was elevated and normalized upon TNF neutralization.  
62 In conclusion, the inflammatory cytokine TNF contributes to elevated systemic FGF23  
63 levels and triggers also ectopic renal *Fgf23* expression in CKD animal models.

## 64 Keywords

65 Fibroblast growth factor 23 (FGF23), tumor necrosis factor (TNF), chronic kidney disease  
66 (CKD), inflammation, cytokine, inflammatory bowel disease, bone.

67

## 68 INTRODUCTION

69 Chronic kidney disease (CKD) causes a severe disturbance of mineral metabolism, one  
70 of the leading factors for morbidity and mortality in patients with end stage renal disease  
71 (ESRD) <sup>1,2</sup>. Fibroblast growth factor 23 (FGF23) increases early during CKD progression  
72 and is required to maintain serum phosphate levels while kidney function declines . In  
73 CKD patients, high FGF23 levels are associated with an increased risk of mortality  
74 independent of plasma phosphate <sup>3</sup>. FGF23 promotes left ventricular hypertrophy in  
75 rodents <sup>4</sup> and elevated FGF23 is a risk factor in the general population for all-cause and  
76 cardiovascular mortality <sup>5</sup>.

77 FGF23 is critical for the regulation of phosphate homeostasis and vitamin D<sub>3</sub> metabolism  
78 . The main target organ of FGF23 is the kidney where FGF23 binds together with αKlotho  
79 to FGF receptors and inhibits phosphate reabsorption and decreases 1,25-(OH)<sub>2</sub> vitamin  
80 D<sub>3</sub> (1,25(OH)<sub>2</sub>D) <sup>6,7</sup>. FGF23 levels are regulated by a variety of stimuli including calcitriol,  
81 PTH, insulin, aldosterone, erythropoietin, and adipokinines <sup>6,8-11</sup>. Moreover, FGF23 may  
82 be linked to inflammation. In the *Chronic Renal Insufficiency Cohort* elevated FGF23 is  
83 independently associated with higher IL-6 and TNF and also in a smaller cohort with  
84 only 103 CKD patients, RANTES and IL-12 associated with higher FGF23 <sup>12</sup>. The  
85 association between FGF23 and inflammation markers is not limited to CKD. *The*  
86 *Reasons for Geographic and Racial Differences in Stroke* study found a positive  
87 correlation of FGF23 with IL-6 and IL-10 in a non-CKD population <sup>13</sup>. Children during an  
88 acute phase of inflammatory bowel disease (IBD) had elevated FGF23 that normalized  
89 in the remission phase <sup>14</sup>. Furthermore, chondrocytes from patients with osteoarthritis  
90 have elevated *Fgf23* gene expression <sup>15</sup>. Microarray data from mouse models with  
91 FGF23 excess (*Col4a3* KO, *Hyp*, and *Fgf23* transgenic mice) show an activation of genes  
92 important in the regulation of the inflammatory response such as transforming growth  
93 factor beta (TGFβ), tumor necrosis factor (TNF) and nuclear factor of kappa light  
94 polypeptide gene enhancer in B-cells (NFκB) <sup>16</sup>. Further, inflammatory stimuli and the  
95 hypoxia inducible transcription factor HIF-1 enhance FGF23 expression: TNF and TGFβ2

TNF stimulates FGF23

1  
2  
3  
4 96 increases FGF23 expression in bone cells *in vitro* and HIF-1, interleukin-1 beta (IL-1 $\beta$ ),  
5  
6 97 lipopolysaccharide (LPS) increase FGF23 expression *in vitro* and *in vivo* <sup>17-22</sup>. Also, in an  
7  
8 98 obesity induced model, TNF is necessary for the increase in FGF23 levels . Some  
9  
10 99 inflammatory stimuli, including TNF, may act on *Fgf23* transcription via a 16 kb enhancer  
11  
12 100 element . Moreover, in the folic-acid induced AKI model as well as in the adenine CKD  
13  
14 101 model, genetic ablation of Il-6 reduced the increase in FGF23 . Thus, inflammatory  
15  
16 102 cytokines may play an important role at least in the early phase of CKD to induce FGF23.  
17  
18 103 However, whether TNF is a critical player has not been demonstrated.  
19  
20 104 Here, we investigated the association between inflammatory cytokines with plasma  
21  
22 105 FGF23 in a population-based cohort and evaluated the effect of TNF on the regulation of  
23  
24 106 plasma FGF23 in CKD animal models and in a non-renal inflammation model.  
25  
26 107 Furthermore, we evaluated the role of hypoxia on *Fgf23* gene expression. Our results  
27  
28 108 demonstrate a critical role for TNF to stimulate FGF23 in models of renal and non-renal  
29  
30 109 inflammatory diseases.  
31  
32  
33  
34 110  
35  
36  
37  
38  
39  
40  
41  
42  
43  
44  
45  
46  
47  
48  
49  
50  
51  
52  
53  
54  
55  
56  
57  
58  
59  
60



## 111 Results

### 112 Plasma TNF positively correlated with intact FGF23 in the SKIPOGH 113 population based cohort

114 The *Swiss Kidney Project on Genes in Hypertension* (SKIPOGH) is a family and  
115 population-based, multicenter, cross-sectional study including 1131 subjects randomly  
116 selected<sup>23</sup>. We assessed the relationship between plasma intact FGF23 (iFGF23) and  
117 parameters of phosphate metabolism, inflammatory cytokines, and iron metabolism while  
118 considering familial correlation. Participants with drugs interacting with calcium,  
119 magnesium and phosphate metabolism, inflammation and iron metabolism or have  
120 diuretic action were excluded. Based on a linear mixed model with family as random  
121 effect, 1,25(OH)<sub>2</sub>D, 25-(OH) vitamin D<sub>3</sub> (25(OH)D), TNF and calcium showed the highest  
122 fixed effects and were considered significant predictors of plasma iFGF23 while holding  
123 all the other variables constant (Figure 1). The standard deviation of the random effect  
124 was low compared to the standard deviation of the residuals (0.26 vs 0.93), which means  
125 that most of the variation in iFGF23 levels was due to the fixed effects (i.e. hormones,  
126 cytokines, etc.). There was no correlation between plasma iFGF23 and plasma  
127 phosphate, PTH, or eGFR. Besides TNF, no other inflammatory cytokine such as  
128 interferon gamma (IFN $\gamma$ ), IL-1 $\beta$ , IL-6, or IL-10 correlated with plasma iFGF23.

129 We also analyzed the cohort without applying exclusion criteria based on drugs.  
130 1,25(OH)<sub>2</sub>D, 25(OH)D, and calcium remained as predictors of iFGF23 while phosphate,  
131 PTH and eGFR arose as additional predictors of iFGF23 (Figure S1). The TNF effect on  
132 iFGF23 is reduced in this population. . First quartile, median, mean and third quartile of  
133 continuous  
134 variables in the SKIPOGH population with and without drug intake criteria applied are  
135 listed in Tables S1 and S2.

### 136 **Inflammation in kidneys of *Pkd1* conditional KO mice**

137 TNF is increased in CKD patients, stimulates FGF23 expression in an osteocyte cell line,  
138 and was the only inflammatory cytokine associated with iFGF23 in the SKIPOGH cohort  
139 <sup>19, 24-26</sup>. Thus, we tested in two CKD mouse models whether TNF contributes to the rise  
140 of iFGF23 during the early phase of kidney disease. First, slowly progressing polycystic  
141 kidney disease (PKD) was induced in *Pkd1* conditional KO mice . Kidney function and  
142 two-kidney per body weight ratio were similar in 6 week old mice whereas kidney function  
143 was decreased and two-kidney per body weight ratio was increased in 12 week old *Pkd1*,  
144 *cre+* mice (Figure S2). At week 6, iFGF23, TmP/GFR as well as renal *Tnf* and *Tgfb* mRNA  
145 expression were similar in *Pkd1<sup>fl/fl</sup>*, *cre-* and *Pkd1<sup>fl/fl</sup>*, *cre+* mice (Figure 2 a - d).  
146 Progression of kidney disease was accompanied by increased plasma iFGF23,  
147 decreased TmP/GFR as well as increased *Tnf* and *Tgfb* mRNA expression in *Pkd1<sup>fl/fl</sup>*,  
148 *cre+* mice (Figure 2 a - d). TNF binding to TNF receptors activates the NFκB signaling  
149 pathway. The ratio of phospho-NFκB p65 to total NFκB p65 protein in the nuclear fraction  
150 of total kidney was significantly elevated in *Pkd1<sup>fl/fl</sup>*, *cre+* mice (Figure 2 e). Increased  
151 renal inflammatory cytokines in 12 week old *Pkd1<sup>fl/fl</sup>*, *cre+* mice were paralleled by the  
152 appearance of renal *Fgf23* expression and by the upregulation of the osteogenic marker  
153 gene *Runx2* in the kidney (Figure 2 f and S2 e). Bone *Fgf23* and *Runx2* mRNA  
154 expression were unchanged (Figure 2 g and S2 f).

### 155 **TNF blockade in *Pkd1* conditional KO mice suppressed FGF23**

156 The effect of acute TNF blockade on FGF23 expression in PKD kidneys and on plasma  
157 iFGF23 was investigated. We injected intraperitoneally (i.p.) a single dose of 0.5 mg anti-  
158 TNF antibody or isotypic IgG control into 12 week old *Pkd1<sup>fl/fl</sup>*, *cre+* and *Pkd1<sup>fl/fl</sup>*, *cre-* mice.  
159 After 24 hours, anti-TNF treated mice had a significant reduction of plasma TNF  
160 compared to the IgG control treated mice confirming the efficacy of the anti-TNF antibody  
161 (Figure 3 a). There was no difference in plasma TNF between IgG control treated *Pkd1<sup>fl/fl</sup>*,  
162 *cre+* and *Pkd1<sup>fl/fl</sup>*, *cre-* mice. Importantly, elevated plasma iFGF23 in *Pkd1<sup>fl/fl</sup>*, *cre+* mice

1  
2  
3  
4 163 was normalized by anti-TNF but not IgG control treatment (Figure 3 b). Plasma C-terminal  
5  
6 164 FGF23 (cFGF23) was increased in IgG control treated *Pkd1<sup>fl/fl</sup>, cre+* and anti-TNF treated  
7  
8 165 *Pkd1<sup>fl/fl</sup>, cre-* compared to IgG control treated *Pkd1<sup>fl/fl</sup>, cre-* mice consequently the  
9  
10 166 iFGF23/cFGF23 ratio was elevated in IgG control treated *Pkd1<sup>fl/fl</sup>, cre-* mice (Figure S4 a  
11  
12 167 – c). There was no change in plasma phosphate and urea.(Figure 3 c and d). The  
13  
14 168 abundance of the sodium dependent phosphate co-transporter NaPi-IIa in the brush  
15  
16 169 border membrane (BBM) showed a trend to increase in *Pkd1<sup>fl/fl</sup>, cre+* mice when treated  
17  
18 170 with anti-TNF antibodies (Figure 3 e). In *Pkd1<sup>fl/fl</sup>, cre+* mice, TNF neutralization decreased  
19  
20 171 ectopic renal *Fgf23* mRNA expression while *Fgf23* mRNA expression in bone (Figure 3 f  
21  
22 172 and g) and *Tnf*, and *Tgfb* mRNA expression in kidney (Figure 3 h and i) were unchanged.  
23  
24 173 The mRNA expression of the inflammatory cytokines *Il1b* and *Il6* was elevated in PKD  
25  
26 174 kidneys but did not change with anti-TNF treatment (Figure S3).

27  
28  
29 175 The orphan nuclear receptor Nurr1 is downstream of TNF signaling and activates *Fgf23*  
30  
31 176 mRNA expression in rat osteosarcoma cells upon PTH treatment<sup>27, 28</sup>. *Nurr1* mRNA was  
32  
33 177 detected in mouse kidney and bone (Figure S5). In the kidney of 12 week old *Pkd1<sup>fl/fl</sup>,*  
34  
35 178 *cre+* mice, *Nurr1* mRNA expression was upregulated and Nurr1 protein was  
36  
37 179 predominantly localized in the cell nucleus compared to *Pkd1<sup>fl/fl</sup>, cre-* mice where Nurr1  
38  
39 180 was mainly distributed in the cytoplasm (Figure S6). Further, nuclear Nurr1 staining in  
40  
41 181 *Pkd1<sup>fl/fl</sup>, cre+* mice was often co-localized with FGF23.

## 182 **TNF but not hypoxia increased FGF23 levels**

43  
44  
45  
46  
47  
48 183 We evaluated the effect of systemic TNF administration on plasma iFGF23. Therefore  
49  
50 184 we injected wild type mice for two consecutive days with 2 µg recombinant mouse TNF.  
51  
52 185 After 48-hours, plasma iFGF23 increased while cFGF23 and the iFGF23/cFGF23 ratio  
53  
54 186 were unchanged (Figure 4a and S4 d – f). Furthermore plasma TNF and fractional  
55  
56 187 excretion of phosphate increased, plasma urea decreased while plasma phosphate and  
57  
58 188 creatinine levels were unchanged (Figure 4 b - f). In bone and spleen *Fgf23* mRNA  
59  
60 189 expression decreased in TNF injected compared to vehicle injected mice whereas *Fgf23*

## TNF stimulates FGF23

1  
2  
3  
4 190 mRNA expression in thymus and bone marrow was unchanged (Figure 4 g -j). We  
5  
6 191 cultured primary osteocytes from tibias and femurs of mice <sup>29,30</sup> for 2 weeks before being  
7  
8 192 supplemented for 24 hours either with 10 ng/ml TNF or 10 nM 1,25(OH)<sub>2</sub>D. TNF as well  
9  
10 193 as 1,25(OH)<sub>2</sub>D increased *Fgf23* mRNA expression (Figure 4 k). TNF and 1,25(OH)<sub>2</sub>D  
11  
12 194 decreased the expression of *Dmp1* (Figure 4 l). *Dmp1* inhibits *Fgf23* gene expression  
13  
14 195 and loss of *DMP1* in patients causes hypophosphatemic rickets due to high FGF23 levels  
15  
16 196 . TNF but not 1,25(OH)<sub>2</sub>D increased the expression of *Galnt3* and *Nurr1* (Figure 4 m and  
17  
18 197 n). *Galnt3* mediates O-glycosylation of FGF23 preventing proteolytic cleavage of FGF23  
19  
20 198 **Error! Reference source not found.Error! Reference source not found..**

21  
22  
23 199 CKD kidneys are commonly affected by hypoxia <sup>31,32</sup> which was recently suggested to  
24  
25 200 stimulate FGF23 expression through the hypoxia inducible transcription factor HIF-1 <sup>17,</sup>  
26  
27 201 <sup>18,21</sup>. We studied in MC3T3-E1 mouse preosteoblasts the effect of hypoxia on *Fgf23* gene  
28  
29 202 expression. MC3T3-E1 did not display intrinsic *Fgf23* expression. Nevertheless, after 2  
30  
31 203 weeks osteogenic differentiation of MC3T3-E1, *Fgf23* mRNA expression was induced by  
32  
33 204 10 nM 1,25(OH)<sub>2</sub>D. 1,25(OH)<sub>2</sub>D-induced *Fgf23* mRNA expression was completely  
34  
35 205 repressed by hypoxic conditions (0.2% O<sub>2</sub>) for 24 or 48 hours and hypoxia alone failed  
36  
37 206 to trigger *Fgf23* expression (Figure S7 a). The upregulation of the HIF-1 target genes  
38  
39 207 carbonic anhydrase 9 (*Car9*) and prolyl hydroxylase domain containing protein 2 (*Phd2*)  
40  
41 208 confirmed the presence of hypoxia (Figure S7 b and c). Similarly, hypoxia had no effect  
42  
43 209 on *Fgf23* mRNA expression in U2OS rat osteosarcoma and primary osteoblast cells (data  
44  
45 210 not shown). We analyzed also kidneys of von Hippel-Lindau (*Vhl*) KO animals <sup>33</sup>. Lack of  
46  
47 211 VHL prevents HIF hydroxylation and degradation and activates hypoxia sensitive genes  
48  
49 212 <sup>34</sup>. Neither the kidneys of *Vhl* KO animals nor primary kidney cells lacking *Vhl* <sup>35</sup>  
50  
51 213 expressed any detectable *Fgf23* (data not shown).  
52  
53  
54  
55  
56  
57  
58  
59  
60

1  
2  
3  
4 214 **TNF blockade lowers FGF23 levels in mouse models of oxalate nephropathy**  
5  
6 215 **and colitis**  
7

8  
9 216 We expanded our observations to another CKD mouse model, the oxalate nephropathy  
10  
11 217 model in order to test for the relationship between TNF and FGF23 in a non-genetically  
12  
13 218 modified mouse model and during early stages of kidney disease <sup>36</sup>. After induction of  
14  
15 219 oxalate nephropathy, 48 hours prior to sacrifice, mice received a single i.p. injection of  
16  
17 220 0.5 mg anti-TNF or isotypic IgG control antibodies. IgG injected oxalate nephropathy  
18  
19 221 mice had elevated plasma iFGF23 compared to control mice and TNF blockade  
20  
21 222 normalized the elevated plasma iFGF23 in oxalate nephropathy mice (Figure 5 a).  
22  
23 223 Plasma cFGF23 and iFGF23/cFGF23 did not differ between the groups (Figure S4 g –  
24  
25 224 i). Plasma TNF was significantly reduced in the anti-TNF treated groups confirming the  
26  
27 225 efficacy of the anti-TNF antibody (Figure 5 b). There was no difference in plasma TNF  
28  
29 226 between IgG control treated oxalate nephropathy and control mice. Renal *Tnf* mRNA  
30  
31 227 expression showed a trend to increase in oxalate nephropathy mice and was not affected  
32  
33 228 by the anti-TNF antibody (Figure 5 c). There was no change in plasma phosphate and  
34  
35 229 urine phosphate per urine creatinine ratio while the renal function parameters plasma  
36  
37 230 creatinine and urea showed a trend to increase in the oxalate nephropathy mice (Figure  
38  
39 231 5 d – g).

40  
41  
42 232 To demonstrate that TNF regulates plasma iFGF23 independent from impaired kidney  
43  
44 233 function, we analyzed a non-renal inflammation model, the *Il10* KO mouse developing  
45  
46 234 spontaneously colitis <sup>37</sup>. Twelve to fourteen weeks old *Il10* KO mice had elevated plasma  
47  
48 235 iFGF23 and increased colon *Tnf* mRNA expression (Figure 6 a and b). After 48 hours of  
49  
50 236 a single i.p. injection of 0.5 mg anti-TNF or IgG control, anti-TNF treated *Il10* KO mice  
51  
52 237 had reduced plasma iFGF23 compared to IgG treated animals whereas cFGF23 levels  
53  
54 238 were similar (Figure 6 c and S4 k). There was a reduction in the iFGF23/cFGF23 ratio in  
55  
56 239 anti-TNF treated *Il10* KO compared to IgG control treated *Il10* KO mice (Figure S4 l).  
57  
58 240 Anti-TNF treatment had no effect on plasma phosphate levels (Figure 6 d) or kidney  
59  
60 241 function parameters (Figure 6 e and f). But there was an increase in abundance of NaPi-

TNF stimulates FGF23

1  
2  
3  
4 242 Ila at the BBM in *I110* KO mice treated with anti-TNF antibodies compared to IgG control  
5  
6 243 mice (Figure 6 g)  
7  
8 244  
9  
10  
11  
12  
13  
14  
15  
16  
17  
18  
19  
20  
21  
22  
23  
24  
25  
26  
27  
28  
29  
30  
31  
32  
33  
34  
35  
36  
37  
38  
39  
40  
41  
42  
43  
44  
45  
46  
47  
48  
49  
50  
51  
52  
53  
54  
55  
56  
57  
58  
59  
60

For Peer Review Only

## 245 Discussion

246 We provide a novel explanation for high iFGF23 levels in patients with chronic kidney  
247 disease or inflammation of non-renal origin. Our data demonstrate that TNF is positively  
248 and independently associated with plasma iFGF23 in humans. We show that exogenous  
249 TNF stimulates iFGF23 expression both *in vivo* and *in vitro*. TNF neutralization  
250 suppresses plasma iFGF23 in two CKD mouse models and triggers renal *Fgf23*  
251 expression in PKD kidneys. TNF also contributes to high iFGF23 in a model of intestinal  
252 inflammation with normal kidney function.

253 In humans, TNF levels correlated with plasma iFGF23 in the SKIPOGH multi-centric  
254 population based cohort. Dhayat et al. found in the same cohort associations between  
255 cFGF23 and plasma phosphate, 1,25(OH)<sub>2</sub>D, 25(OH)D, the ratio of TmP/GFR, age, sex,  
256 and renal function. However, there are relevant differences between both analyses: 1)  
257 we have measured both the biologically active iFGF23 and the biologically inactive C-  
258 terminal fragment, while Dhayat et al.<sup>38</sup> used a method that detects the sum of the intact  
259 form and the C-terminal fragment. 2) in addition to the subjects excluded by Dhayat et al.  
260 we excluded individuals taking drugs interacting with inflammation and subjects without  
261 complete data available for all variables. However, both analyses identified 1,25(OH)<sub>2</sub>D  
262 and 25(OH)D as strong predictors of FGF23 variation in the SKIPOGH population while  
263 the correlation of PTH and eGFR in our study was dependent on drug exclusion criteria.  
264 The overall effect of TNF on iFGF23 may explain only a small part of the overall variability  
265 of iFGF23 in this cohort.

266 TNF increases in kidney disease and associates with CKD progression<sup>24-26</sup>. TNF  
267 stimulates *Fgf23* mRNA expression in an osteocyte-derived cell line<sup>19</sup> and may be  
268 involved in obesity induced increases in FGF23. We tested the relevance of FGF23  
269 regulation by TNF in pathological situations such as kidney disease or colitis. We used  
270 two distinct CKD mouse models, the *Pkd1* conditional KO mouse and the oxalate  
271 nephropathy model. PKD kidneys are affected by inflammation<sup>39, 40</sup> as confirmed by

TNF stimulates FGF23

1  
2  
3  
4 272 higher renal *Tnf* and *Tgfb* expression as well as enhanced NFκB subunit p65  
5  
6 273 phosphorylation. Similarly, in oxalate nephropathy the inflammasome is activated and  
7  
8 274 various proinflammatory cytokines are released <sup>36, 41</sup>**Error! Reference source not**  
9  
10 275 **found..** Ectopic renal FGF23 gene and protein expression occurs in rodents with either  
11  
12 276 diabetic nephropathy, PKD, or 5/6 nephrectomy <sup>42-44</sup>. The increase of renal *Tnf* and *Tgfb*  
13  
14 277 mRNA expression in PKD kidneys was paralleled by the increase in plasma iFGF23  
15  
16 278 levels, and the appearance of renal *Fgf23* and *Runx-2* expression. Renal FGF23  
17  
18 279 production may promote inflammation and fibrosis in the affected kidney <sup>45-47</sup>. We did not  
19  
20 280 detect any change in bone *Fgf23* mRNA expression or plasma TNF levels in both CKD  
21  
22 281 models. Similarly, in *Col4a3* KO mice, another CKD model, the early rise in plasma  
23  
24 282 FGF23 is not accompanied by increased *Fgf23* expression in bone <sup>48</sup>. TNF blockade in  
25  
26 283 both CKD models normalized plasma iFGF23 levels without changes in plasma  
27  
28 284 phosphate levels. In the PKD model, TNF neutralization also reduced renal *Fgf23*  
29  
30 285 expression. TNF may regulate renal *Fgf23* expression through NFκB stimulating orphan  
31  
32 286 nuclear receptor *Nurr1* gene expression <sup>28</sup>. *Nurr1* mediates the PTH dependent  
33  
34 287 regulation of *Fgf23* in bone <sup>27</sup>. *Nurr1* was upregulated in PKD kidneys and predominantly  
35  
36 288 localized in the cell nucleus whereas in wild type kidneys it was localized in the  
37  
38 289 cytoplasm. *Nurr1* nuclear localization often overlapped with renal FGF23 protein  
39  
40 290 expression. Thus, *Nurr1* may contribute to renal FGF23 expression.

41  
42  
43  
44 291 In patients with CKD, TNF increases with ascending FGF23 quartiles and correlates with  
45  
46 292 FGF23 levels independent of renal function and measures of mineral metabolism .  
47  
48 293 Likewise, markers of inflammation correlate with ascending FGF23 quartiles in non-CKD  
49  
50 294 stroke patients <sup>13</sup>. Inoculation of mice with LPS or bacteria stimulates serum FGF23 levels  
51  
52 295 <sup>20, 49</sup>. In the diabetic nephropathy rat model, renal FGF23 was reduced by ramipril, an  
53  
54 296 angiotensin-converting enzyme inhibitor , which also reduces inflammation <sup>50</sup>. Non-renal  
55  
56 297 diseases characterized by inflammation such as inflammatory bowel disease (IBD) or  
57  
58 298 osteoarthritis are linked to elevated plasma FGF23 <sup>14, 15</sup>. Patients with IBD or mouse  
59  
60 299 colitis models show elevated FGF23 levels, lower 1,25(OH)<sub>2</sub>D and impaired intestinal



1  
2  
3  
4 300 phosphate absorption<sup>14, 51-54</sup> **Error! Reference source not found. Error! Reference**  
5  
6 301 **source not found. Error! Reference source not found. Error! Reference source not**  
7  
8 302 **found.** These disturbances are partially caused by TNF and in patients with IBD, TNF  
9  
10 303 neutralizing therapy can reverse some of these abnormalities. We tested whether  
11  
12 304 inflammation *per se* without renal disease could increase FGF23. Consistently, in *Il-10*  
13  
14 305 KO mice, a model of IBD, plasma FGF23 increased and was reduced by TNF  
15  
16 306 neutralization without affecting renal function parameters. Thus, extrarenal inflammation  
17  
18 307 also stimulates FGF23 levels in mouse models and may play a role in humans.

21 308 David et al. reported that 6 hours after administration of the inflammatory cytokine IL-1 $\beta$   
22  
23 309 only cFGF23 increased while it required 4 days of consecutive IL-1 $\beta$  injections to  
24  
25 310 increase also iFGF23 levels<sup>21</sup>, whereas Onal et al showed higher FGF23 levels already  
26  
27 311 3 hours after IL-1 $\beta$  injection<sup>49</sup>. We demonstrate that TNF administration in wild type mice  
28  
29 312 stimulated plasma iFGF23 levels within 48 hours without altering plasma phosphate and  
30  
31 313 creatinine but increasing fractional excretion of phosphate demonstrating that iFGF23 is  
32  
33 314 functional. TNF may exert even faster effects as indicated by higher FGF23 levels in mice  
34  
35 315 3 hours after TNF injection. The stimulation of *Fgf23* mRNA expression by TNF was  
36  
37 316 confirmed *in vitro* in primary mouse osteocytes and comparable to the effect of  
38  
39 317 1,25(OH)<sub>2</sub>D. TNF but not 1,25(OH)<sub>2</sub>D increased *Nurr1* and *Galnt3* expression in primary  
40  
41 318 osteocytes suggesting that TNF but not 1,25(OH)<sub>2</sub>D may regulate *Fgf23* expression in a  
42  
43 319 *Nurr1*-dependent manner. TNF may also modulate FGF23 protein stability by regulating  
44  
45 320 the expression of *Galnt3* which mediates the O-glycosylation of FGF23 making it more  
46  
47 321 resistant to proteolytic degradation. In bone, C-terminal DMP-1 binds to PHEX and  
48  
49 322 thereby inhibits *Fgf23* expression<sup>55</sup>. In primary osteocytes, *Dmp1* expression was  
50  
51 323 strongly decreased by TNF and 1,25(OH)<sub>2</sub>D. The upregulation of *Fgf23* expression by  
52  
53 324 TNF and 1,25(OH)<sub>2</sub>D is paralleled by the downregulation of its suppressor. Our data  
54  
55 325 expand previous observations in IDG-SW3 mouse osteocyte cells where TNF, IL-1 $\beta$ , and  
56  
57 326 LPS increased *Fgf23* and reduced *Dmp1* mRNA expression<sup>19</sup>. TNF also stimulated  
58  
59 327 *Fgf23* mRNA expression in rat UMR106 osteosarcoma cells and is required to increase  
60

TNF stimulates FGF23

1  
2  
3  
4 328 circulating FGF23 levels in a mouse obesity model . Deletion of an 16kb enhancer  
5  
6 329 element in the *Fgf23* murine gene abolishes TNF induced FGF23 increases and reduces  
7  
8 330 the effect of LPS and IL-1 $\beta$  on circulating FGF23 levels without altering bone structure or  
9  
10 331 plasma phosphate and PTH. Induction of *Fgf23* mRNA in various organs is organ-  
11  
12 332 specifically responsive to LPS, TNF and IL-1 $\beta$  and the deletion of the enhancer  
13  
14 333 suggesting a complex and cell- and/or organ-specific regulation <sup>49</sup>. The enhancer  
15  
16 334 element is also required for the early induction of FGF23 in the oxalate nephropathy  
17  
18 335 model <sup>49</sup>. Thus, our work demonstrates the critical role of TNF in inducing FGF23  
19  
20 336 production and thereby complements previous work that identified a genetic element  
21  
22 337 responding to TNF and possibly other regulators of *Fgf23* mRNA transcription .  
23  
24 338 Furthermore, we expand these observations from kidney disease to at least one other  
25  
26 339 clinically important condition, inflammatory bowel disease.

27  
28  
29  
30 340 IL-6 has been recently identified as another important proinflammatory cytokine that  
31  
32 341 associates with FGF23 levels in the CRIC cohort and that stimulates *Fgf23* mRNA in  
33  
34 342 the IDG-SW3 osteocyte cell line <sup>19</sup>. Durlacher-Betzer et al. showed increased expression  
35  
36 343 of IL-6 in kidney of folic-acid and adenine AKI and CKD mouse models and a partly  
37  
38 344 blunted increase of circulating FGF23 levels in IL-6 deficient mice treated with adenine .  
39  
40 345 While IL-6 may participate in the regulation of FGF23 in CKD, IL-6 plays also an important  
41  
42 346 role in normal bone biology and IL-6 deficient mice have altered bone architecture <sup>56, 57</sup>.  
43  
44 347 Thus, IL-6 may contribute to the upregulation of FGF23 in early CKD but TNF may act  
45  
46 348 either upstream or is a critical permissive factor as indicated by the complete  
47  
48 349 normalization of FGF23 levels in our experiments. In our population-based cohort, TNF  
49  
50 350 but not IL-6 associated with intact FGF23 levels further strengthening the concept that  
51  
52 351 TNF may play a central role in mediating effects of inflammation on bone.

53  
54  
55  
56 352 Renal hypoxia is a common complication in CKD kidneys <sup>31, 32</sup>. Hypoxia increased *Fgf23*  
57  
58 353 expression in UMR-106 rat osteosarcoma cells, and plasma cFGF23 but not iFGF23 in  
59  
60 354 rats under hypobaric hypoxia conditions <sup>18</sup>. We cultured MC3T3-E1 cells, a mouse

1  
2  
3  
4 355 preosteoblast cell line and primary mouse osteoblasts for 24 and 48 hours in 0.2%  
5  
6 356 hypoxia and we did not observe any stimulation of *Fgf23* expression. In contrast, hypoxia  
7  
8 357 suppressed the stimulatory effect of 1,25(OH)<sub>2</sub>D on *Fgf23*. TNF and IL-1 $\beta$  increase HIF-  
9  
10 358 1 binding to DNA under normoxia while in combination with hypoxia both cytokines  
11  
12 359 strongly increase HIF-1 activity<sup>58</sup>. IL-1 $\beta$  but not TNF enhance nuclear accumulation of  
13  
14 360 HIF-1 $\alpha$  in a hepatoma cell line<sup>58</sup> and increase FGF23 mRNA expression in bones and  
15  
16 361 kidneys<sup>21</sup>. Inhibition of HIF-1 $\alpha$  attenuated the positive effect of IL-1 $\beta$  on FGF23  
17  
18 362 expression<sup>21</sup>. Combined with the fact that we did not find any effect of constitutively  
19  
20 363 activated HIF-1 $\alpha$  in *Vhl* KO animals as well as in primary kidney cells lacking *Vhl*, these  
21  
22 364 results suggest that the HIF-1 $\alpha$  mediated upregulation of *Fgf23* expression may depend  
23  
24 365 on IL-1 $\beta$  or other factors such as erythropoietin<sup>9, 21, 59, 60</sup>.

26  
27  
28 366 In summary, TNF stimulates iFGF23 in renal and non-renal inflammatory mouse models  
29  
30 367 and in primary bone cell culture; triggers renal *Fgf23* expression in CKD animal models  
31  
32 368 and is positively associated with plasma iFGF23 in a population-based cohort. These  
33  
34 369 findings question the concept that the early rise in plasma FGF23 in CKD is solely to  
35  
36 370 balance plasma phosphate while kidney function declines. The data suggest that other  
37  
38 371 non-renal inflammatory processes may strongly impact on plasma FGF23 levels. Our  
39  
40 372 study suggests novel therapeutic options to reduce excessive FGF23 levels in kidney  
41  
42 373 and other diseases as drugs lowering TNF are widely clinically used and have proven to  
43  
44 374 be safe in humans.

45  
46  
47  
48 375  
49  
50  
51  
52  
53  
54  
55  
56  
57  
58  
59  
60

## 376 **Methods**

### 377 **SKIPOGH cohort**

378 We obtained 1098 out of 1131 human EDTA plasma samples from SKIPOGH cohort  
379 (Swiss Kidney Project on Genes in Hypertension)<sup>23, 61, 62</sup>. Plasma iFGF23 was measured  
380 with the human intact FGF23 ELISA kit (Immutopics International, USA). For statistical  
381 modeling the following 18 previously determined parameters were used: plasma calcium,  
382 phosphate, ferritin, transferrin, iron, 1,25(OH)<sub>2</sub>D, 25(OH) vitamin D<sub>3</sub>, PTH, TNF, IFN $\gamma$ , IL-  
383 1 $\beta$ , IL-6, IL-10 and cFGF23 as well as body mass index, age, sex and estimated renal  
384 function calculated by the CKD-EPI equation.

385 Exclusion criteria followed the pipeline described in the Table S3. Participants with  
386 incomplete data sets (n = 261) were excluded. TNF followed a bimodal distribution with  
387 40 values close to undetectable (TNF < 1 pg/ml) without continuity with the rest of the  
388 distribution, highly suggestive for measurement failures. Therefore the 40 participants  
389 with TNF < 1 pg/ml were excluded from the study. Next, the ratio between iFGF23  
390 (detects only iFGF23) and cFGF23 (detects iFGF23 and cFGF23) was calculated. One  
391 Ru/ml cFGF23 corresponds to 1.5 pg/ml iFGF23 (information provided by Immutopics);  
392 participants with ratios higher than 1.5 were excluded (n = 40). To avoid confounding  
393 effects by drug intake we eliminated 4 major drug categories that interact with FGF23  
394 metabolism: 1) calcium, phosphate and magnesium (n = 41); 2) inflammation (pro or anti-  
395 inflammatory) (n = 390); 3) iron metabolism (n = 6); 4) kidney function (i.e. diuretics) (n =  
396 54) (Table S4). A total of 361 participants were excluded due to intake of drugs of one or  
397 more of these drug categories. The final dataset contains either 429 participants (198  
398 female / 231 male) with or 790 (424 female / 366 male) without drug exclusion criteria.

### 399 **Animals**

400 *Pkd1* floxed/floxed (*Pkd1*<sup>fl/fl</sup>) tamoxifen inducible *cre* mice were kindly provided by  
401 Gregory Germino<sup>63, 64</sup>. *Cre* recombinase expression is under the control of the  $\beta$ -actin  
402 promoter which drives high levels of expression in most tissues. Male and female *Pkd1*<sup>fl/fl</sup>,

1  
2  
3  
4 403 *cre+* and *Pkd1<sup>fl/fl</sup>*, *cre-* mice were used. Cre recombinase activity was induced at postnatal  
5  
6 404 days 15, 17, and 19 by injecting pups with 100  $\mu$ l tamoxifen (2.5 mg/ml) in corn oil causing  
7  
8 405 slow onset disease. Without further interventions, 24-hour urine was collected from 6 and  
9  
10 406 12 weeks old animals (e.g. 3 or 9 weeks after induction, respectively) which were  
11  
12 407 thereafter sacrificed to collect plasma and organs. For TNF blockade, animals were  
13  
14 408 treated at the age of 11-12 weeks with a single i.p. injection of 0.5 mg *InVivoMAb* anti-  
15  
16 409 Tnfa (Clone XT3.11, Lot4653-1/0413, BioXCell, USA) or *InVivoMAb* rat IgG1 (Clone  
17  
18 410 HRPN, Lot 5339/1014, BioXCell, USA)<sup>65, 66</sup>. Twenty-four hours after antibody application,  
19  
20 411 animals were sacrificed and plasma and organs were collected. The effect of TNF in wild-  
21  
22 412 type mice was assessed by injecting 13 weeks old C57Bl/6J mice on two consecutive  
23  
24 413 days with 2  $\mu$ g TNF. After 48 hours, plasma and organs were collected.  
25  
26 414 Nephropathy was induced in 10 to 12 weeks old C57Bl/6J mice. After 3 days of  
27  
28 415 adaptation with calcium-free diet (irradiated S7042-E005S, Sniff Spezialdiäten GmbH,  
29  
30 416 Germany), mice were fed for 10 days with either calcium free diet or 0.67% oxalate in  
31  
32 417 calcium-free diet (irradiated S7042-E010) followed by a 5-day recovery phase in standard  
33  
34 418 diet (3433, Kliba, Kaiseraugst, Switzerland). Forty-eight hours prior to sacrifice, mice  
35  
36 419 received a single i.p. injection of 0.5 mg anti-TNF or isotypic IgG1 control. Mice were  
37  
38 420 sacrificed and plasma and organs were collected.  
39  
40 421 *Il10* deficient mice (*Il10<sup>-/-</sup>*) develop spontaneous colitis and were used as a non-renal  
41  
42 422 inflammatory disease model<sup>37</sup>. *Il10<sup>-/-</sup>* mice between 12-14 weeks were sacrificed to  
43  
44 423 collect plasma and organs. *Il10<sup>-/-</sup>* mice were treated with a single i.p. injection of 0.5 mg  
45  
46 424 *InVivoMAb* anti-Tnfa (Clone XT3.11, Lot4653-1/0413, BioXCell, USA) or *InVivoMAb* rat  
47  
48 425 IgG1 (Clone HRPN, Lot 5339/1014, BioXCell, USA)<sup>65, 66</sup> 48 hours prior to sacrifice and  
49  
50 426 plasma and organs were collected. For some experiments, kidneys from kidney-specific  
51  
52 427 von-Hippel-Lindau deficient mice were used<sup>33</sup>. All animal studies were performed  
53  
54 428 according to protocols approved by the legal authority (Veterinary Office of the Canton  
55  
56 429 of Zurich or the Committee on Animal Research, University of California San Francisco).  
57  
58  
59  
60

TNF stimulates FGF23

### 430 **Plasma and urine analysis**

431 Blood and 24 hours urine were collected from *Pkd1<sup>fl/fl</sup>, cre+* and *Pkd1<sup>fl/fl</sup>, cre-* mice at 6  
432 and 12 weeks after birth. Briefly, *Pkd1<sup>fl/fl</sup>, cre* mice were kept for three days in metabolic  
433 cages (Tecniplast, Italy) whereas the last day was used for 24 hours urine collection.  
434 Afterwards mice were anesthetized with isoflurane and blood was collected from the  
435 heart. Plasma and urine aliquots were rapidly frozen and stored at -80 °C until  
436 measurement. Urine and plasma laboratory analyses were performed on a UniCel DxC  
437 800 Synchron (Beckman Coulter, Switzerland) by the Zurich Integrative Rodent  
438 Physiology (ZIRP) core facility. The ratio of the maximum rate of tubular phosphate  
439 reabsorption to the glomerular filtration rate (TmP/GFR) was calculated as follows:

440  $TmP/GFR \text{ in } mmol/L = P_P - [U_P \times P_{crea} / U_{crea}]^{67}$ . The fractional excretion of phosphate  
441 was calculated according to the following equation:  $FE_{Pi} = (U_{Pi} \times P_{crea}) / (P_{Pi} \times U_{crea}) \times 100$ .  
442  $P_{Pi}$ ,  $U_{Pi}$ ,  $P_{crea}$ , and  $U_{crea}$  refer to the plasma and urinary concentration of phosphate and  
443 creatinine, respectively. The plasma concentration of intact FGF23 (Kainos Laboratories,  
444 Japan or Immutopics International, USA), cFGF23 (Immutopics International, USA),  
445 intact PTH (Immutopics International, USA) and TNF (Bio-Techne AG, Switzerland) were  
446 measured by enzyme-linked immunosorbent assays according to the manufacturers  
447 protocols.

### 448 **Cell culture**

449 All cell culture reagents were from Life Technologies Europe B.V. (Switzerland) unless  
450 stated otherwise. Two to four month old *Pkd1<sup>fl/fl</sup>, cre* mice (4-6 mice per experiment, male  
451 and female mixed) were sacrificed with carbon dioxide. Tibias and femurs from the  
452 hindlegs were harvested. The epiphyses were cut and bones were flushed with Hank's  
453 Balanced Salt Solution (HBSS) containing 1% penicillin streptomycin (Pen Strep) to  
454 remove the bone marrow. Bones were cut into small pieces of 1-2 mm<sup>2</sup>. Bone cell  
455 extraction was performed according to established protocols<sup>29, 30</sup>. Briefly, small bone  
456 pieces were repeatedly digested with either a solution containing 2 mg/ml collagenase

1  
2  
3  
4 457 type II, 0.05% (w/v) soybean trypsin inhibitor (Sigma-Aldrich, Switzerland), 20 mM  
5  
6 458 HEPES, 1% Pen Strep in HBSS or 10 nM EDTA, 1% fetal bovine serum (FBS), 1% Pen  
7  
8 459 Strep in phosphate buffered saline (PBS) for 25 min at 37°C. Cells from digestion steps  
9  
10 460 6-9 or cells and bone pieces from digestion step >9 were cultured for 2 weeks in an  
11  
12 461 osteogenic medium (minimal essential medium  $\alpha$  (MEM $\alpha$ ) containing 10% FBS, 1% Pen  
13  
14 462 Strep, 50  $\mu$ g/ml 2-phospho-L-ascorbic acid trisodium salt (Sigma-Aldrich, Switzerland),  
15  
16 463 and 1 mM  $\beta$ -glycerophosphate (Sigma-Aldrich, Switzerland)). After 2 weeks, cells were  
17  
18 464 supplemented for 24 hours with either 10 nM 1,25(OH)<sub>2</sub>D (CaymanChemical, USA) or 10  
19  
20 465 ng/ml mouse TNF (R&D Systems, USA) and total mRNA was extracted.

21  
22 466 MC3T3-E1 subclone 4 preostoblast cells (CRL-2593, Lot 59899932, ATCC France)  
23  
24 467 passage 17/4 were expanded for 4-5 days with MEM $\alpha$  medium supplemented with 10%  
25  
26 468 FBS and 1% PenStrep. After reaching 80-90% confluence, MC3T3-E1 cells were  
27  
28 469 trypsinized and plated in collagen coated 6-well plates (80'000 cells/well). Medium was  
29  
30 470 changed to osteogenic differentiation medium (MEM $\alpha$  supplemented with 10% FBS, 1%  
31  
32 471 PenStrep, 50 $\mu$ g/ml 2-phospho-L-ascorbic acid trisodium salt (Sigma-Aldrich,  
33  
34 472 Switzerland), and 1 mM beta glycerophosphate (Sigma-Aldrich, Switzerland)). After 2  
35  
36 473 weeks differentiation along the osteogenic lineage cells were supplemented for 24 or 48  
37  
38 474 hours with either 10 nM 1,25(OH)<sub>2</sub>D (CaymanChemical, USA) or an equal amount of  
39  
40 475 ethanol and incubated for 24 or 48 hours under hypoxic (0.2% O<sub>2</sub>) or normoxic conditions.  
41  
42 476 Hypoxia experiments were performed in a gas-controlled workstation (InvivoO<sub>2</sub>, Baker  
43  
44 477 Ruskinn, UK).

#### 48 **RNA extraction, reverse transcription and qPCR**

49  
50  
51 479 Organs and scraped colonic mucosa were harvested and rapidly frozen in liquid nitrogen.  
52  
53 480 Tissues were homogenized using either a Precellys homogenizer or a liquid nitrogen  
54  
55 481 cooled mortar and pestle (bone). Total mRNA from bone as well as from cultured cells  
56  
57 482 was extracted with TRIzol (Life Technologies Europe B.V., Switzerland) followed by  
58  
59 483 purification with RNeasy Mini Kit (Qiagen, Switzerland) according to the manufacturers  
60  
484 protocol. Total mRNA from kidney and colonic mucosa were extracted with RNeasy Mini

TNF stimulates FGF23

1  
2  
3  
4 485 Kit (Qiagen, Switzerland) according to the manufacturer's protocol. DNase digestion was  
5  
6 486 performed using the RNase-free DNAase Set (Qiagen, Switzerland). Total RNA  
7  
8 487 extractions were analyzed for purity and concentration using the NanoDrop ND-1000  
9  
10 488 spectrophotometer (Wilmington, Germany). RNA samples were diluted to a final  
11  
12 489 concentration of 100 ng/ $\mu$ l and cDNA was prepared using the TaqMan Reverse  
13  
14 490 Transcriptase Reagent Kit (Applied Biosystems, Roche, Foster City, CA). In brief, in a  
15  
16 491 reaction volume of 40  $\mu$ l, 300 ng of RNA was used as template and mixed with the  
17  
18 492 following final concentrations of RT buffer (1x): MgCl<sub>2</sub> (5.5 mmol/l), random hexamers  
19  
20 493 (2.5  $\mu$ mol/l), dNTP mix (500  $\mu$ mol/l each), RNase inhibitor (0.4 U/ $\mu$ l), multiscribe reverse  
21  
22 494 transcriptase (1.25 U/ $\mu$ l), and RNase-free water. Reverse transcription was performed  
23  
24  
25 495 with temperature conditions set at 25 °C for 10 min, 48 °C for 30 min, and 95 °C for 5  
26  
27 496 min on a thermocycler (Biometra, Germany). Quantitative PCR (qPCR) was performed  
28  
29 497 on the ABI PRISM 7700 Sequence Detection System (Applied Biosystems). Primers for  
30  
31 498 genes of interest were designed using Primer 3 software. Primers were chosen to span  
32  
33 499 exon - exon boundaries to exclude the amplification of contaminating genomic DNA  
34  
35 500 (primer and probe sequence see Table S5). The specificity of all primers was tested and  
36  
37 501 always resulted in a single product of the expected size (data not shown). Probes were  
38  
39 502 labeled with the reporter dye FAM at the 5'-end and the quencher dye TAMRA at the 3'-  
40  
41 503 end (Microsynth, Switzerland). qPCR reactions were performed using the KAPA PROBE  
42  
43 504 FAST qPCR Kit (KappaBiosystems, USA) or PowerUp™ SYBR® Green Master Mix  
44  
45 505 (Applied Biosystems, Switzerland).

### 506 **Protein extraction and Western blot analysis**

507 Organs were rapidly frozen in liquid nitrogen. Tissues were homogenized in  
508 homogenization buffer containing 0.27 M sucrose, 2 mM EDTA (pH8), 0.5% NP-40, 60  
509 mM KCl, 15 mM NaCl, 15 mM HEPES (pH7.5) (all Sigma-Aldrich, Switzerland) and  
510 complete protease inhibitor cocktail (Roche, Switzerland) using Precellys homogenizer.  
511 Nuclei were separated by a sucrose cushion and resuspended in a nuclear extraction  
512 buffer containing 20 mM HEPES (pH 7.5), 400 mM NaCl, 1 mM EDTA (pH 8), 1 mM DTT



1  
2  
3  
4 513 and 1 mM PMSF (all Sigma-Aldrich, Switzerland). BBM vehicles were prepared using the  
5  
6 514 Mg<sup>2+</sup> precipitation technique <sup>68</sup>. After measurement of protein concentration (Bio-Rad,  
7  
8 515 Hercules, CA, USA), 60 µg of nuclear proteins or 20 µg of BBM proteins were solubilized  
9  
10 516 in loading buffer containing DTT and separated on a 10% polyacrylamide gel. For  
11  
12 517 immunoblotting, proteins were transferred electrophoretically to polyvinylidene fluoride  
13  
14 518 membranes (Immobilon-P, Millipore, Bedford, MA, USA). After blocking with 5% milk  
15  
16 519 powder in Tris-buffered saline/0.1% Tween-20 or 5% bovine serum albumin (BSA) in  
17  
18 520 Tris-buffered saline/0.1% Tween-20 for 60 min, blots were incubated with the primary  
19  
20 521 antibodies: mouse monoclonal anti-phospho-NFκB p65 (Ser536)(7F1) (Cell Signaling  
21  
22 522 Technology, USA; 1:1000), rabbit monoclonal NFκB p65 (D14E12) (Cell Signaling  
23  
24 523 Technology, USA; 1:1000), rabbit polyclonal anti-NaPi-IIa (<sup>69</sup>; 1:3000) or mouse  
25  
26 524 monoclonal anti-β-actin either for 2 h at room temperature or overnight at 4 °C.  
27  
28 525 Membranes were then incubated for 1 h at room temperature with secondary goat anti-  
29  
30 526 rabbit or donkey anti-mouse antibodies (1:5000) linked to alkaline phosphatase  
31  
32 527 (Promega, USA) or HRP (Amersham, MA, USA or R&D Systems, USA). The protein  
33  
34 528 signal was detected with the appropriate substrates using the DIANA III-  
35  
36 529 chemiluminescence detection system (Raytest, Straubenhardt, Germany). All images  
37  
38 530 were analyzed using the software Advanced Image Data Analyser AIDA, Raytest to  
39  
40 531 calculate the ratio between phosphorylated protein to total protein.  
41  
42  
43  
44

### 532 **Immunofluorescence staining**

45  
46  
47 533 Mouse kidneys were perfused through the left heart ventricle with a fixative solution  
48  
49 534 containing 3% paraformaldehyde in phosphate buffered saline (PBS). Kidneys were  
50  
51 535 embedded in TissueTec and frozen in liquid nitrogen. Five µm cryosections were cut.  
52  
53 536 Slides were rehydrated with PBS, treated for 5 min with 0.5% SDS in PBS followed by  
54  
55 537 10 min treatment with 0.5% Triton-X-100 in PBS (Sigma-Aldrich, Switzerland). Unspecific  
56  
57 538 sites were blocked with 1% bovine serum albumin (BSA) in PBS for 1 h at room  
58  
59 539 temperature. Primary antibodies were diluted in 1% BSA in PBS (rat anti-FGF23 clone  
60 540 #283507 (R&D Systems, USA) 1:1000; rabbit anti-Nurr1 N-20 sc-991 (Santa-Cruz, USA)

1  
2  
3  
4 541 1:200) and kidney sections were incubated with the primary antibody overnight at 4 ° C.  
5  
6 542 After washing with PBS, sections were incubated with the corresponding secondary  
7  
8 543 antibody (1:500) (anti-rabbit DyLight 594 (Jackson ImmunoResearch, Europe), anti-rat  
9  
10 544 NL493 (R&D Systems, USA)), and DAPI (Life Technologies Europe B.V., Switzerland,  
11  
12 545 1:1000) for 1 h at room temperature. Slides were washed twice with PBS before they  
13  
14 546 were mounted with Dako glycergel mounting medium (Dako, Switzerland). Sections were  
15  
16 547 visualized on a Leica DM 5500B fluorescence microscope and images processed with  
17  
18 548 ImageJ.

### 549 **Statistical analysis**

550 Statistics were performed using unpaired Student's t-test, ANOVA, or Two-Way-ANOVA  
551 (GraphPad Prism version 7, GraphPad, San Diego, CA) and R programming  
552 environment including the nlme, visreg, data.table, car, lmtest, and forestplot  
553 packages. **Error! Reference source not found. Error! Reference source not**  
554 **found. Error! Reference source not found. Error! Reference source not found. Error!**  
555 **Reference source not found.** P < 0.05 was considered significant.

556 The identification of predictors for iFGF23 variation in the SKIPOGH population was  
557 performed using linear mixed models with random intercept. The distribution of all  
558 parameters was analyzed in histograms. Due to a heavily skewed distribution, IL-6, IL-  
559 10, IFN $\gamma$  and IL1- $\beta$  were log-transformed. All parameters were centralized and then  
560 normalized by their standard deviations. Linear or nonlinear relationship of each variable  
561 with iFGF23 was assessed using a component residual plot. However, all parameters  
562 were considered linear. Assumptions on the within-group error were checked with plots  
563 of the standardized residuals versus fitted values and a Q-Q plot of the residuals. The  
564 assumptions on the random effects were checked with a Q-Q plot of the random effects.

### 565 **Author contributions**

566 Conceptualization, D. E-S., P.H.I.S., and C.A.W; Methodology, D. E-S., P.H.I.S., and  
567 C.A.W; Formal analysis, D. E-S. and P.H.I.S.; Investigation, D. E-S., P.H.I.S., B.G., N.G.,

1  
2  
3  
4 568 C.B., M.Z., D.S., M.R., D.A., B.P., M.P., A.L., V.B., and G.-M. F; Resources C.A.W., D.H.,  
5  
6 569 F.K., I.F-W., G.R., M. B., F.P., M.F., F.L., R.H.W., S.H.- and I.F.; Writing – Original Draft,  
7  
8 570 D. E-S. Writing -Review & Editing, D. E-S., P.H.I.S., and C.A.W; Visualization, D. E-S.  
9  
10 571 and P.H.I.S.; Supervision, C.A.W.; Funding Acquisition, C.A.W, all authors read, edited  
11  
12 572 and approved the manuscript.

### 13 14 573 **Acknowledgments**

15  
16  
17 574 This study was supported by grants from the Swiss National Center for Competence in  
18  
19 575 Research NCCR Kidney.CH to C. A. Wagner, the Novartis Foundation for medical-  
20  
21 576 biological research to C. A. Wagner and D. Egli-Spichtig, the SNSF early postdoc mobility  
22  
23 577 grant to D. Egli-Spichtig and the Deutsche Forschungsgemeinschaft to Michael Föller  
24  
25 578 and Florian Lang (La315-15). P.H. Imenez Silva was recipient of a fellowship from the  
26  
27 579 IKPP Kidney.CH under the European Union Seventh Framework Programme for  
28  
29 580 Research, Technological Development and Demonstration under the grant agreement  
30  
31 581 no 608847 and Conselho Nacional de Desenvolvimento Científico e Tecnológico (CNPq)  
32  
33 582 grant number 205625/2014-2. The use of the ZIRP Core facility for Rodent Physiology is  
34  
35 583 gratefully acknowledged. SKIPOGH was supported by a SPUM grant from the Swiss  
36  
37 584 National Center for Competence in Research (FN 33CM30-124087) and by intramural  
38  
39 585 support of Lausanne, Geneva, and Bern University Hospitals. cFGF23, PTH and vitamin  
40  
41 586 D measurements were supported by an unrestricted research grant from Abbvie (Daniel  
42  
43 587 Fuster and Nasser Dhayat) and by intramural support of Bern University Hospital. We  
44  
45 588 thank the study nurses Marie-Odile Levy, Guler Gök-Sogüt, Ulla Schüpbach, and  
46  
47 589 Dominique Siminski for their involvement and help with recruitment. We also thank  
48  
49 590 Sandrine Estoppey for her help in logistic and database management. SKIPOGH  
50  
51 591 investigators include Murielle Bochud (PI), Fred Paccaud and Michel Burnier, Lausanne  
52  
53 592 University Hospital, Lausanne; Pierre-Yves Martin and Antoinette Péchère-Bertschi,  
54  
55 593 Geneva University Hospitals, Geneva; Bruno Vogt, Inselspital, Bern and Olivier Devuyst,  
56  
57 594 University of Zürich, Zürich. SNFR-supported SKIPOGH-1 fellows include Daniel  
58  
59 595 Ackermann (Inselspital, Bern), Georg Ehret, Idris Guessous and Belen Ponte (Geneva  
60

TNF stimulates FGF23

1  
2  
3  
4 596 University Hospitals, Geneva) and Menno Pruijm (Lausanne University Hospital,  
5  
6 597 Lausanne).

7  
8 598 **Conflict of interests**

9  
10  
11 599 C.A. Wagner has been a member of an advisory board to Bayer Pharma AG, and  
12  
13 600 provided consultancy to Medice. No other financial interests are reported.

14  
15 601  
16 602  
17 603  
18  
19  
20  
21  
22  
23  
24  
25  
26  
27  
28  
29  
30  
31  
32  
33  
34  
35  
36  
37  
38  
39  
40  
41  
42  
43  
44  
45  
46  
47  
48  
49  
50  
51  
52  
53  
54  
55  
56  
57  
58  
59  
60

604 **Figure legends**605 **Figure 1**

606 **Identification of plasma iFGF23 predictors in a human cohort.** (a) Forest plot  
 607 showing the fixed effects calculated for all predictors used in the mixed linear model for  
 608 the subpopulation of 429 participants after all the exclusion criteria applied. Fixed effect  
 609 estimates ( $\beta$ ), standard error, ratio between the estimates and their standard errors (t-  
 610 value), and associated p-value from a t-distribution. The parameters are ordered by fixed  
 611 effect estimates. (b) Association between plasma TNF and iFGF23 in the SKIPOGH  
 612 cohort in a subpopulation of 429 participants after all the exclusion criteria applied. The  
 613 regression line and confidence band were obtained from the linear mixed model  
 614 containing all the predictors.

615 **Figure 2**

616 **FGF23 and inflammation in *Pkd1* KO mice.** Plasma FGF23 (a) and TmP/GFR (b) as  
 617 well as renal *Tnf* (c) and renal *Tgfb* (d) mRNA expression relative to 18SrRNA in *Pkd1<sup>fl/fl</sup>*,  
 618 *cre-* (white squares) and *Pkd1<sup>fl/fl</sup>*, *cre+* (black squares) animals after 6 and 12 weeks.  
 619 Phosphorylation of NF $\kappa$ B p65 (e) in the nuclear fraction of total kidney protein  
 620 homogenates in *Pkd1<sup>fl/fl</sup>*, *cre-* (white squares) and *Pkd1<sup>fl/fl</sup>*, *cre+* (black squares) animals  
 621 after 12 weeks. Renal (f) and bone (g) *Fgf23* mRNA expression relative to 18SrRNA in  
 622 *Pkd1<sup>fl/fl</sup>*, *cre-* (white squares) and *Pkd1<sup>fl/fl</sup>*, *cre+* (black squares) animals after 12 weeks.  
 623 ND = not detected. Two-way ANOVA with Bonferroni correction (a - d) or unpaired t-test  
 624 (e - g), \*  $p < 0.05$ .

625 **Figure 3**

626 **TNF neutralization lowers FGF23 in *Pkd1* KO mice.** Plasma TNF (a), iFGF23 (b),  
 627 phosphate (c), and urea (d) levels, bone (e) and renal (f) *Fgf23*, renal *Tnf* (g), and renal  
 628 *Tgfb* (h) mRNA expression relative to *Hprt* as well as abundance of NaPi-IIa (i) in the  
 629 renal BBM relative to  $\beta$ -actin 24 hours after injection of 0.5mg isotypic IgG control or anti-  
 630 TNF neutralizing antibodies in 11-12 weeks old *Pkd1<sup>fl/fl</sup>*, *cre-* (white squares) and *Pkd1<sup>fl/fl</sup>*,  
 631 *cre+* (black squares) animals. ND = not detected. Two-way ANOVA with Bonferroni  
 632 correction \*  $p < 0.05$ .

633 **Figure 4**

634 **TNF stimulates FGF23 *in vivo* and *in vitro*.** Plasma iFGF23 (a), TNF (b), phosphate  
 635 (c), creatinine (d), urea (e) and  $FE_{P_i}$  (f) as well as bone (g), spleen (h) thymus (i) and  
 636 bone marrow (j) *Fgf23* mRNA expression relative to *Hprt* (g,h) or *18SrRNA* (i,j) 48 hours  
 637 after two consecutive injections of vehicle or 2  $\mu$ g recombinant mouse TNF in 12 weeks  
 638 old wild type mice. Unpaired t-test \*  $p < 0.05$ . Fold increase of *Fgf23* (k), *Dmp1* (l), *Galnt3*  
 639 (m), and *Nurr1* (n) mRNA expression compared to untreated control in primary murine  
 640 osteocytes after stimulation with 1,25(OH) $_2$ D (white squares) or 10ng/ml TNF (black  
 641 squares) for 24 hours. Single experiments were normalized to their untreated control  
 642 (dashed line = 1). Number of independent experiments 9-10; One-way ANOVA with  
 643 Bonferroni correction \*  $p < 0.05$  compared to 1,25(OH) $_2$ D treated cells, #  $p < 0.05$  compared  
 644 to untreated cells.

645 **Figure 5**

646 **TNF neutralization lowers plasma iFGF23 in mice with oxalate nephropathy.**  
647 Oxalate-nephropathy was induced in wild type mice. Plasma iFGF23 (a), plasma TNF  
648 (b), renal *Tnf* (c) mRNA expression relative to *Hprt*, plasma phosphate (d), urinary  
649 phosphate to creatinine ratio (e), plasma creatinine (f) and plasma urea (g) 48 hours after  
650 injection of 0.5 mg isotypic IgG control or anti-TNF neutralizing antibodies in control diet  
651 (white squares) and oxalate nephropathy (black squares) induced mice. One-way  
652 ANOVA with Bonferroni correction \*  $p < 0.05$ .

653 **Figure 6**

654 **Colonic inflammation increases plasma iFGF23 via TNF in *Il-10* KO mice.** Plasma  
655 iFGF23 (a) levels and colonic *Tnf* (b) mRNA expression relative to 18SrRNA in 14 weeks  
656 old *Il-10*<sup>+/+</sup> and *Il-10*<sup>-/-</sup> mice. Plasma iFGF23 (c), phosphate (d), creatinine (e), and urea  
657 (f) levels as well as abundance of NaPi-IIa at the renal BBM 48 hours after injection of  
658 0.5 mg isotypic IgG control or anti-TNF neutralizing antibodies in 12 weeks old *Il-10*<sup>-/-</sup>  
659 mice. Unpaired t-test \*  $p < 0.05$ .

660

## 661 REFERENCES

- 662  
663 1. Isakova T, Wahl P, Vargas GS, *et al.* Fibroblast growth factor 23 is elevated  
664 before parathyroid hormone and phosphate in chronic kidney disease. *Kidney Int*  
665 2011; **79**: 1370-1378.  
666
- 667 2. Block GA, Klassen PS, Lazarus JM, *et al.* Mineral metabolism, mortality, and  
668 morbidity in maintenance hemodialysis. *J Am Soc Nephrol* 2004; **15**: 2208-2218.  
669
- 670 3. Gutierrez OM. Fibroblast growth factor 23 and disordered vitamin D metabolism  
671 in chronic kidney disease: updating the "trade-off" hypothesis. *Clin J Am Soc*  
672 *Nephrol* 2010; **5**: 1710-1716.  
673
- 674 4. Gutierrez OM, Mannstadt M, Isakova T, *et al.* Fibroblast growth factor 23 and  
675 mortality among patients undergoing hemodialysis. *N Engl J Med* 2008; **359**: 584-  
676 592.  
677
- 678 5. Faul C, Amaral AP, Oskouei B, *et al.* FGF23 induces left ventricular hypertrophy.  
679 *J Clin Invest* 2011; **121**: 4393-4408.  
680
- 681 6. Souma N, Isakova T, Lipiszko D, *et al.* Fibroblast Growth Factor 23 and Cause-  
682 Specific Mortality in the General Population: The Northern Manhattan Study. *J*  
683 *Clin Endocrinol Metab* 2016; **101**: 3779-3786.  
684
- 685 7. Quarles LD. Skeletal secretion of FGF-23 regulates phosphate and vitamin D  
686 metabolism. *Nat Rev Endocrinol* 2012; **8**: 276-286.  
687
- 688 8. Hu MC, Shiizaki K, Kuro-o M, *et al.* Fibroblast growth factor 23 and Klotho:  
689 physiology and pathophysiology of an endocrine network of mineral metabolism.  
690 *Annu Rev Physiol* 2013; **75**: 503-533.  
691
- 692 9. Urakawa I, Yamazaki Y, Shimada T, *et al.* Klotho converts canonical FGF  
693 receptor into a specific receptor for FGF23. *Nature* 2006; **444**: 770-774.  
694
- 695 10. Zhang B, Umbach AT, Chen H, *et al.* Up-regulation of FGF23 release by  
696 aldosterone. *Biochem Biophys Res Commun* 2016; **470**: 384-390.  
697
- 698 11. Daryadel A, Bettoni C, Haider T, *et al.* Erythropoietin stimulates Fibroblast Growth  
699 Factor 23 (FGF23) in mice and men. *Pflügers Arch* 2018; **470**: 1569-1582  
700
- 701 12. Bar L, Feger M, Fajol A, *et al.* Insulin suppresses the production of fibroblast  
702 growth factor 23 (FGF23). *Proc Natl Acad Sci U S A* 2018; **115**: 5804-5809.  
703
- 704 13. Kuro OM, Moe OW. FGF23-alphaKlotho as a paradigm for a kidney-bone  
705 network. *Bone* 2017; **100**: 4-18.  
706
- 707 14. Mendoza JM, Isakova T, Ricardo AC, *et al.* Fibroblast Growth Factor 23 and  
708 Inflammation in CKD. *Clin J Am Soc Nephrol* 2012; **7**: 1155-1162.  
709
- 710 15. Wallquist C, Mansouri L, Norrback M, *et al.* Associations of Fibroblast Growth  
711 Factor 23 with Markers of Inflammation and Leukocyte Transmigration in Chronic  
712 Kidney Disease. *Nephron* 2018; **138**: 287-295.  
713

## TNF stimulates FGF23

- 1  
2  
3  
4 714 16. Hanks LJ, Casazza K, Judd SE, *et al.* Associations of fibroblast growth factor-23  
5 715 with markers of inflammation, insulin resistance and obesity in adults. *PLoS One*  
6 716 2015; **10**: e0122885.  
7 717
- 8 718 17. El-Hodhod MA, Hamdy AM, Abbas AA, *et al.* Fibroblast growth factor 23  
9 719 contributes to diminished bone mineral density in childhood inflammatory bowel  
10 720 disease. *BMC Gastroenterol* 2012; **12**: 44.  
11 721
- 12 722 18. Iliopoulos D, Malizos KN, Oikonomou P, *et al.* Integrative microRNA and  
13 723 proteomic approaches identify novel osteoarthritis genes and their collaborative  
14 724 metabolic and inflammatory networks. *PLoS One* 2008; **3**: e3740.  
15 725
- 16 726 19. Dai B, David V, Martin A, *et al.* A comparative transcriptome analysis identifying  
17 727 FGF23 regulated genes in the kidney of a mouse CKD model. *PLoS One* 2012;  
18 728 **7**: e44161.  
19 729
- 20 730 20. Farrow EG, Davis SI, Summers LJ, *et al.* Initial FGF23-mediated signaling occurs  
21 731 in the distal convoluted tubule. *J Am Soc Nephrol* 2009; **20**: 955-960.  
22 732
- 23 733 21. Clinkenbeard EL, Farrow EG, Summers LJ, *et al.* Neonatal iron deficiency causes  
24 734 abnormal phosphate metabolism by elevating FGF23 in normal and ADHR mice.  
25 735 *J Bone Miner Res* 2014; **29**: 361-369.  
26 736
- 27 737 22. Ito N, Wijenayaka AR, Prideaux M, *et al.* Regulation of FGF23 expression in IDG-  
28 738 SW3 osteocytes and human bone by pro-inflammatory stimuli. *Mol Cell*  
29 739 *Endocrinol* 2015; **399**: 208-218.  
30 740
- 31 741 23. Masuda Y, Ohta H, Morita Y, *et al.* Expression of Fgf23 in activated dendritic cells  
32 742 and macrophages in response to immunological stimuli in mice. *Biol Pharm Bull*  
33 743 2015; **38**: 687-693.  
34 744
- 35 745 24. David V, Martin A, Isakova T, *et al.* Inflammation and functional iron deficiency  
36 746 regulate fibroblast growth factor 23 production. *Kidney Int* 2016; **89**: 135-146.  
37 747
- 38 748 25. Feger M, Hase P, Zhang B, *et al.* The production of fibroblast growth factor 23 is  
39 749 controlled by TGF-beta2. *Sci Rep* 2017; **7**: 4982.  
40 750
- 41 751 26. Glosse P, Fajol A, Hirche F, *et al.* A high-fat diet stimulates fibroblast growth factor  
42 752 23 formation in mice through TNFalpha upregulation. *Nutr Diabetes* 2018; **8**: 36.  
43 753
- 44 754 27. Onal M, Carlson AH, Thostenson JD, *et al.* A Novel Distal Enhancer Mediates  
45 755 Inflammation-, PTH-, and Early Onset Murine Kidney Disease-Induced  
46 756 Expression of the Mouse Fgf23 Gene. *JBMR Plus* 2018; **2**: 32-47.  
47 757
- 48 758 28. Durlacher-Betzer K, Hassan A, Levi R, *et al.* Interleukin-6 contributes to the  
49 759 increase in fibroblast growth factor 23 expression in acute and chronic kidney  
50 760 disease. *Kidney Int* 2018; **94**: 315-325  
51 761
- 52 762 29. Alwan H, Pruijm M, Ponte B, *et al.* Epidemiology of masked and white-coat  
53 763 hypertension: the family-based SKIPOGH study. *PLoS One* 2014; **9**: e92522.  
54 764
- 55 765 30. Farrow EG, Yu X, Summers LJ, *et al.* Iron deficiency drives an autosomal  
56 766 dominant hypophosphatemic rickets (ADHR) phenotype in fibroblast growth  
57 767 factor-23 (Fgf23) knock-in mice. *Proc Natl Acad Sci U S A* 2011; **108**: E1146-  
58 768 1155.  
59 769  
60



- 1  
2  
3  
4 770 31. Amdur RL, Feldman HI, Gupta J, *et al.* Inflammation and Progression of CKD:  
5 771 The CRIC Study. *Clin J Am Soc Nephrol* 2016; **11**: 1546-56  
6 772
- 7 773 32. Feng YM, Thijs L, Zhang ZY, *et al.* Glomerular function in relation to circulating  
8 774 adhesion molecules and inflammation markers in a general population. *Nephrol*  
9 775 *Dial Transplant* 2018; **33**: 426-435.  
10 776
- 11 777 33. Piontek K, Menezes LF, Garcia-Gonzalez MA, *et al.* A critical developmental  
12 778 switch defines the kinetics of kidney cyst formation after loss of Pkd1. *Nat Med*  
13 779 2007; **13**: 1490-1495.  
14 780
- 15 781 34. Mace ML, Gravesen E, Nordholm A, *et al.* Kidney fibroblast growth factor 23 does  
16 782 not contribute to elevation of its circulating levels in uremia. *Kidney Int* 2017; **92**:  
17 783 165-178  
18 784
- 19 785 35. Smith ER, Holt SG, Hewitson TD. FGF23 activates injury-primed renal fibroblasts  
20 786 via FGFR4-dependent signalling and enhancement of TGF-beta autoinduction.  
21 787 *Int J Biochem Cell Biol* 2017; **92**: 63-78.  
22 788
- 23 789 36. Smith ER, Tan SJ, Holt SG, *et al.* FGF23 is synthesised locally by renal tubules  
24 790 and activates injury-primed fibroblasts. *Sci Rep* 2017; **7**: 3345.  
25 791
- 26 792 37. Meir T, Durlacher K, Pan Z, *et al.* Parathyroid hormone activates the orphan  
27 793 nuclear receptor Nurr1 to induce FGF23 transcription. *Kidney Int* 2014; **86**: 1106-  
28 794 1115.  
29 795
- 30 796 38. McEvoy AN, Murphy EA, Ponnio T, *et al.* Activation of nuclear orphan receptor  
31 797 NURR1 transcription by NF-kappa B and cyclic adenosine 5'-monophosphate  
32 798 response element-binding protein in rheumatoid arthritis synovial tissue. *J*  
33 799 *Immunol* 2002; **168**: 2979-2987.  
34 800
- 35 801 39. Bakker AD, Klein-Nulend J. Osteoblast isolation from murine calvaria and long  
36 802 bones. *Methods Mol Biol* 2012; **816**: 19-29.  
37 803
- 38 804 40. Stern AR, Stern MM, Van Dyke ME, *et al.* Isolation and culture of primary  
39 805 osteocytes from the long bones of skeletally mature and aged mice.  
40 806 *Biotechniques* 2012; **52**: 361-373.  
41 807
- 42 808 41. Feng JQ, Ward LM, Liu S, *et al.* Loss of DMP1 causes rickets and osteomalacia  
43 809 and identifies a role for osteocytes in mineral metabolism. *Nat Genet* 2006; **38**:  
44 810 1310-1315.  
45 811
- 46 812 42. Topaz O, Shurman, D L, Bergman, R, Indelman, M, Ratajczak, P, Mizrachi, M,  
47 813 Khamaysi, Z, Behar, D, Petronius, D, Friedman, V, Zelikovic, I, Raimer, S,  
48 814 Metzker, A, Richard, G, Sprecher, E. Mutations in *GALNT3*, encoding a protein  
49 815 involved in O-linked glycosylation, cause familial tumoral calcinosis. *Nat Genet*  
50 816 2004; **36**: 579-581.  
51 817
- 52 818 43. Kato K, Jeanneau, C, Tarp, M A, Benet-Pages, A, Lorenz-Depiereux, B, Bennett,  
53 819 E P, Mandel, U, Strom, T M, Clausen H. Polypeptide GalNAc-transferase T3 and  
54 820 familial tumoral calcinosis: secretion of FGF23 requires O-glycosylation. *J Biol*  
55 821 *Chem* 2006; **281**: 18370-18377.  
56 822
- 57 823 44. Fine LG, Bandyopadhyay D, Norman JT. Is there a common mechanism for the  
58 824 progression of different types of renal diseases other than proteinuria? Towards  
59 825 the unifying theme of chronic hypoxia. *Kidney Int Suppl* 2000; **75**: S22-26.

- 1  
2  
3  
4 826  
5 827 45. Eckardt KU, Bernhardt WM, Weidemann A, *et al.* Role of hypoxia in the  
6 828 pathogenesis of renal disease. *Kidney Int Suppl* 2005; S46-51.  
7 829  
8 830 46. Frew IJ, Thoma CR, Georgiev S, *et al.* pVHL and PTEN tumour suppressor  
9 831 proteins cooperatively suppress kidney cyst formation. *EMBO J* 2008; **27**: 1747-  
10 832 1757.  
11 833  
12 834 47. Maxwell PH, Wiesener MS, Chang GW, *et al.* The tumour suppressor protein VHL  
13 835 targets hypoxia-inducible factors for oxygen-dependent proteolysis. *Nature* 1999;  
14 836 **399**: 271-275.  
15 837  
16 838 48. Schonenberger D, Harlander S, Rajski M, *et al.* Formation of Renal Cysts and  
17 839 Tumors in Vhl/Trp53-Deficient Mice Requires HIF1alpha and HIF2alpha. *Cancer*  
18 840 *Res* 2016; **76**: 2025-2036.  
19 841  
20 842 49. Mulay SR, Eberhard JN, Pfann V, *et al.* Oxalate-induced chronic kidney disease  
21 843 with its uremic and cardiovascular complications in C57BL/6 mice. *Am J Physiol*  
22 844 *Renal Physiol* 2016; **310**: F785-F795  
23 845  
24 846 50. Kullberg MC, Rothfuchs AG, Jankovic D, *et al.* Helicobacter hepaticus-induced  
25 847 colitis in interleukin-10-deficient mice: cytokine requirements for the induction and  
26 848 maintenance of intestinal inflammation. *Infect Immun* 2001; **69**: 4232-4241.  
27 849  
28 850 51. Dhayat NA, Ackermann D, Pruijm M, *et al.* Fibroblast growth factor 23 and  
29 851 markers of mineral metabolism in individuals with preserved renal function.  
30 852 *Kidney Int* 2016; **90**: 648-657.  
31 853  
32 854 52. Zeier M, Fehrenbach P, Geberth S, *et al.* Renal histology in polycystic kidney  
33 855 disease with incipient and advanced renal failure. *Kidney Int* 1992; **42**: 1259-  
34 856 1265.  
35 857  
36 858 53. Li X, Magenheimer BS, Xia S, *et al.* A tumor necrosis factor-alpha-mediated  
37 859 pathway promoting autosomal dominant polycystic kidney disease. *Nat Med*  
38 860 2008; **14**: 863-868.  
39 861  
40 862 54. Mulay SR, Anders HJ. Crystallopathies. *N Engl J Med* 2016; **374**: 2465-2476.  
41 863  
42 864 55. Spichtig D, Zhang H, Mohebbi N, *et al.* Renal expression of FGF23 and peripheral  
43 865 resistance to elevated FGF23 in rodent models of polycystic kidney disease.  
44 866 *Kidney Int* 2014 ; **85**: 1340-50  
45 867  
46 868 56. Zanchi C, Locatelli M, Benigni A, *et al.* Renal Expression of FGF23 in Progressive  
47 869 Renal Disease of Diabetes and the Effect of Ace Inhibitor. *PLoS One* 2013; **8**:  
48 870 e70775.  
49 871  
50 872 57. Zhang X, Guo K, Xia F, *et al.* FGF23(C-tail) improves diabetic nephropathy by  
51 873 attenuating renal fibrosis and inflammation. *BMC Biotechnol* 2018; **18**: 33.  
52 874  
53 875 58. Stubbs JR, He N, Idiculla A, *et al.* Longitudinal evaluation of FGF23 changes and  
54 876 mineral metabolism abnormalities in a mouse model of chronic kidney disease. *J*  
55 877 *Bone Miner Res* 2012; **27**: 38-46.  
56 878  
57 879 59. Fernandez M, Triplitt C, Wajcberg E, *et al.* Addition of pioglitazone and ramipril to  
58 880 intensive insulin therapy in type 2 diabetic patients improves vascular dysfunction  
59 881 by different mechanisms. *Diabetes Care* 2008; **31**: 121-127.

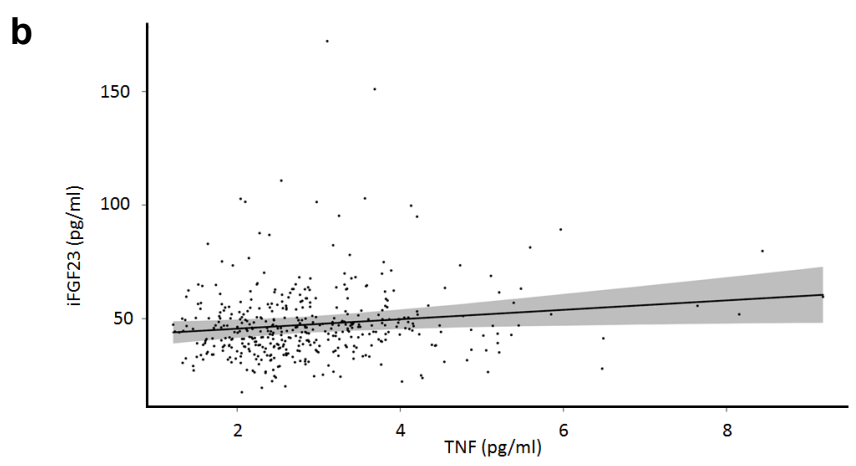
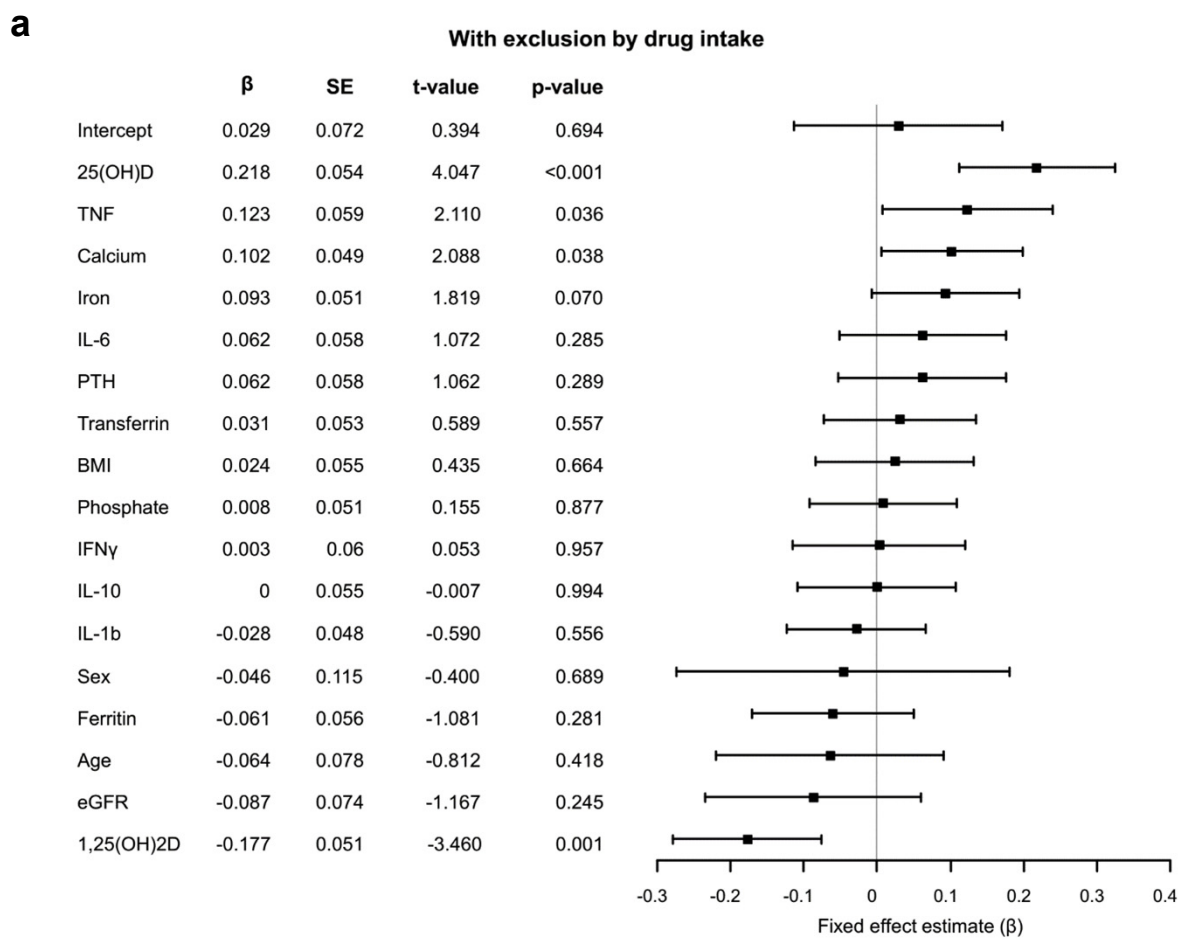
1  
2  
3  
4  
5  
6  
7  
8  
9  
10  
11  
12  
13  
14  
15  
16  
17  
18  
19  
20  
21  
22  
23  
24  
25  
26  
27  
28  
29  
30  
31  
32  
33  
34  
35  
36  
37  
38  
39  
40  
41  
42  
43  
44  
45  
46  
47  
48  
49  
50  
51  
52  
53  
54  
55  
56  
57  
58  
59  
60

- 882  
883 60. Liu N, Nguyen L, Chun RF, *et al.* Altered endocrine and autocrine metabolism of  
884 vitamin D in a mouse model of gastrointestinal inflammation. *Endocrinology* 2008;  
885 **149**: 4799-4808.  
886  
887 61. Chen H, Xu H, Dong J, *et al.* Tumor necrosis factor-alpha impairs intestinal  
888 phosphate absorption in colitis. *Am J Physiol Gastrointest Liver Physiol* 2009;  
889 **296**: G775-781.  
890  
891 62. Augustine MV, Leonard MB, Thayu M, *et al.* Changes in vitamin D-related mineral  
892 metabolism after induction with anti-tumor necrosis factor-alpha therapy in  
893 Crohn's disease. *J Clin Endocrinol Metab* 2014; **99**: E991-998.  
894  
895 63. Agrawal M, Arora S, Li J, *et al.* Bone, inflammation, and inflammatory bowel  
896 disease. *Curr Osteoporos Rep* 2011; **9**: 251-257.  
897  
898 64. Martin A, David V, Li H, *et al.* Overexpression of the DMP1 C-terminal fragment  
899 stimulates FGF23 and exacerbates the hypophosphatemic rickets phenotype in  
900 Hyp mice. *Mol Endocrinol* 2012; **26**: 1883-1895.  
901  
902 65. Bellido T, Jilka RL, Boyce BF, *et al.* Regulation of interleukin-6,  
903 osteoclastogenesis, and bone mass by androgens. The role of the androgen  
904 receptor. *J Clin Invest* 1995; **95**: 2886-2895.  
905  
906 66. Wang C, Tian L, Zhang K, *et al.* Interleukin-6 gene knockout antagonizes high-  
907 fat-induced trabecular bone loss. *J Mol Endocrinol* 2016; **57**: 161-170.  
908  
909 67. Hellwig-Burgel T, Rutkowski K, Metzen E, *et al.* Interleukin-1beta and tumor  
910 necrosis factor-alpha stimulate DNA binding of hypoxia-inducible factor-1. *Blood*  
911 1999; **94**: 1561-1567.  
912  
913 68. Clinkenbeard EL, Hanudel MR, Stayrook KR, *et al.* Erythropoietin stimulates  
914 murine and human fibroblast growth factor-23, revealing novel roles for bone and  
915 bone marrow. *Haematologica* 2017; **102**: e427-e430.  
916  
917 69. Flamme I, Ellinghaus P, Urrego D, *et al.* FGF23 expression in rodents is directly  
918 induced via erythropoietin after inhibition of hypoxia inducible factor proline  
919 hydroxylase. *PLoS One* 2017; **12**: e0186979.  
920  
921 70. Pruijm M, Ponte B, Ackermann D, *et al.* Heritability, determinants and reference  
922 values of renal length: a family-based population study. *Eur Radiol* 2013; **23**:  
923 2899-2905.  
924  
925 71. Ponte B, Pruijm M, Ackermann D, *et al.* Reference values and factors associated  
926 with renal resistive index in a family-based population study. *Hypertension* 2014;  
927 **63**: 136-142.  
928  
929 72. Piontek KB, Huso DL, Grinberg A, *et al.* A functional floxed allele of Pkd1 that can  
930 be conditionally inactivated in vivo. *J Am Soc Nephrol* 2004; **15**: 3035-3043.  
931  
932 73. Grinberg-Bleyer Y, Saadoun D, Baeyens A, *et al.* Pathogenic T cells have a  
933 paradoxical protective effect in murine autoimmune diabetes by boosting Tregs.  
934 *J Clin Invest* 2010; **120**: 4558-4568.  
935

TNF stimulates FGF23

- 1  
2  
3  
4 936 74. Carlson MJ, West ML, Coghill JM, *et al.* In vitro-differentiated TH17 cells mediate  
5 937 lethal acute graft-versus-host disease with severe cutaneous and pulmonary  
6 938 pathologic manifestations. *Blood* 2009; **113**: 1365-1374.  
7 939  
8 940 75. Brodehl J, Krause A, Hoyer PF. Assessment of maximal tubular phosphate  
9 941 reabsorption: comparison of direct measurement with the nomogram of Bijvoet.  
10 942 *Pediatr Nephrol* 1988; **2**: 183-189.  
11 943  
12 944 76. Biber J, Stieger B, Stange G, *et al.* Isolation of renal proximal tubular brush-border  
13 945 membranes. *Nat Protoc* 2007; **2**: 1356-1359.  
14 946  
15 947 77. Custer M, Lötscher, M, Biber, J, Murer, H, Kaissling, B. Expression of Na-P<sub>i</sub>  
16 948 cotransport in rat kidney: localization by RT-PCR and immunohistochemistry. *Am*  
17 949 *J Physiol* 1994; **266**: F767-774.  
18 950  
19  
20  
21  
22  
23  
24  
25  
26  
27  
28  
29  
30  
31  
32  
33  
34  
35  
36  
37  
38  
39  
40  
41  
42  
43  
44  
45  
46  
47  
48  
49  
50  
51  
52  
53  
54  
55  
56  
57  
58  
59  
60

# Figure 1



1  
2  
3  
4  
5  
6  
7  
8  
9  
10  
11  
12  
13  
14  
15  
16  
17  
18  
19  
20  
21  
22  
23  
24  
25  
26  
27  
28  
29  
30  
31  
32  
33  
34  
35  
36  
37  
38  
39  
40  
41  
42  
43  
44  
45  
46  
47

Figure 2

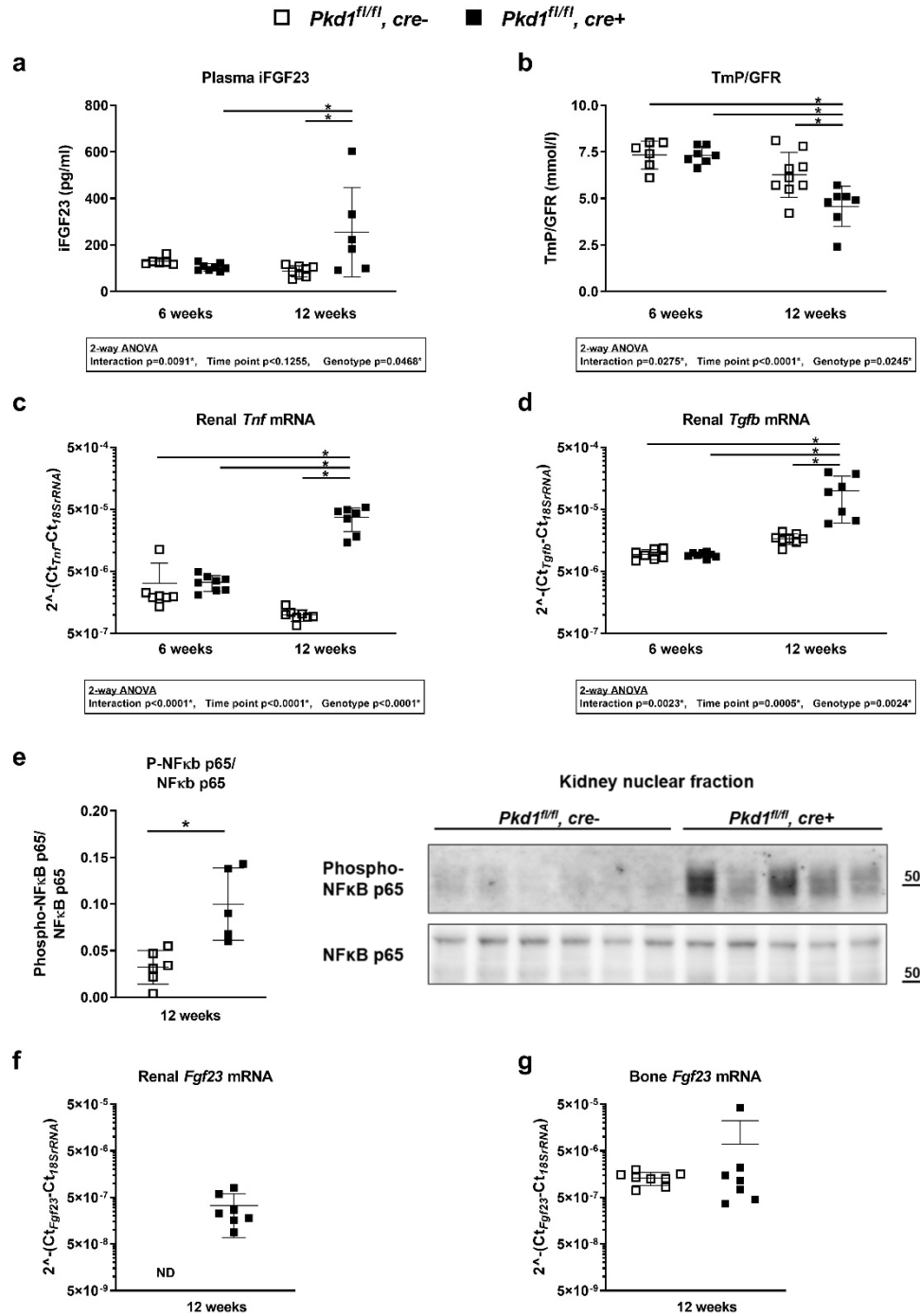


# Figure 3

□ *Pkd1<sup>fl/fl</sup>, cre-*    ■ *Pkd1<sup>fl/fl</sup>, cre+*

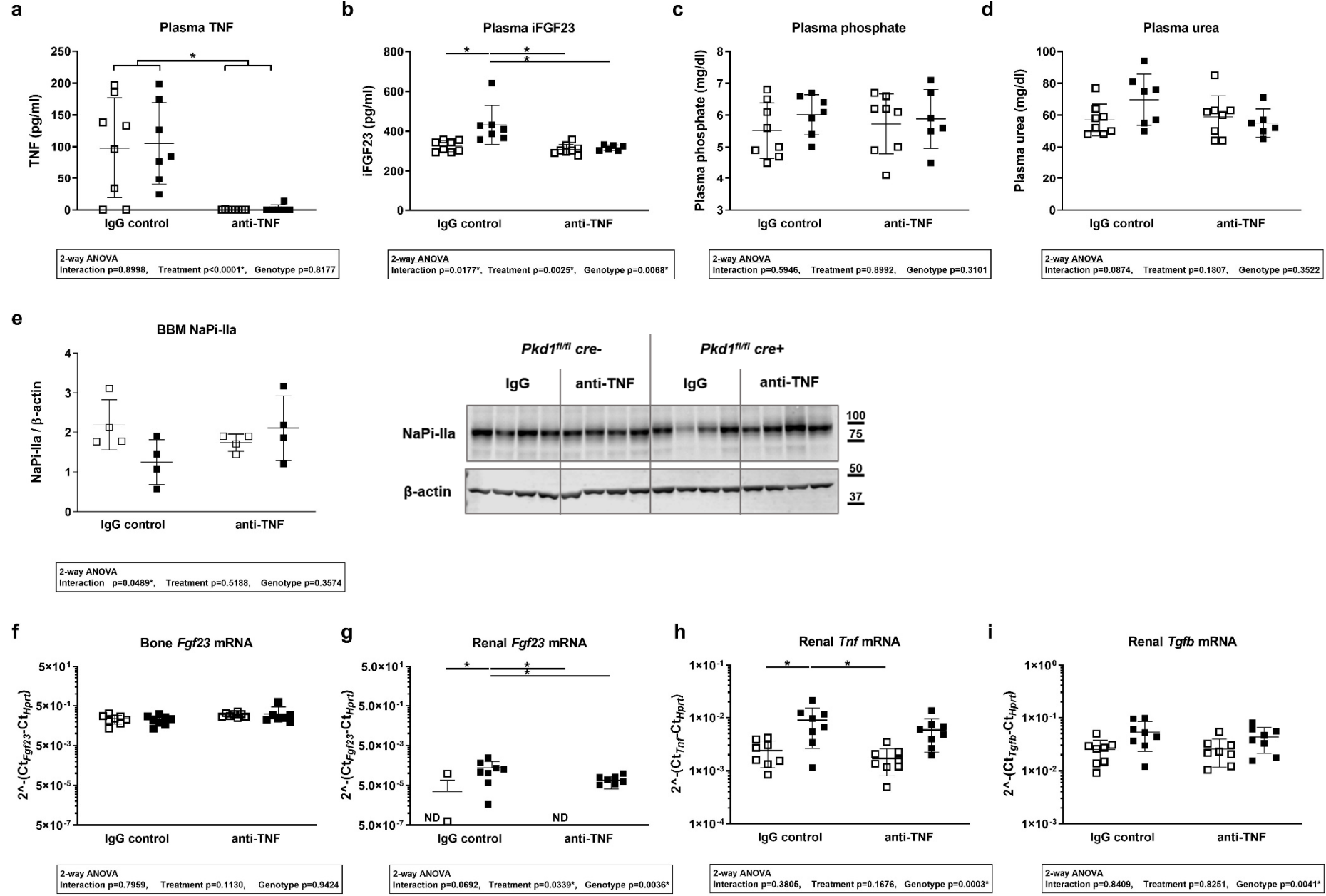
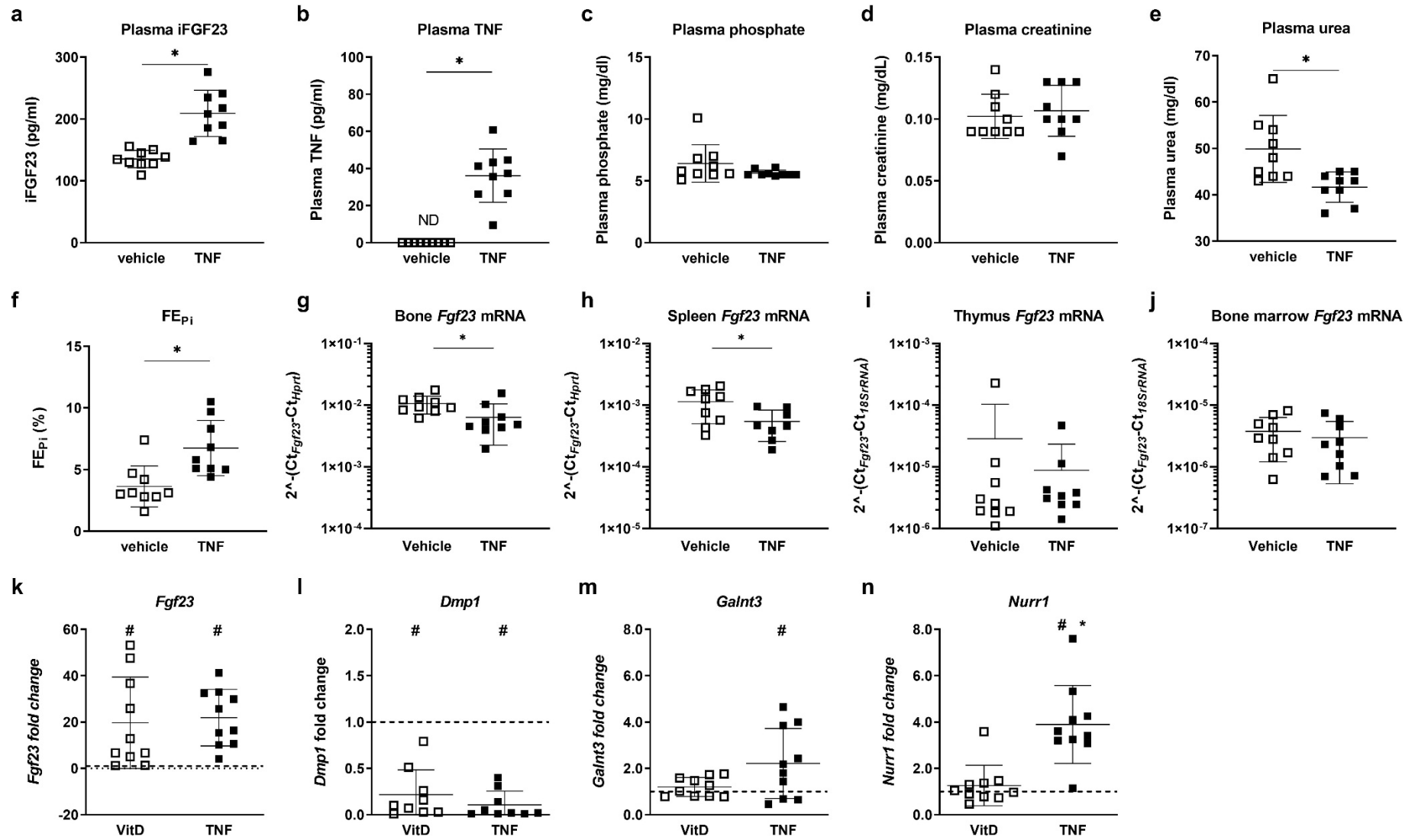
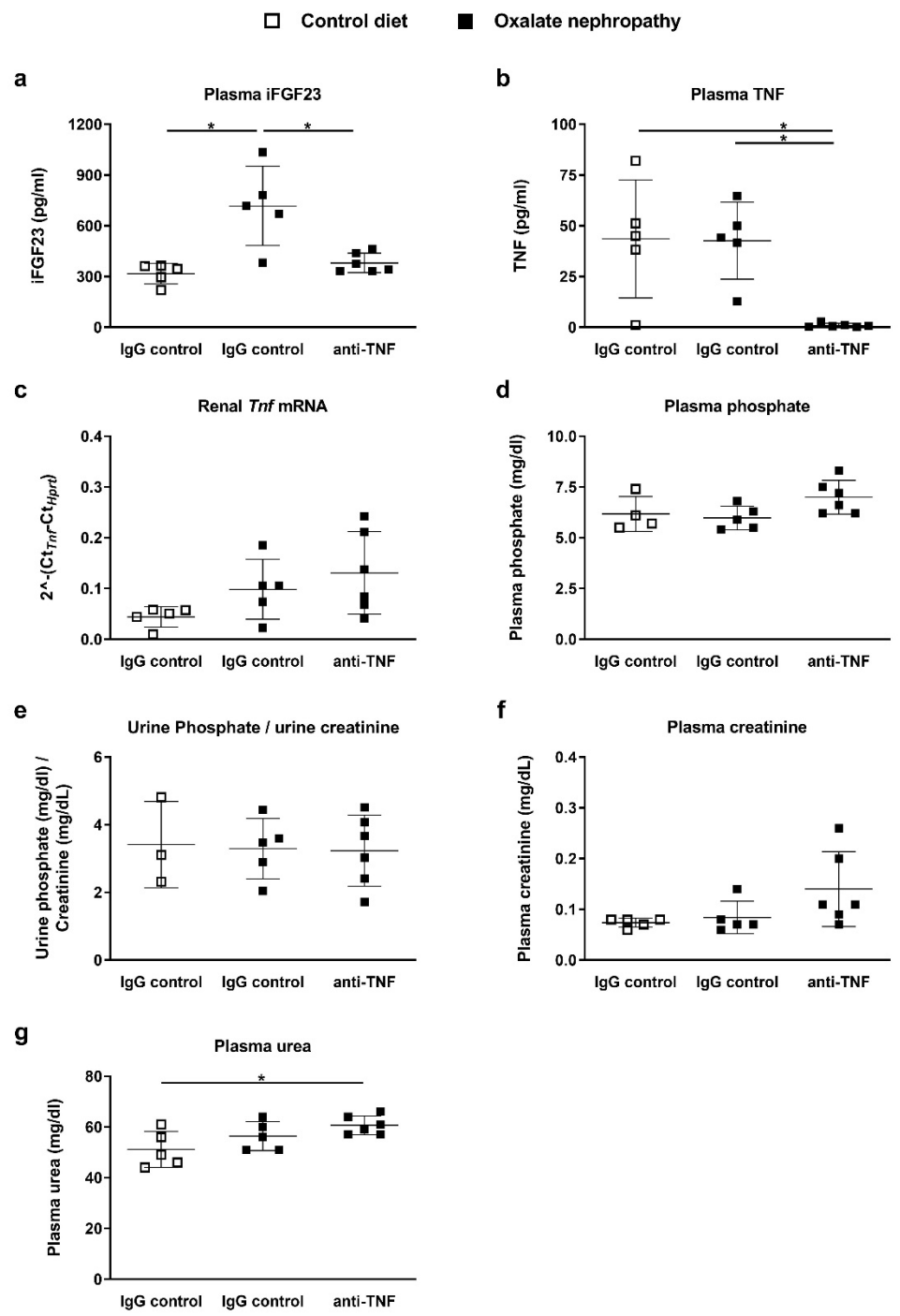


Figure 4

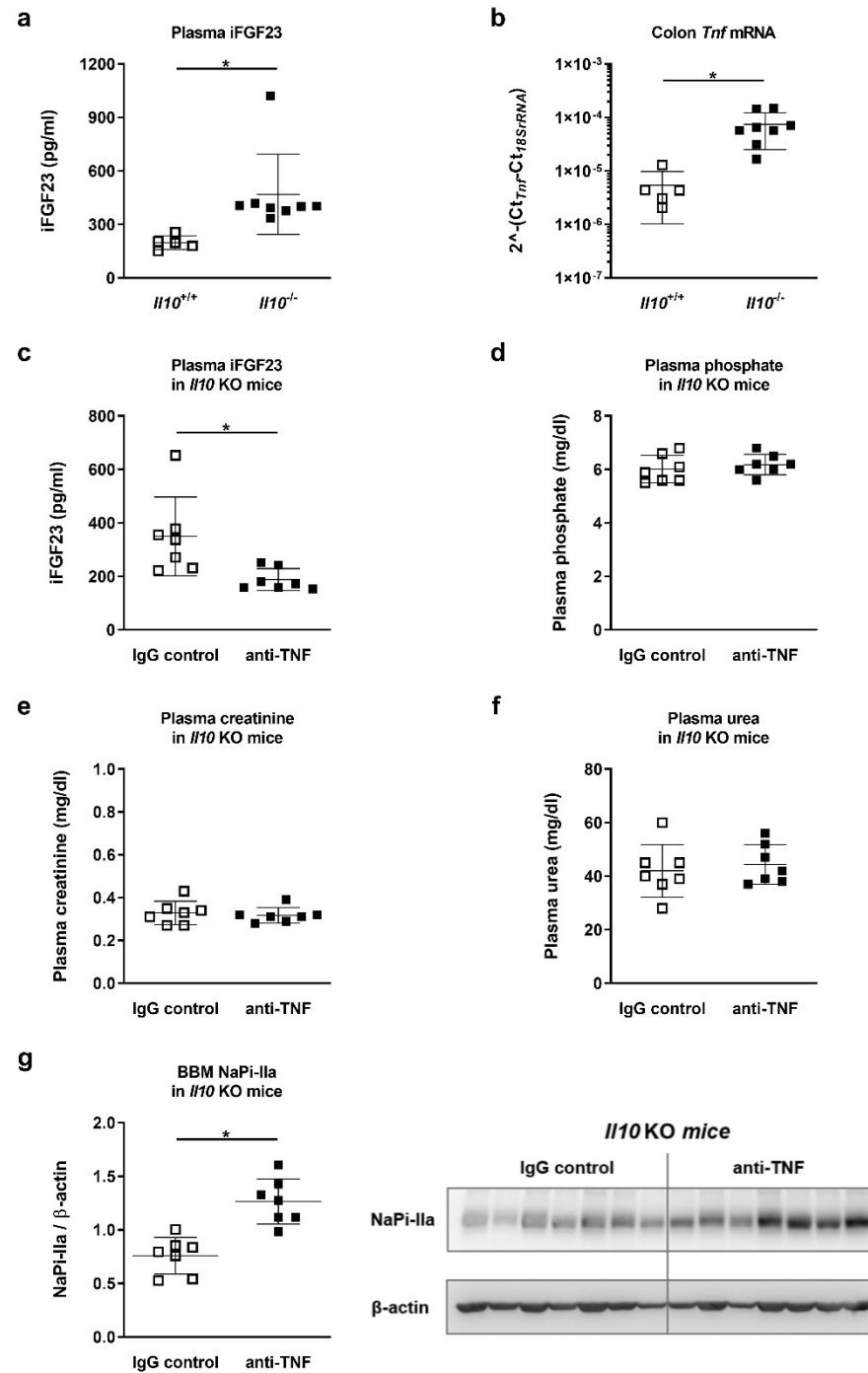




1 **Figure 5**



## Figure 6



## Supplementary Tables

**Supplementary Table 1** First quartile, median, mean and third quartile of continuous variables in the SKIPOGH population after full exclusion criteria applied (429 subjects).

Variable	1st Qu.	Median	Mean	3rd Qu.
Age (yr)	29.7	46.6	45.7	57.9
BMI (kg/m <sup>2</sup> )	21.8	24.3	24.6	26.7
eGFR (CKD-EPI) (mL/min/1.73 m <sup>2</sup> )	87.1	98.4	98.1	110.1
IFN $\gamma$ (pg/ml)	3.2	4.7	9.0	7.1
IL-10 (pg/ml)	0.2	0.3	0.5	0.4
IL-1 $\beta$ (pg/ml)	0.0	0.1	0.1	0.1
IL-6 (pg/ml)	0.4	0.6	0.9	0.8
TNF (pg/ml)	2.2	2.7	2.9	3.4
iFGF23 (pg/ml)	38.8	46.2	49.2	55.3
cFGF23 (Ru/ml)	63.7	79.4	97.3	103.4
Ratio iFGF23 (pg/ml) / cFGF23 (Ru/ml)	0.4	0.6	0.6	0.7
Iron ( $\mu$ mol/l)	13.9	17.3	18.7	22.5
Transferrin ( $\mu$ mol/l)	28.0	31.0	32.2	35.0
Ferritin ( $\mu$ g/l)	62.0	119.0	143.2	192.0
Phosphate (mmol/l)	0.9	1.0	1.0	1.1
Calcium (mmol/l)	2.2	2.3	2.3	2.3
PTH (pg/ml)	29.8	37.1	38.8	45.0
25(OH)D (nmol/l)	33.0	44.0	47.4	61.0
1,25(OH) <sub>2</sub> D (pmol/l)	67.0	88.0	92.3	116.0

**SupplementaryTable 2** First quartile, median, mean and third quartile of continuous variables in the SKIPOGH population without drug intake criteria applied (790 subjects).

Variable	1st Qu.	Median	Mean	3rd Qu.
Age (yr)	32.3	48.7	47.9	61.8
BMI (kg/m <sup>2</sup> )	21.8	24.3	24.9	27.3
eGFR (CKD-EPI) (mL/min/1.73 m <sup>2</sup> )	84.7	96.9	96.0	108.3
IFN $\gamma$ (pg/ml)	3.4	4.9	9.0	7.6
IL-10 (pg/ml)	0.2	0.3	0.5	0.4
IL-1 $\beta$ (pg/ml)	0.0	0.1	0.1	0.1
IL-6 (pg/ml)	0.4	0.6	0.9	0.9
TNF (pg/ml)	2.2	2.8	3.1	3.6
iFGF23 (pg/ml)	39.0	47.2	50.6	57.6
cFGF23 (Ru/ml)	64.7	81.4	103.2	107.9
Ratio iFGF23 (pg/ml) / cFGF23 (Ru/ml)	0.4	0.6	0.6	0.7
Iron ( $\mu$ mol/l)	13.6	17.3	18.3	22.0
Transferrin ( $\mu$ mol/l)	28.0	31.0	32.0	35.0
Ferritin ( $\mu$ g/l)	62.2	115.5	142.4	180.1
Phosphate (mmol/l)	0.9	1.0	1.0	1.2
Calcium (mmol/l)	2.2	2.3	2.3	2.3
PTH (pg/ml)	29.8	37.4	39.4	45.8
25(OH)D (nmol/l)	33.0	45.0	48.0	61.0
1,25(OH) <sub>2</sub> D (pmol/l)	68.0	88.0	92.8	115.0

**Supplementary Table 3** Exclusion criteria for SKIPOGH subjects

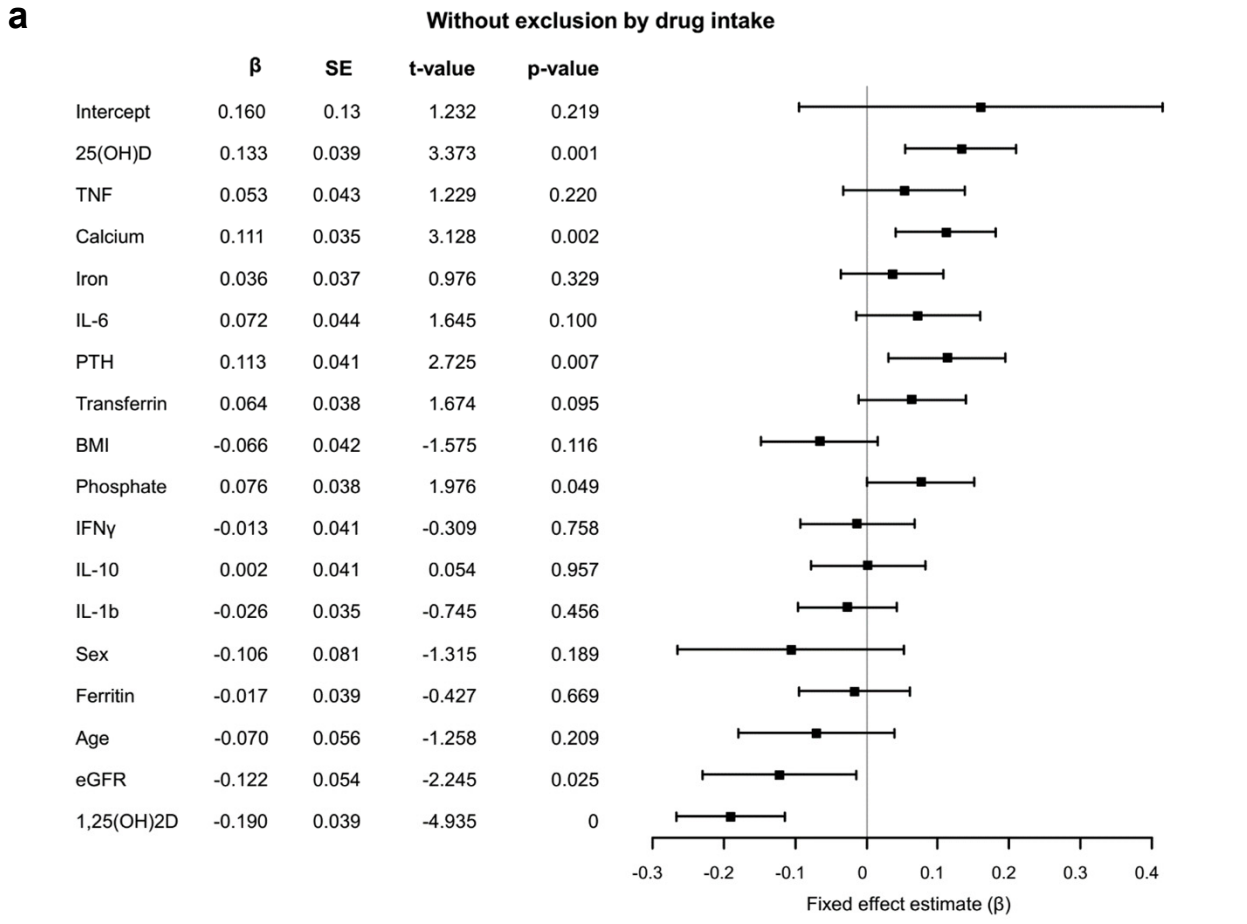
Exclusion criteria	N
Total SKIPOGH subjects	1131
Incomplete data	- 261
No TNF detected	- 40
Odd iFGF23/ cFGF23 ratio	- 40
Drugs	- 361
Total study subjects	429

**Supplementary Table 4** Drug types which led to exclusion of SKIPOGH subjects for data analysis. The table shows 491 drug intake entries (N) for 361 subjects. Each entry represents each time a drug appears in the data base of 429 subjects after all exclusion criteria applied.

Drug type	N
Interaction with Ca, Mg or Pi	41
Interaction with iron	6
Diuretic or diuretic action	54
Interaction with inflammation	390

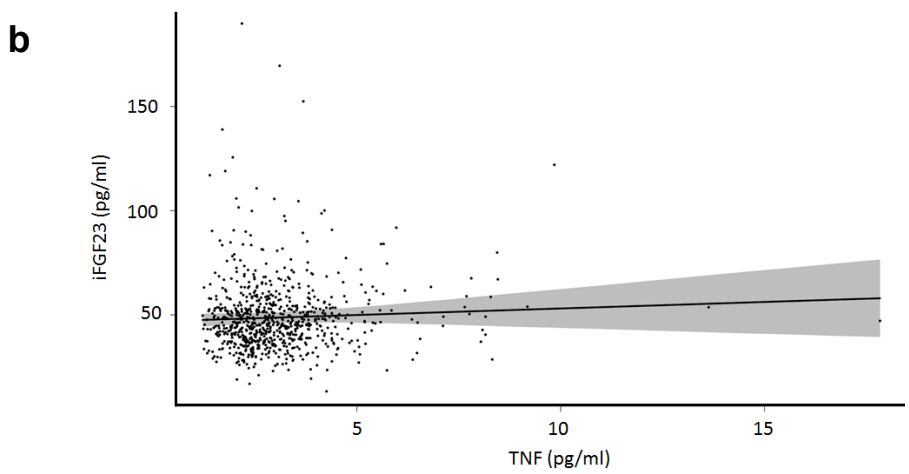
**Supplementary Table 5** Primer and probe sequences used for qPCR

Gene	Type	Sequence
Mouse <i>Pkd1</i>	Fwd	5'-GGCCAACCTCTCCTCAGTATC-3'
	Rev	5'-GAAGGGTACTGCTGCCACA-3'
	Probe	5'-CTGTGGTGAGGAATATGTCGCCTGC-3'
Mouse <i>Fgf23</i>	Fwd	5'-TCGAAGGTTCCCTTTGTATGGAT-3'
	Rev	5'-AGTGATGCTTCTGCGACAAGT-3'
	Probe	5'-TTTTTGGATCGCTTCACT-3'
Mouse <i>Fgf23</i>	Fwd	5'-GTATGGATCTCCACGGCAAC-3'
	Rev	5' AGTGATGCTTCTGCGACAAGT-3'
	Probe	5'-TTTTTGGATCGCTTCACTTCAAGCCC-3'
Mouse <i>Fgf23</i>	Fwd	5'-GACCAGCTATCACCTACAGATCCA-3'
	Rev	5' CGGCGTCCTCTGATGTAATCA-3'
Mouse <i>Galnt3</i>	Fwd	5'-GAGAAAGAGCGAGGGGAAAC-3'
	Rev	5'-GTGGACCATGCTTCATTGTG-3'
	Probe	5'-ACACCCGACCACCTGAATGTATTGAAC-3'
Mouse <i>Dmp1</i>	Fwd	5'-TCTCCCAGTTGCCAGATACC-3'
	Rev	5'-TCTCCAGATTCAGTCTGTCC-3'
	Probe	5'-CTCTGAAGAGAGGACGGGTGATTTGG-3'
Mouse <i>Runx2</i>	Fwd	5'-CCCTGAACTCTGCACCAAGT-3'
	Rev	5'-AGTGGATGGATGGGGATGT-3'
	Probe	5'-TCAGATTACAGATCCCAGGCAGGCA-3'
Mouse <i>Nurr1</i>	Fwd	5'-CATCGACATTTCTGCCTTCTC-3'
	Rev	5'-CTTCCACTCTTTGGGTTCTC-3'
	Probe	5'-TGCCCTGGCTATGGTCACAGAGAGA-3'
Mouse <i>Tnf</i>	Fwd	5'-CAGACCCTCACACTCAGATCATCT-3'
	Rev	5'-CCTCCACTTGGTGGTTTGCT-3'
	Probe	5'-ATTTCAGTGACAAGCCTGTAGCCCACGT-3'
Mouse <i>Tgfb</i>	Fwd	5'-AGAGGTCACCCGCGTGCTA-3'
	Rev	5'-GCTTCCCGAATGTCTGACGTA-3'
	Probe	5'-ACCGCAACAACGCCATCTATGAGAAAACC-3'
Mouse <i>Car9</i>	Fwd	5'-GCACCTCAGTACTGCTTTCTCC-3'
	Rev	5'-TTCCTCCGAGATTTCTTCCA-3'
	Probe	5'-CCTTTCTGCAGGAGAGCCCAGAAGA-3'
Mouse <i>Phd2</i>	Fwd	5'-TGGGCAACTACAGGATAAACG-3'
	Rev	5'-TGTCACGCATCTTCCATCTC-3'
	Probe	5'-CGAAAGCCATGGTTGCTTGTACCC-3'



**Figure S1**

**Identification of plasma iFGF23 predictors in a human cohort.** (a) Forest plot showing the fixed effects calculated for all predictors used in the mixed linear model for the subpopulation of 790 participants without drug intake criteria applied. Fixed effect estimates ( $\beta$ ), standard error, ratio between the estimates and their standard errors (t-value), and associated p-value from a t-distribution. (b) Association between plasma TNF and iFGF23 in the SKIPOGH cohort in a subpopulation of 790 participants after all the exclusion criteria applied. The regression line and confidence band were obtained from the linear mixed model containing all the predictors.



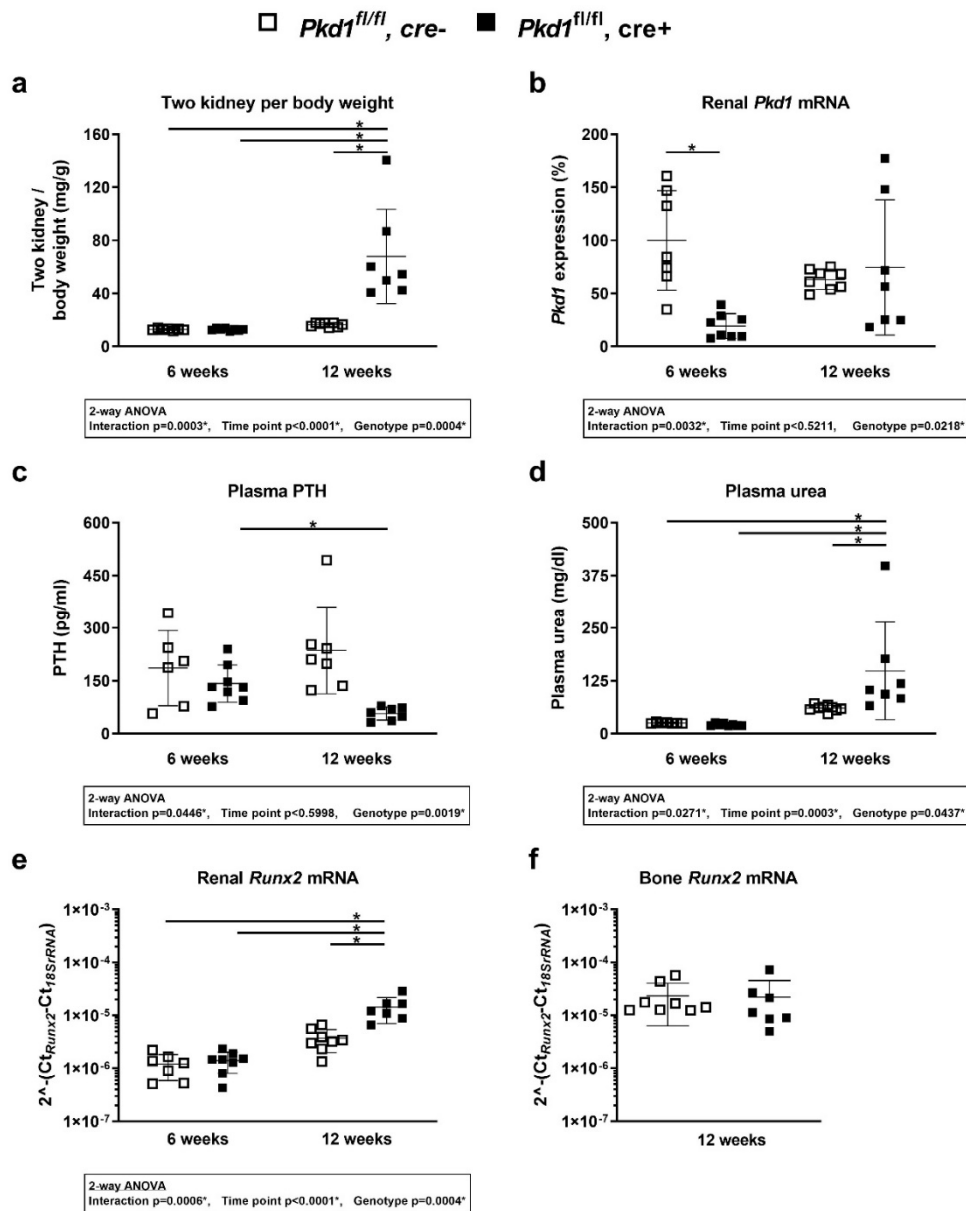
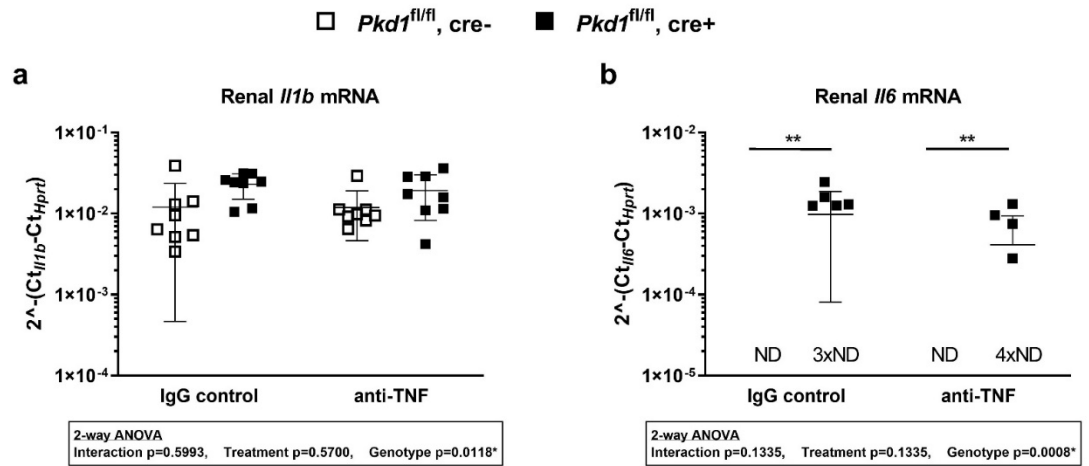


Figure S2

**Baseline characteristics of *Pkd1* KO mice.** Two-kidney per body weight ratio (a), *Pkd1* gene expression normalized to *Pkd1<sup>fl/fl</sup>, cre-* mice (6 weeks) (b), plasma iFGF23 (c), plasma PTH (d) and plasma urea (d) as well as *Runx-2* (e, f) mRNA expression relative to 18SrRNA in kidney and bone in *Pkd1<sup>fl/fl</sup>, cre-* (white squares) and *Pkd1<sup>fl/fl</sup>, cre+* (black squares) animals at the age of 6 and 12 weeks. Two-way ANOVA with Bonferroni correction (a-d, f) or unpaired t-test (e), \*  $p<0.05$ .





**Figure S3**

**Expression of inflammation markers in the kidney of *Pkd1* KO mice.** Renal *Il1b* (a), and renal *Il6* (b) mRNA expression relative to 18SrRNA in *Pkd1<sup>fl/fl</sup>, cre<sup>-</sup>* (white squares) and *Pkd1<sup>fl/fl</sup>, cre<sup>+</sup>* (black squares) animals at the age of 6 and 12 weeks. Two-way ANOVA with Bonferroni correction, \* p<0.05.

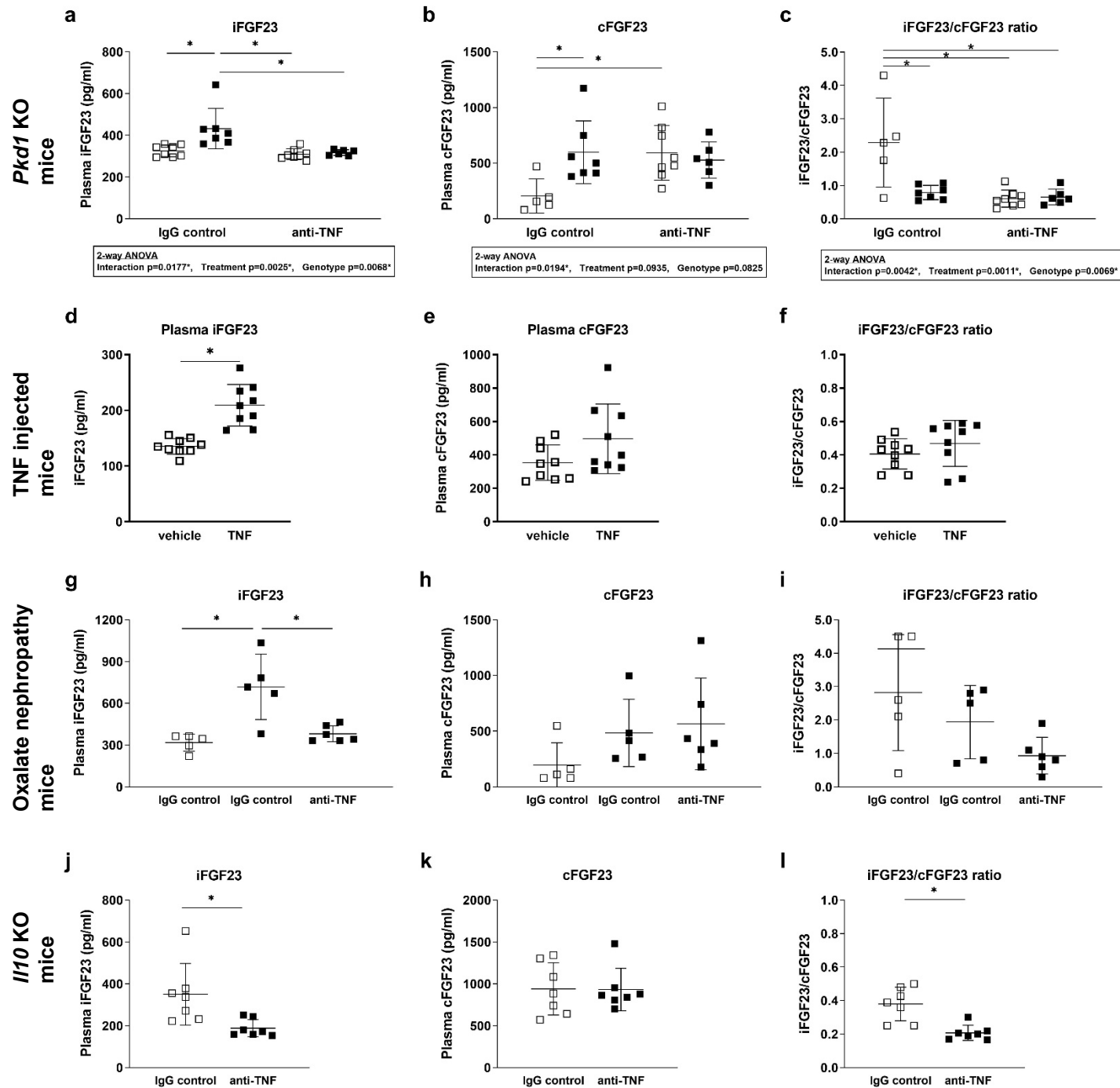
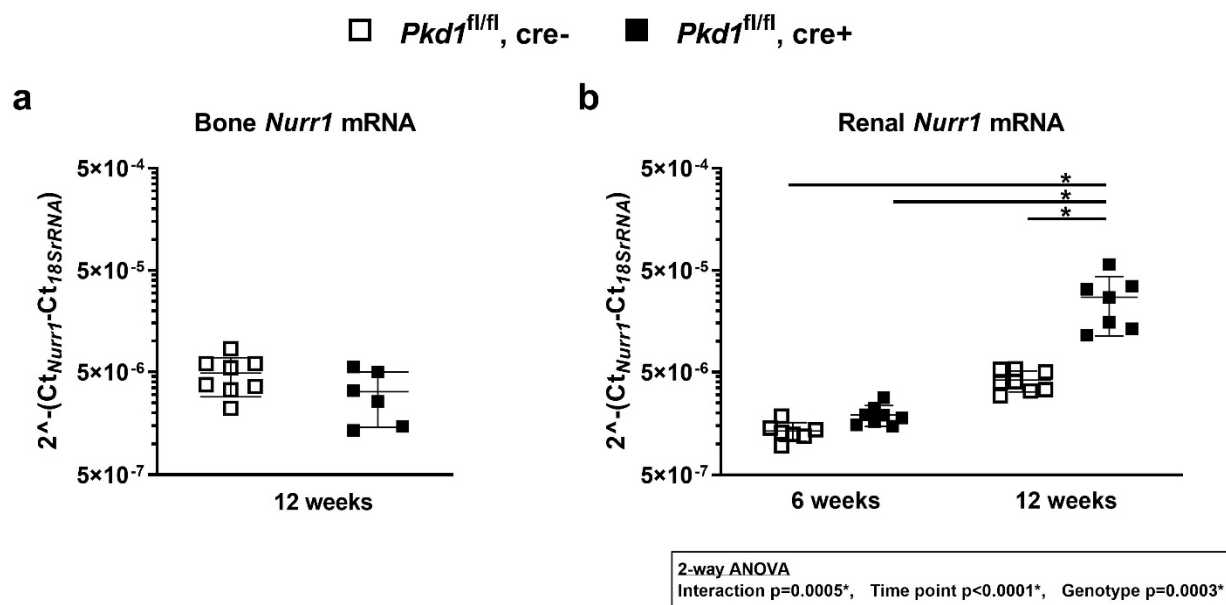


Figure S4

Comparison of plasma iFGF23, cFGF23 and iFGF23 to cFGF23 ratio. Plasma iFGF23 (a, d, g, j), plasma cFGF23 (b, e, h, k) and iFGF23/cFGF23 ratio (c, f, i, l) in *Pkd1* KO mice (*Pkd1*<sup>fl/fl</sup>, *cre*<sup>-</sup> (white squares) and *Pkd1*<sup>fl/fl</sup>, *cre*<sup>+</sup> (black squares)), TNF injected mice (2ug/day for two consecutive days), oxalate nephropathy mice (control diet (white squares) and oxalate nephropathy (black squares)). Two-way ANOVA with Bonferroni correction (a-c), One-way ANOVA with Bonferroni correction (g-i) or unpaired t-test (d-f, j-l), \* p<0.05.



**Figure S5**

**Bone and renal *Nurr1* mRNA expression in *Pkd1* KO mice.** *Nurr1* mRNA expression relative to 18SrRNA in kidney (a) and bone (b) in *Pkd1*<sup>fl/fl</sup>, cre- (white squares) and *Pkd1*<sup>fl/fl</sup>, cre+ (black squares) animals at the age of 6 and 12 weeks. Unpaired t-test (a), or Two-way ANOVA with Bonferroni correction (b), \* p<0.05.

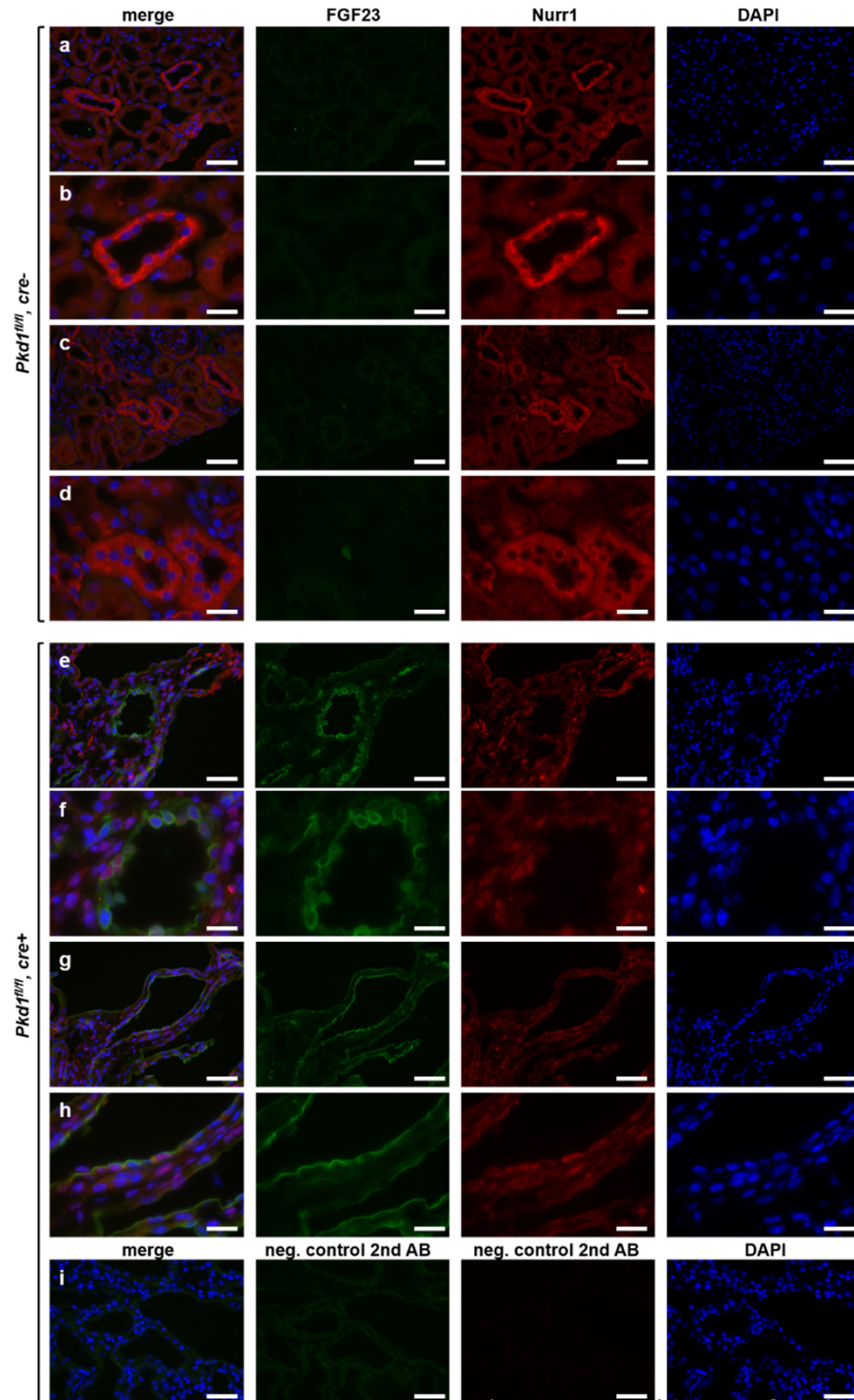


Figure S6

**Colocalization of Nurr1 and FGF23 in *Pkd1* kidneys.**

Immunofluorescence staining for FGF23 (green), Nurr1 (red), and DAPI (blue, cell nuclei) merge and single channels in kidneys of 12 weeks old *Pkd1<sup>fl/fl</sup>, cre-* (a-d), *Pkd1<sup>fl/fl</sup>, cre+* (e-h) and *Pkd1<sup>fl/fl</sup>, cre+* incubated with secondary antibodies alone (i). Original magnification (a, c, e, g) 400x (scale bar 50  $\mu$ m) and (b, d, f, h) 1000x (scale bar 20  $\mu$ m).

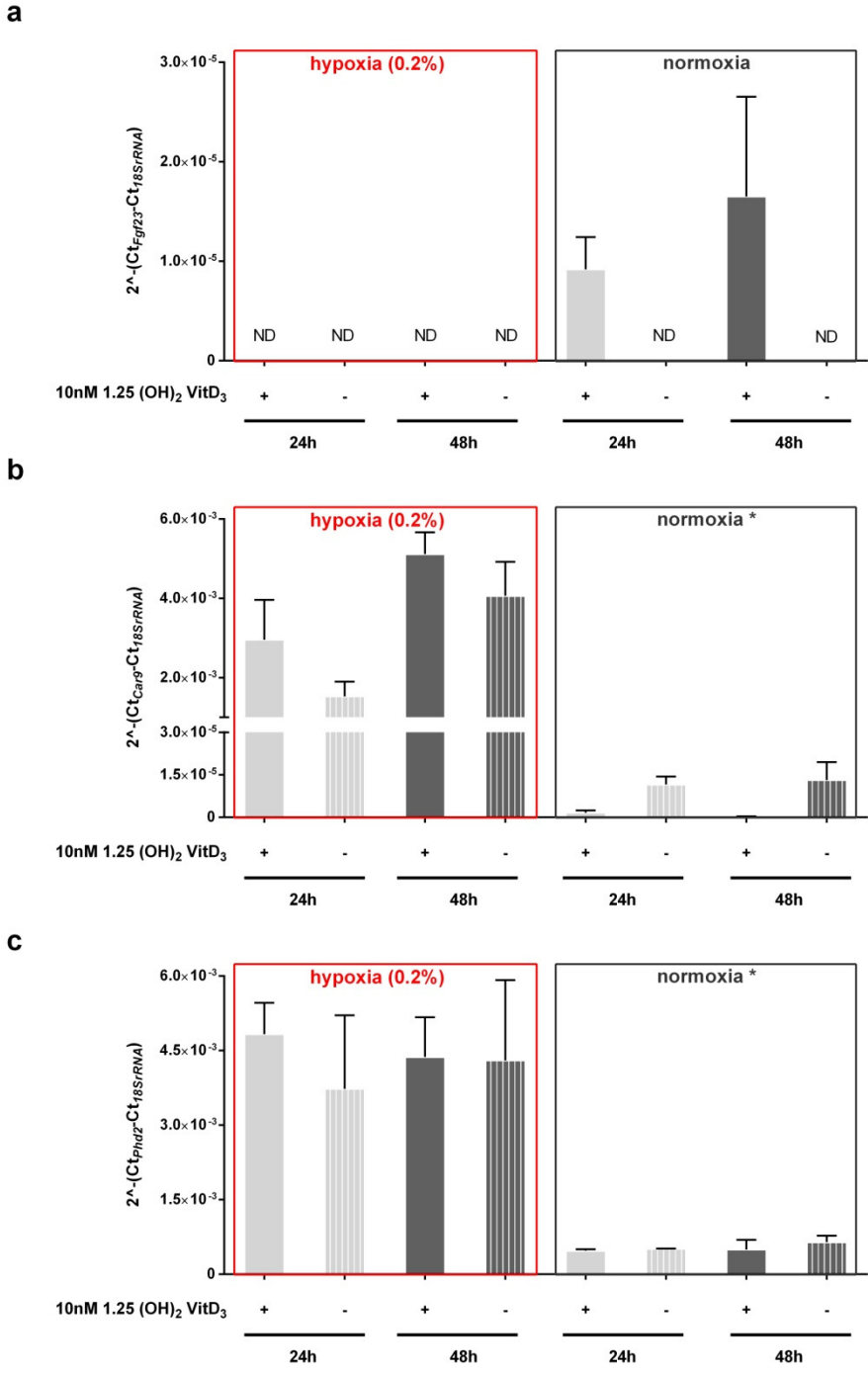


Figure S7

**1,25 (OH)<sub>2</sub> vitamin D<sub>3</sub> dependent *Fgf23* expression in MC3T3-E1 cells under hypoxic conditions.** MC3T3-E1 cells were differentiated for two weeks along the osteogenic lineage. Subsequently, cells were supplemented for 24 or 48 hours with 10nM 1,25 (OH)<sub>2</sub> vitamin D<sub>3</sub> and incubated under hypoxic (0.2% oxygen) or normoxic conditions. *Fgf23* (a), *Car9* (b), and *Phd2* (c) mRNA expression relative to 18SrRNA. Mean ±SD; 3 independent experiments; ANOVA with Bonferroni correction, \* p<0.05.

1 **Antibody mediated TNF stimulates neutralization decreases**  
 2 **FGF23 levels in animal models of chronic kidney disease and**  
 3 **non-renal inflammation**

4 Daniela Egli-Spichtig<sup>1,2#</sup>, Pedro Henrique Imenez Silva<sup>1#</sup>, Bob Glaudemans<sup>1</sup>, Nicole  
 5 Gehring<sup>1</sup>, Carla Bettoni<sup>1</sup>, Martin Zhang<sup>2</sup>, Eva Pastor Arroyo<sup>1</sup>, Désirée Schönenberger<sup>1</sup>,  
 6 Michal Rajski<sup>1</sup>, David Hoogewijis<sup>1</sup>, Felix Knauf<sup>3</sup>, Benjamin Misselwitz<sup>4</sup>, Isabelle Frey-  
 7 Wagner<sup>4</sup>, Gerhard Rogler<sup>4</sup>, Daniel Ackermann<sup>5</sup>, Belen Ponte<sup>6</sup>, Menno Pruijm<sup>7</sup>, Alexander  
 8 Leichtle<sup>8</sup>, Georg-Martin Fiedler<sup>8</sup>, Murielle Bochud<sup>9</sup>, [Virginia Ballotta<sup>10</sup>](#), [Sandra Hofmann<sup>10</sup>](#),  
 9 Farzana Perwad<sup>2</sup>, Michael Föller<sup>10</sup>, Florian Lang<sup>11</sup>, Roland H. Wenger<sup>1</sup>, Ian Frew<sup>1</sup>,  
 10 Carsten A. Wagner<sup>1\*</sup>

11  
 12 # contributed equally to the manuscript

13  
 14 <sup>1</sup>Institute of Physiology, University of Zurich, Zurich, Switzerland and National Center of  
 15 Competence in Research NCCR Kidney.CH, Switzerland

16 <sup>2</sup>Department of Pediatrics, Division of Nephrology, University of California San Francisco,  
 17 San Francisco, California, United States of America

18 <sup>3</sup>Division of Nephrology, Charité - Universitätsmedizin Berlin, Berlin, Germany

19 <sup>4</sup>University Hospital Zurich, Clinic for Gastroenterology and Hepatology, Zürich,  
 20 Switzerland

21 <sup>5</sup>Department of Nephrology and Hypertension, Inselspital, Bern University Hospital and  
 22 University of Bern, Switzerland

23 <sup>6</sup>Department of Nephrology, University Hospital of Geneva (HUG), Switzerland

24 <sup>7</sup>Department of Nephrology, Lausanne University Hospital (CHUV), Switzerland

25 <sup>8</sup>Institute of Clinical Chemistry, Inselspital, Bern University Hospital, University of Bern,  
 26 Switzerland.

27 <sup>9</sup>Institute of Social and Preventive Medicine (IUMSP), Lausanne University Hospital  
 28 (CHUV), Switzerland

29 ~~<sup>10</sup>Martin-Luther-Universität Halle-Wittenberg, Ernährungsphysiologie – Halle/S.–~~  
 30 ~~Germany~~

31 [<sup>10</sup>Department of Biomedical Engineering and Institute for Complex Molecular Systems,](#)  
 32 [Eindhoven University of Technology, P.O. Box 513, 5600 MB Eindhoven, The](#)  
 33 [Netherlands](#)

34 [<sup>11</sup>Institute of Physiology, University of Hohenheim, 70599 Stuttgart, Germany.](#)

1  
2  
3  
4  
5  
6  
7  
8  
9  
10  
11  
12  
13  
14  
15  
16  
17  
18  
19  
20  
21  
22  
23  
24  
25  
26  
27  
28  
29  
30  
31  
32  
33  
34  
35  
36  
37  
38  
39  
40  
41  
42  
43  
44  
45  
46  
47  
48  
49  
50  
51  
52  
53  
54  
55  
56  
57  
58  
59  
60

35 Martin-Luther-Universität Halle-Wittenberg, Ernährungsphysiologie – Halle/S.  
36 Germany<sup>14</sup>Institute  
37 <sup>12</sup>Institute of Physiology I, University of Tübingen, Germany  
38

For Peer Review Only

39 **\* Corresponding author**

40  
41 Carsten A. Wagner  
42 Institute of Physiology  
43 University of Zurich  
44 Winterthurerstrasse 190  
45 CH-8057 Zurich  
46 Switzerland  
47 Phone: +41-44-63 55023  
48 Fax: +41-44-63 56814  
49 Email: [Wagnerca@access.uzh.ch](mailto:Wagnerca@access.uzh.ch)

50

For Peer Review Only



## 51 Abstract

52 Fibroblast growth factor 23 (FGF23) regulates phosphate homeostasis and its early rise  
53 in patients with chronic kidney disease (CKD) is ~~directly linked to~~independently  
54 associated with all-cause mortality. Since inflammation is characteristic for CKD and has  
55 been associated with plasma FGF23 we examined whether inflammation directly  
56 stimulates FGF23. In a population-based cohort, plasma tumor necrosis factor (TNF) was  
57 the only inflammatory cytokine that independently and positively correlated with plasma  
58 FGF23. Mouse models of CKD showed signs of renal inflammation, renal FGF23  
59 expression and elevated systemic FGF23. Renal FGF23 expression coincided with  
60 expression of the orphan nuclear receptor Nurr1 regulating FGF23 in other organs.  
61 Antibody-mediated neutralization of TNF normalized plasma FGF23 and ectopic renal  
62 *Fgf23* expression. Conversely, TNF administration to control mice increased plasma  
63 FGF23 without altering plasma phosphate. Similarly, in ~~H-10110~~H-10110 deficient mice with  
64 inflammatory bowel disease and normal kidney function, FGF23 was elevated and  
65 normalized upon TNF neutralization. In conclusion, the inflammatory cytokine TNF  
66 contributes to elevated systemic FGF23 levels and triggers also ectopic renal *Fgf23*  
67 expression in CKD animal models.

## 68 Keywords

69 Fibroblast growth factor 23 (FGF23), tumor necrosis factor (TNF), chronic kidney disease  
70 (CKD), inflammation, cytokine, inflammatory bowel disease, bone.

71

## 72 INTRODUCTION

73 Chronic kidney disease (CKD) causes a severe disturbance of mineral metabolism, one  
74 of the leading factors for morbidity and mortality in patients with end stage renal disease  
75 (ESRD) <sup>1,2</sup>. Fibroblast growth factor 23 (FGF23) increases early during CKD progression  
76 and is required to maintain serum phosphate levels while kidney function declines <sup>3</sup>. In  
77 CKD patients, high FGF23 levels are associated with an increased risk of mortality  
78 independent of plasma phosphate <sup>4</sup>. FGF23 promotes left ventricular hypertrophy in  
79 rodents <sup>5</sup> and elevated FGF23 is a risk factor in the general population for all-cause and  
80 cardiovascular mortality <sup>6</sup>.

81 FGF23 is critical for the regulation of phosphate homeostasis and vitamin D<sub>3</sub> metabolism  
82 <sup>7</sup>. The main target organ of FGF23 is the kidney where FGF23 binds together with  
83  $\alpha$ Klotho to FGF receptors and inhibits phosphate reabsorption and decreases 1,25-(OH)<sub>2</sub>  
84 vitamin D<sub>3</sub> (1,25(OH)<sub>2</sub>D) <sup>8,9</sup>. FGF23 levels are regulated by a variety of stimuli including  
85 calcitriol, PTH, insulin, aldosterone, erythropoietin, and adipokines <sup>8, 10-13</sup>. Moreover,  
86 FGF23 may be linked to inflammation. In the *Chronic Renal Insufficiency Cohort* elevated  
87 FGF23 is independently associated with higher IL-6 and TNF <sup>14</sup> and also in a smaller  
88 cohort with only 103 CKD patients, RANTES and IL-12 associated with higher FGF23 <sup>15</sup>.  
89 The association between FGF23 and inflammation markers is not limited to CKD. *The*  
90 *Reasons for Geographic and Racial Differences in Stroke* study found a positive  
91 correlation of FGF23 with IL-6 and IL-10 in a non-CKD population <sup>16</sup>. Children during an  
92 acute phase of inflammatory bowel disease (IBD) had elevated FGF23 that normalized  
93 in the remission phase <sup>17</sup>. Furthermore, chondrocytes from patients with osteoarthritis  
94 have elevated *Fgf23* gene expression <sup>18</sup>. Microarray data from mouse models with  
95 FGF23 excess (*Col4a3* KO, *Hyp*, and *Fgf23* transgenic mice) show an activation of genes  
96 important in the regulation of the inflammatory response such as transforming growth  
97 factor beta (TGF $\beta$ ), tumor necrosis factor (TNF) and nuclear factor of kappa light  
98 polypeptide gene enhancer in B-cells (NF $\kappa$ B) <sup>19</sup>. Further, inflammatory stimuli and the  
99 hypoxia inducible transcription factor HIF-1 enhance FGF23 expression: TNF and TGF $\beta$ 2

1  
2  
3  
4 100 increases FGF23 expression in bone cells *in vitro* and HIF-1, interleukin-1 beta (IL-1 $\beta$ ),  
5  
6 101 lipopolysaccharide (LPS) increase FGF23 expression *in vitro* and *in vivo* <sup>20-25</sup>. Also, in an  
7  
8 102 obesity induced model, TNF is necessary for the increase in FGF23 levels <sup>26</sup>. Some  
9  
10 103 inflammatory stimuli, including TNF, may act on *Fgf23* transcription via a 16 kb enhancer  
11  
12 104 element <sup>27</sup>. Moreover, in the folic-acid induced AKI model as well as in the adenine CKD  
13  
14 105 model, genetic ablation of Il-6 reduced the increase in FGF23 <sup>28</sup>. Thus, inflammatory  
15  
16 106 cytokines may play an important role at least in the early phase of CKD to induce FGF23.  
17  
18 107 However, whether TNF is a critical player has not been demonstrated.  
19  
20 108 Here, we investigated the association between inflammatory cytokines with plasma  
21  
22 109 FGF23 in a population-based cohort and evaluated the effect of TNF on the regulation of  
23  
24 110 plasma FGF23 in CKD animal models and in a non-renal inflammation model.  
25  
26 111 Furthermore, we evaluated the role of hypoxia on *Fgf23* gene expression. Our results  
27  
28 112 demonstrate a critical role for TNF to stimulate FGF23 in models of renal and non-renal  
29  
30 113 inflammatory diseases.  
31  
32  
33  
34 114  
35  
36  
37  
38  
39  
40  
41  
42  
43  
44  
45  
46  
47  
48  
49  
50  
51  
52  
53  
54  
55  
56  
57  
58  
59  
60

## 115 Results

### 116 Plasma TNF positively correlated with intact FGF23 in the SKIPOGH 117 population based cohort

118 The *Swiss Kidney Project on Genes in Hypertension* (SKIPOGH) is a family and  
119 population-based, multicenter, cross-sectional study including 1131 subjects randomly  
120 selected<sup>29</sup>. We assessed the relationship between plasma intact FGF23 (iFGF23) and  
121 parameters of phosphate metabolism, inflammatory cytokines, and iron metabolism while  
122 considering familial correlation. Participants with drugs interacting with calcium,  
123 magnesium and phosphate metabolism, inflammation and iron metabolism or have  
124 diuretic action were excluded. Based on a linear mixed model with family as random  
125 effect, 1,25-((OH)<sub>2</sub>-vitamin-D<sub>3</sub>D, 25-(OH) vitamin D<sub>3</sub>, (25(OH)D), TNF, and calcium, and  
126 iron are showed the highest fixed effects and were considered significant predictors of  
127 plasma iFGF23 while holding all the other variables constant (Figure 1 and Table S1).  
128 The standard deviation of the random effect was low compared to the standard deviation  
129 of the residuals (0.26 vs 0.93), which means that most of the variation in iFGF23 levels  
130 was due to the fixed effects (i.e. hormones, cytokines, etc.). There was no correlation  
131 between plasma iFGF23 and plasma phosphate, PTH, or eGFR. Besides TNF, no other  
132 inflammatory cytokine such as interferon gamma (IFN $\gamma$ ), IL-1 $\beta$ , IL-6, or IL-10 correlated  
133 with plasma iFGF23.

134 ~~Iron metabolism affects plasma FGF23 in mice<sup>21, 24, 30</sup>. In the SKIPOGH cohort iron is~~  
135 ~~associated with plasma iFGF23, however, there was no correlation between plasma~~  
136 ~~iFGF23 and ferritin and transferrin. Plasma iFGF23 was not dependent on age, body~~  
137 ~~mass index, or sex.~~

138 We also analyzed the cohort without applying exclusion criteria based on drugs. ~~TNF~~  
139 ~~remained together with 1,25-((OH)<sub>2</sub>-vitamin-D<sub>3</sub>D, 25-((OH)-vitamin-D<sub>3</sub>D, and calcium~~  
140 ~~remained as a predictor/predictors~~ of iFGF23 while phosphate, PTH and eGFR arose as

1  
2  
3  
4 141 additional predictors of iFGF23 (Figure S1 ~~and Table S2~~). ~~The TNF effect on iFGF23 is~~  
5 142 ~~reduced in this population.~~ . ~~First quartile, median, mean and third quartile of continuous~~  
6  
7  
8 143 ~~variables in the SKIPOGH population with and without drug intake criteria applied are~~  
9  
10 144 ~~listed in the Tables S1 and S2.~~

### 145 **Inflammation in kidneys of *Pkd1* conditional KO mice**

146 TNF is increased in CKD patients, stimulates FGF23 expression in an osteocyte cell line,  
147 and was the only inflammatory cytokine associated with iFGF23 in the SKIPOGH cohort  
148 <sup>14, 22, 31, 32</sup>. Thus, we tested in two CKD mouse models whether TNF contributes to the  
149 rise of iFGF23 during the early phase of kidney disease. First, slowly progressing  
150 polycystic kidney disease (PKD) was induced in ~~*Pkd1*~~*Pkd1* conditional KO mice <sup>33</sup>.  
151 Kidney function and two-kidney per body weight ratio were similar in 6 week old mice  
152 whereas kidney function was decreased and two-kidney per body weight ratio was  
153 increased in 12 week old *Pkd1*, *cre*+ mice (Figure S2). At week 6, ~~iFGF23, TmP/GFR as~~  
154 ~~well as~~ renal *Tnf* and *Tgfb* mRNA expression were similar in *Pkd1*<sup>fl/fl</sup>, *cre*- and *Pkd1*<sup>fl/fl</sup>,  
155 *cre*+ ~~animals~~ mice (Figure 2 a ~~and b- d~~). Progression of kidney disease ~~correlated with was~~  
156 ~~accompanied by increased plasma iFGF23, decreased TmP/GFR as well as increased~~  
157 *Tnf* and *Tgfb* mRNA expression in *Pkd1*<sup>fl/fl</sup>, *cre*+ mice (Figure 2 a ~~and b- d~~). TNF binding  
158 to TNF receptors activates the NFκB signaling pathway. The ratio of phospho-NFκB p65  
159 to total NFκB p65 protein in the nuclear fraction of total kidney was significantly elevated  
160 in *Pkd1*<sup>fl/fl</sup>, *cre*+ mice (Figure ~~2e2 e~~). Increased renal inflammatory cytokines in 12 week  
161 old *Pkd1*<sup>fl/fl</sup>, *cre*+ mice were paralleled by the appearance of renal *Fgf23* expression and  
162 by the upregulation of the osteogenic marker gene *Runx2* ~~in the kidney~~ (Figure ~~S3-a2 f~~  
163 and ~~eS2 e~~). Bone *Fgf23* and *Runx2* mRNA expression were unchanged (Figure ~~S3-b2 g~~  
164 and ~~dS2 f~~).

### 165 TNF blockade in *Pkd1* conditional KO mice suppressed FGF23

166 The effect of acute TNF blockade on FGF23 expression in PKD kidneys and on plasma  
 167 iFGF23 was investigated. We injected intraperitoneally (i.p.) a single dose of 0.5 mg anti-  
 168 TNF antibody or isotypic IgG control into 12 week old *Pkd1<sup>fl/fl</sup>, cre+* and *Pkd1<sup>fl/fl</sup>, cre-* mice.  
 169 After 24 hours, anti-TNF treated mice had a significant reduction of plasma TNF  
 170 compared to the IgG control treated mice confirming the efficacy of the anti-TNF antibody  
 171 (Figure 3 a). There was no difference in plasma TNF between IgG control treated *Pkd1<sup>fl/fl</sup>,*  
 172 *cre+* and *Pkd1<sup>fl/fl</sup>, cre-* mice. Importantly, elevated plasma iFGF23 in *Pkd1<sup>fl/fl</sup>, cre+* mice  
 173 was normalized by anti-TNF but not IgG control treatment (Figure 3 b). ~~There was no~~  
 174 ~~change in plasma phosphate or urea levels (Figure 3 c and d).~~ Plasma C-terminal FGF23  
 175 (cFGF23) was increased in IgG control treated *Pkd1<sup>fl/fl</sup>, cre+* and anti-TNF treated  
 176 *Pkd1<sup>fl/fl</sup>, cre-* compared to IgG control treated *Pkd1<sup>fl/fl</sup>, cre-* mice consequently the  
 177 iFGF23/cFGF23 ratio was elevated in IgG control treated *Pkd1<sup>fl/fl</sup>, cre-* mice (Figure S4 a  
 178 – c). There was no change in plasma phosphate and urea. as well as t(Figure 3 c and d).  
 179 The abundance of the sodium dependent phosphate co-transporter NaPi-IIa inat the  
 180 brush border membrane (BBM) increased in *Pkd1<sup>fl/fl</sup>, cre+* mice when treated with anti-  
 181 TNF antibodies showed a trend to increase in *Pkd1<sup>fl/fl</sup>, cre+* mice when treated with anti-  
 182 TNF antibodies– (Figure 3 e–e). In *Pkd1<sup>fl/fl</sup>, cre+* mice, TNF neutralization decreased  
 183 ectopic renal *Fgf23* mRNA expression while *Fgf23* mRNA expression in bone (Figure 3  
 184 ~~ef and fg) and renal *Tnf- $\alpha$*  and *Tgfb* mRNA expression in kidney (Figure 3 g and h and~~  
 185 ~~i) were unchanged. The mRNA expression of the inflammatory cytokines *Il1b* and *Il6* was~~  
 186 ~~elevated in PKD kidneys but did not affected change with anti-TNF treatment (Figure S3).~~  
 187 ~~Mace et al. showed that renal *Fgf23* expression did not contribute to total circulating~~  
 188 ~~FGF23 levels<sup>34</sup>. Here, TNF blockade also reduced renal *Fgf23* expression in *Pkd1<sup>fl/fl</sup>,*~~  
 189 ~~*cre+* mice. TNF itself may trigger renal *Fgf23* expression which in turn may promote~~  
 190 ~~further local inflammation and fibrosis<sup>35, 36</sup>. The orphan nuclear receptor *Nurr1* is~~  
 191 downstream of TNF signaling and activates *Fgf23* mRNA expression in rat osteosarcoma  
 192 cells upon PTH treatment<sup>37, 38</sup>. *Nurr1* mRNA was detected in mouse kidney and bone

1  
2  
3  
4 193 (Figure ~~S4 a and b~~S5). In the kidney of 12 week old *Pkd1<sup>fl/fl</sup>*, *cre+* mice, *Nurr1* mRNA  
5  
6 194 expression was upregulated and Nurr1 protein was predominantly localized in the cell  
7  
8 195 nucleus compared to *Pkd1<sup>fl/fl</sup>*, *cre-* mice where Nurr1 was mainly distributed in the  
9  
10 196 cytoplasm (Figure ~~S5~~S6). Further, nuclear Nurr1 staining in *Pkd1<sup>fl/fl</sup>*, *cre+* mice was often  
11  
12 197 co-localized with FGF23. ~~We assessed the relationship between renal *Fgf23* and *Nurr1*~~  
13  
14 198 ~~expression in C57Bl/6J mice undergoing unilateral ureteral ligation (UUO). Fourteen days~~  
15  
16 199 ~~after surgery, we detected *Fgf23* mRNA expression only in the UUO kidney but not in the~~  
17  
18 200 ~~contralateral control kidney. Ectopic *Fgf23* expression was paralleled by higher *Tnf* and~~  
19  
20 201 ~~*Nurr1* mRNA expression (Figure S4 c – e).~~

## 202 TNF but not hypoxia increased FGF23 levels

203 We evaluated the effect of systemic TNF administration on plasma iFGF23,  
204 ~~and therefore we~~ injected wild type mice ~~for two consecutive days~~ with ~~a single dose of~~  
205 2 µg recombinant mouse TNF. After 48-hours, plasma iFGF23 increased while ~~cFGF23~~  
206 ~~and the iFGF23/cFGF23 ratio were unchanged (Figure 4a and S4 d – f). Furthermore~~  
207 plasma ~~TNF and fractional excretion of phosphate,~~ ~~increased, plasma urea decreased~~  
208 ~~while plasma phosphate and creatinine, and urea~~ levels were unchanged (Figure 4 ~~a–~~  
209 ~~d)-b - f). In bone and spleen *Fgf23* mRNA expression decreased in TNF injected~~  
210 ~~compared to vehicle injected mice whereas *Fgf23* mRNA expression in thymus and bone~~  
211 ~~marrow was unchanged (Figure 4 g -j). We cultured primary osteocytes from tibias and~~  
212 femurs of mice <sup>39, 40</sup> for 2 weeks before being supplemented for 24 hours either with 10  
213 ng/ml TNF or 10 nM 1,25-((OH)<sub>2</sub>-~~vitamin D<sub>32</sub>D~~. TNF as well as 1,25-((OH)<sub>2</sub>-~~vitamin D<sub>32</sub>D~~  
214 increased *Fgf23* mRNA expression (Figure 4 ~~ek~~). TNF and 1,25-((OH)<sub>2</sub>-~~vitamin D<sub>32</sub>D~~  
215 decreased the expression of *Dmp1* (Figure 4 ~~fl~~). *Dmp1* inhibits *Fgf23* gene expression  
216 and loss of *DMP1* in patients causes hypophosphatemic rickets due to high FGF23 levels  
217 <sup>44</sup>. TNF but not 1,25-((OH)<sub>2</sub>-~~vitamin D<sub>32</sub>D~~ increased the expression of *Galnt3* and *Nurr1*  
218 (Figure 4 ~~gm~~ and ~~hn~~). *Galnt3* mediates O-glycosylation of FGF23 preventing proteolytic

TNF stimulates FGF23

219 cleavage of FGF23 <sup>42,43</sup>**Error! Reference source not found.****Error! Reference source**  
220 **not found..**

221 CKD kidneys are commonly affected by hypoxia <sup>44, 45</sup> which was recently suggested to  
222 stimulate FGF23 expression through the hypoxia inducible transcription factor HIF-1 <sup>20,</sup>  
223 <sup>21, 24</sup>. We studied in MC3T3-E1 mouse preosteoblasts the effect of hypoxia on *Fgf23* gene  
224 expression. MC3T3-E1 did not display intrinsic *Fgf23* expression. Nevertheless, after 2  
225 weeks osteogenic differentiation of MC3T3-E1, *Fgf23* mRNA expression was induced by  
226 10 nM 1,25-((OH)<sub>2</sub>-vitamin-D<sub>3</sub>D. 1,25-((OH)<sub>2</sub>-vitamin-D<sub>3</sub>D-induced *Fgf23* mRNA  
227 expression was completely repressed by hypoxic conditions (0.2% O<sub>2</sub>) for 24 or 48 hours  
228 and hypoxia alone failed to trigger *Fgf23* expression (Figure [S6S7](#) a). The upregulation  
229 of the HIF-1 target genes carbonic anhydrase 9 (*Car9*) and prolyl hydroxylase domain  
230 containing protein 2 (*Phd2*) confirmed the presence of hypoxia (Figure [S6S7](#) b and c).  
231 Similarly, hypoxia had no effect on *Fgf23* mRNA expression in U2OS rat osteosarcoma  
232 and primary osteoblast cells (data not shown). We analyzed also kidneys of von Hippel-  
233 Lindau (*Vhl*) KO animals <sup>46</sup>. Lack of VHL prevents HIF hydroxylation and degradation and  
234 activates hypoxia sensitive genes <sup>47</sup>. Neither the kidneys of *Vhl* KO animals nor primary  
235 kidney cells lacking *Vhl* <sup>48</sup> expressed any detectable *Fgf23* (data not shown).

## 236 **TNF blockade lowers FGF23 levels in mouse models of oxalate nephropathy** 237 **and colitis**

238 We expanded our observations to another CKD mouse model, the oxalate nephropathy  
239 model in order to test for the relationship between TNF and FGF23 in a non-genetically  
240 modified mouse model and during early stages of kidney disease <sup>49</sup>. After induction of  
241 oxalate nephropathy, 48 hours prior to sacrifice, mice received a single i.p. injection of  
242 0.5 mg anti-TNF or isotypic IgG control antibodies. IgG injected oxalate nephropathy  
243 mice had elevated plasma iFGF23 compared to control mice and TNF blockade  
244 normalized the elevated plasma iFGF23 in oxalate nephropathy mice (Figure 5 a).  
245 Plasma cFGF23 and iFGF23/cFGF23 did not differ between the groups (Figure S4 g –



1  
2  
3  
4 246 i). Plasma TNF was significantly reduced in the anti-TNF treated groups confirming the  
5  
6 247 efficacy of the anti-TNF antibody (Figure 5 b). There was no difference in plasma TNF  
7  
8 248 between IgG control treated oxalate nephropathy and control mice. Renal *Tnf* mRNA  
9  
10 249 expression showed a ~~clear~~ trend to increase in oxalate nephropathy mice and was not  
11  
12 250 affected by the anti-TNF antibody (Figure 5 c). There was no change in plasma  
13  
14 251 phosphate and urine phosphate per urine creatinine ratio while the renal function  
15  
16 252 parameters plasma creatinine and urea showed a trend to increase in the oxalate  
17  
18 253 nephropathy mice (Figure 5 d – fg).

20 254 To demonstrate that TNF regulates plasma iFGF23 independent from impaired kidney  
21  
22 255 function, we analyzed a non-renal inflammation model, the ~~*H-10I10*~~ KO mouse  
23  
24 256 developing spontaneously colitis<sup>50</sup>. Twelve to fourteen weeks old ~~*H-10I10*~~ KO mice had  
25  
26 257 elevated plasma iFGF23 and increased colon *Tnf* mRNA expression (Figure 6 a and b).  
27  
28 258 After 48 hours of a single i.p. injection of 0.5 mg anti-TNF or IgG control, anti-TNF treated  
29  
30 259 ~~*H-10I10*~~ KO mice had reduced plasma iFGF23 compared to IgG treated animals  
31  
32 260 ~~without~~ whereas cFGF23 levels were similar (Figure 6 c and S4 k). There was a reduction  
33  
34 261 in the iFGF23/cFGF23 ratio in anti-TNF treated *I10* KO compared to IgG control treated  
35  
36 262 *I10* KO mice (Figure S4 j—l). Anti-TNF treatment had no effect on plasma phosphate  
37  
38 263 levels (Figure 6 ~~e and~~ d) or kidney function parameters (Figure 6 e and f). But there was  
39  
40 264 an increase in abundance of NaPi-IIa at the BBM in *I10* KO mice treated with anti-TNF  
41  
42 265 antibodies compared to IgG control mice (Figure 6 g)  
43  
44  
45  
46 266

TNF stimulates FGF23

## 267 Discussion

268 We provide a novel explanation for high iFGF23 levels in patients with chronic kidney  
269 disease or inflammation of non-renal origin. Our data demonstrate that TNF is positively  
270 and independently associated with plasma iFGF23 in humans. We show that exogenous  
271 TNF stimulates iFGF23 expression both *in vivo* and *in vitro*. TNF neutralization  
272 suppresses plasma iFGF23 in two CKD mouse models and triggers renal *Fgf23*  
273 expression in PKD kidneys. TNF also contributes to high iFGF23 in a model of intestinal  
274 inflammation with normal kidney function.

275 In humans, TNF levels correlated with plasma iFGF23 ~~independent of drug intake~~ in the  
276 SKIPOGH multi-centric population based cohort. Dhayat et al. found in the same cohort  
277 associations between ~~C-terminal FGF23 (cFGF23)~~ and plasma phosphate, 1,25-~~((OH)<sub>2</sub>~~  
278 ~~vitamin D<sub>3</sub>D<sub>2</sub>~~, 25-~~((OH)-vitamin D<sub>3</sub>D<sub>2</sub>~~, the ratio of TmP/GFR, age, sex, and renal function.  
279 However, there are relevant differences between both analyses: 1) we have measured  
280 both the biologically active iFGF23 and the biologically inactive C-terminal fragment,  
281 while Dhayat et al.<sup>51</sup> used a method that detects both the sum of the intact form and the  
282 biologically inactive C-terminal fragment. 2) in addition to the subjects excluded by  
283 Dhayat et al. we excluded individuals taking drugs interacting with inflammation and  
284 subjects without complete data available for all variables. However, both analyses  
285 identified 1,25-~~((OH)<sub>2</sub>-vitamin D<sub>3</sub>D<sub>2</sub>~~ and 25-~~((OH)-vitamin D<sub>3</sub>D<sub>2</sub>~~ as strong predictors of  
286 FGF23 variation in the SKIPOGH population while the correlation of ~~iron~~, PTH and eGFR  
287 in our study was dependent on drug exclusion criteria. The overall effect of TNF on  
288 iFGF23 may explain only a small part of the overall variability of iFGF23 in this cohort.

289 TNF increases in kidney disease and associates with CKD progression<sup>14, 31, 32</sup>. TNF  
290 stimulates *Fgf23* mRNA expression in an osteocyte-derived cell line<sup>22</sup> and may be  
291 involved in obesity induced increases in FGF23<sup>26</sup>. We tested the relevance of FGF23  
292 regulation by TNF in pathological situations such as kidney disease or colitis. We used  
293 two distinct CKD mouse models, the *Pkd1* conditional KO mouse and the oxalate

1  
2  
3  
4 294 nephropathy model. PKD kidneys are affected by inflammation <sup>52, 53</sup> as confirmed by  
5  
6 295 higher renal *Tnf* and *Tgfb* expression as well as enhanced NFκB subunit p65  
7  
8 296 phosphorylation. Similarly, in oxalate nephropathy the inflammasome is activated and  
9  
10 297 various proinflammatory cytokines are released <sup>49, 54</sup>**Error! Reference source not**  
11  
12 298 **found.** Ectopic renal FGF23 gene and protein expression occurs in rodents with either  
13  
14 299 diabetic nephropathy, PKD, or 5/6 nephrectomy <sup>34, 55, 56</sup>. The increase of renal *Tnf* and  
15  
16 300 *Tgfb* mRNA expression in PKD kidneys was paralleled by the increase in plasma iFGF23  
17  
18 301 levels, and the appearance of renal *Fgf23* and *Runx-2* expression. Renal FGF23  
19  
20 302 production may promote inflammation and fibrosis in the affected kidney <sup>35, 36, 57</sup>. We did  
21  
22 303 not detect any change in bone *Fgf23* mRNA expression or plasma TNF levels in both  
23  
24 304 CKD models. Similarly, in *Col4a3* KO mice, another CKD model, the early rise in plasma  
25  
26 305 FGF23 is not accompanied by increased *Fgf23* expression in bone <sup>58</sup>. TNF blockade in  
27  
28 306 both CKD models normalized plasma iFGF23 levels without changes in plasma  
29  
30 307 phosphate levels. In the PKD model, TNF neutralization also reduced renal *Fgf23*  
31  
32 308 expression. TNF may regulate renal *Fgf23* expression through NFκB stimulating orphan  
33  
34 309 nuclear receptor *Nurr1* gene expression <sup>38</sup>. *Nurr1* mediates the PTH dependent  
35  
36 310 regulation of *Fgf23* in bone <sup>37</sup>. *Nurr1* was upregulated in PKD kidneys and predominantly  
37  
38 311 localized in the cell nucleus whereas in wild type kidneys it was localized in the  
39  
40 312 cytoplasm. *Nurr1* nuclear localization often overlapped with renal FGF23 protein  
41  
42 313 expression. Thus, *Nurr1* may contribute to renal FGF23 expression.

43  
44  
45  
46  
47 314 In patients with CKD, TNF increases with ascending FGF23 quartiles and correlates with  
48  
49 315 FGF23 levels independent of renal function and measures of mineral metabolism <sup>14</sup>.  
50  
51 316 Likewise, markers of inflammation correlate with ascending FGF23 quartiles in non-CKD  
52  
53 317 stroke patients <sup>16</sup>. Inoculation of mice with LPS or bacteria stimulates serum FGF23 levels  
54  
55 318 <sup>23, 27</sup>. In the diabetic nephropathy rat model, renal FGF23 was reduced by ramipril, an  
56  
57 319 angiotensin-converting enzyme inhibitor <sup>56</sup>, which also reduces inflammation <sup>59</sup>. Non-  
58  
59 320 renal diseases characterized by inflammation such as inflammatory bowel disease (IBD)  
60  
321 or osteoarthritis are linked to elevated plasma FGF23 <sup>17, 18</sup>. Patients with IBD or mouse

TNF stimulates FGF23

colitis models show elevated FGF23 levels, lower 1,25- $\text{((OH)}_2\text{-vitamin-D}_{32}\text{D}$  and impaired intestinal phosphate absorption <sup>17, 60-63</sup> **Error! Reference source not found.Error! Reference source not found.Error! Reference source not found.** These disturbances are partially caused by TNF and in patients with IBD, TNF neutralizing therapy can reverse some of these abnormalities. We tested whether inflammation *per se* without renal disease could increase FGF23. Consistently, in *Il-10* KO mice, a model of IBD, plasma FGF23 increased and was reduced by TNF neutralization without affecting renal function parameters. Thus, extrarenal inflammation also stimulates FGF23 levels in mouse models and may play a role in humans.

David et al. reported that 6 hours after administration of the inflammatory cytokine IL-1 $\beta$  only cFGF23 increased while it required 4 days of consecutive IL-1 $\beta$  injections to increase also iFGF23 levels <sup>24</sup>, whereas Onal et al showed higher FGF23 levels already 3 ~~hours~~ after IL-1 $\beta$  injection <sup>27,27</sup>. We demonstrate that TNF administration in wild type mice stimulated plasma iFGF23 levels within ~~2448~~ hours without altering plasma phosphate, and creatinine, or urea levels but increasing fractional excretion of phosphate demonstrating that ~~FGF23~~iFGF23 is ~~differently regulated by inflammation and phosphate~~functional. TNF may exert even faster effects as indicated by higher FGF23 levels in mice 3 hours after TNF injection <sup>27</sup>. The stimulation of *Fgf23* mRNA expression by TNF was confirmed *in vitro* in primary mouse osteocytes and comparable to the effect of 1,25- $\text{((OH)}_2\text{-vitamin-D}_{32}\text{D}$ . TNF but not 1,25- $\text{((OH)}_2\text{-vitamin-D}_{32}\text{D}$  increased *Nurr1* and *Galnt3* expression in primary osteocytes suggesting that TNF but not 1,25- $\text{((OH)}_2\text{-vitamin-D}_{32}\text{D}$  may regulate *Fgf23* expression in a *Nurr1*-dependent manner. TNF may also modulate FGF23 protein stability by regulating the expression of *Galnt3* which mediates the O-glycosylation of FGF23 making it more resistant to proteolytic degradation <sup>43</sup>. In bone, C-terminal DMP-1 binds to PHEX and thereby inhibits *Fgf23* expression <sup>64</sup>. In primary osteocytes, *Dmp1* expression was strongly decreased by TNF and 1,25- $\text{((OH)}_2\text{-vitamin-D}_{32}\text{D}$ . The upregulation of *Fgf23* expression by TNF and 1,25- $\text{((OH)}_2\text{-vitamin-D}_{32}\text{D}$  is paralleled by the downregulation of its suppressor. Our data expand previous

1  
2  
3  
4 350 observations in IDG-SW3 mouse osteocyte cells where TNF, IL-1 $\beta$ , and LPS increased  
5  
6 351 *Fgf23* and reduced *Dmp1* mRNA expression <sup>22</sup>. TNF also stimulated *Fgf23* mRNA  
7  
8 352 expression in rat UMR106 osteosarcoma cells and is required to increase circulating  
9  
10 353 FGF23 levels in a mouse obesity model <sup>25</sup>. Deletion of an 16kb enhancer element in the  
11  
12 354 *Fgf23* murine gene abolishes TNF induced FGF23 increases and reduces the effect of  
13  
14 355 LPS and IL-1 $\beta$  on circulating FGF23 levels without altering bone structure or plasma  
15  
16 356 phosphate and PTH. Induction of *Fgf23* mRNA in various organs is organ-specifically  
17  
18 357 responsive to LPS, TNF and IL-1 $\beta$  and the deletion of the enhancer suggesting a complex  
19  
20 358 and cell- and/or organ-specific regulation <sup>27,27</sup>. The enhancer element is also required for  
21  
22 359 the early induction of FGF23 in the oxalate nephropathy model <sup>27,27</sup>. Thus, our work  
23  
24 360 demonstrates the critical role of TNF in inducing FGF23 production and thereby  
25  
26 361 complements previous work that identified a genetic element responding to TNF and  
27  
28 362 possibly ~~some~~ other regulators of *Fgf23* mRNA transcription <sup>27</sup>. Furthermore, we expand  
29  
30 363 these observations from kidney disease to at least one other clinically important  
31  
32 364 condition, inflammatory bowel disease.

33  
34  
35  
36 365 IL-6 has been recently identified as another important proinflammatory cytokine that  
37  
38 366 associates with FGF23 levels in the CRIC cohort <sup>14</sup> and that stimulates *Fgf23* mRNA in  
39  
40 367 the IDG-SW3 osteocyte cell line <sup>22</sup>. Durlacher-Betzer et al. showed increased expression  
41  
42 368 of IL-6 in kidney of folic-acid and adenine AKI and CKD mouse models and a partly  
43  
44 369 blunted increase of circulating FGF23 levels in IL-6 deficient mice treated with adenine <sup>28</sup>.  
45  
46 370 While IL-6 may participate in the regulation of FGF23 in CKD, IL-6 plays also an important  
47  
48 371 role in normal bone biology and IL-6 deficient mice have altered bone architecture <sup>65, 66</sup>.  
49  
50 372 Thus, IL-6 may contribute to the upregulation of FGF23 in early CKD but TNF may act  
51  
52 373 either upstream or is a critical permissive factor as indicated by the complete  
53  
54 374 normalization of FGF23 levels in our experiments. In our population-based cohort, TNF  
55  
56 375 but not IL-6 associated with intact FGF23 levels further strengthening the concept that  
57  
58 376 TNF may play a central role in mediating effects of inflammation on bone.

TNF stimulates FGF23

1  
2  
3  
4 377 Renal hypoxia is a common complication in CKD kidneys<sup>44, 45</sup>. Hypoxia increased *Fgf23*  
5  
6 378 expression in UMR-106 rat osteosarcoma cells, and plasma cFGF23 but not iFGF23 in  
7  
8 379 rats under hypobaric hypoxia conditions<sup>21</sup>. We cultured MC3T3-E1 cells, a mouse  
9  
10 380 preosteoblast cell line and primary mouse osteoblasts for 24 and 48 hours in 0.2%  
11  
12 381 hypoxia and we did not observe any stimulation of *Fgf23* expression. In contrast, hypoxia  
13  
14 382 suppressed the stimulatory effect of 1,25-(OH)<sub>2</sub>-~~vitamin D<sub>3</sub>~~ on *Fgf23*. TNF and IL-1β  
15  
16 383 increase HIF-1 binding to DNA under normoxia while in combination with hypoxia both  
17  
18 384 cytokines strongly increase HIF-1 activity<sup>67</sup>. IL-1β but not TNF enhance nuclear  
19  
20 385 accumulation of HIF-1α in a hepatoma cell line<sup>67</sup> and increase FGF23 mRNA expression  
21  
22 386 in bones and kidneys<sup>24</sup>. Inhibition of HIF-1α attenuated the positive effect of IL-1β on  
23  
24 387 FGF23 expression<sup>24</sup>. Combined with the fact that we did not find any effect of  
25  
26 388 constitutively activated HIF-1α in *Vhl* KO animals as well as in primary kidney cells lacking  
27  
28 389 *Vhl*, these results suggest that the HIF-1α mediated upregulation of *Fgf23* expression  
29  
30 390 may depend on IL-1β or other factors such as erythropoietin<sup>11, 24, 68, 69</sup>.

31  
32  
33  
34 391 In summary, TNF stimulates ~~FGF23~~iFGF23 in renal and non-renal inflammatory mouse  
35  
36 392 models and in primary bone cell culture; ~~triggers renal *Fgf23* expression in CKD animal~~  
37  
38 393 ~~models and~~ is positively associated with plasma iFGF23 in a population-based cohort; ~~it~~  
39  
40 394 ~~triggers renal *Fgf23* expression in CKD animal models.~~ These findings question the  
41  
42 395 concept that the early rise in plasma FGF23 in CKD is a specific marker of the severity  
43  
44 396 of solely to balance plasma phosphate while kidney disease as function declines. The data  
45  
46 397 suggest or if that other non-renal inflammatory processes may strongly impact on plasma  
47  
48 398 FGF23 levels. Our study ~~also provides new insights into possible pathological~~  
49  
50 399 ~~mechanisms through which inflammatory diseases may be linked to bone health. It also~~  
51  
52 400 suggests novel therapeutic options to reduce excessive FGF23 levels in kidney and other  
53  
54 401 diseases as drugs lowering TNF are widely clinically used and have proven to be safe in  
55  
56 402 humans.  
57  
58  
59  
60

403

## 404 **Methods**

### 405 **SKIPOGH cohort**

406 We obtained 1098 out of 1131 human EDTA plasma samples from SKIPOGH cohort  
407 (Swiss Kidney Project on Genes in Hypertension)<sup>29, 70, 71</sup>. Plasma iFGF23 was measured  
408 with the human intact FGF23 ELISA kit (Immutopics International, USA). For statistical  
409 modeling the following 18 previously determined parameters were used: plasma calcium,  
410 phosphate, ferritin, transferrin, iron, 1,25(OH)<sub>2</sub>-~~vitamin D<sub>3</sub>D~~, 25(OH) vitamin D<sub>3</sub>, PTH,  
411 TNF, IFN $\gamma$ , IL-1 $\beta$ , IL-6, IL-10 and cFGF23 as well as body mass index, age, sex and  
412 estimated renal function calculated by the CKD-EPI equation.

413 Exclusion criteria followed the pipeline described in the Table S3. Participants with  
414 incomplete data sets (n = 261) were excluded. TNF followed a bimodal distribution with  
415 40 values close to undetectable (TNF < 1 pg/ml) without continuity with the rest of the  
416 distribution, highly suggestive for measurement failures. Therefore the 40 participants  
417 with TNF < 1 pg/ml were excluded from the study. Next, the ratio between iFGF23  
418 (detects only iFGF23) and cFGF23 (detects iFGF23 and cFGF23) was calculated. One  
419 Ru/ml cFGF23 corresponds to 1.5 pg/ml iFGF23 (information provided by Immutopics);  
420 participants with ratios higher than 1.5 were excluded (n = 40). To avoid confounding  
421 effects by drug intake we eliminated 4 major drug categories that interact with FGF23  
422 metabolism: 1) calcium, phosphate and magnesium (n = 41); 2) inflammation (pro or anti-  
423 inflammatory) (n = 390); 3) iron metabolism (n = 6); 4) kidney function (i.e. diuretics) (n =  
424 54) (Table S4). A total of 361 participants were excluded due to intake of drugs of one or  
425 more of these drug categories. The final dataset contains either 429 participants (198  
426 female / 231 male) with or 790 (424 female / 366 male) without drug exclusion criteria.

### 427 **Animals**

428 *Pkd1* floxed/floxed (*Pkd1<sup>fl/fl</sup>*) tamoxifen inducible *cre* mice were kindly provided by  
429 Gregory Germino<sup>33, 72</sup>. *Cre* recombinase expression is under the control of the  $\beta$ -actin  
430 promoter which drives high levels of expression in most tissues<sup>33</sup>. Male and female

TNF stimulates FGF23

1  
2  
3  
4 431 *Pkd1<sup>fl/fl</sup>*, *cre+* and *Pkd1<sup>fl/fl</sup>*, *cre-* mice were used. Cre recombinase activity was induced at  
5  
6 432 postnatal days 15, 17, and 19 by injecting pups with 100 µl tamoxifen (2.5 mg/ml) in corn  
7  
8 433 oil causing slow onset disease <sup>33</sup>. Without further interventions, 24-hour urine was  
9  
10 434 collected from 6 and 12 weeks old animals (e.g. 3 or 9 weeks after induction, respectively)  
11  
12 435 which were thereafter sacrificed to collect plasma and organs. For TNF blockade, animals  
13  
14 436 were treated at the age of 11-12 weeks with a single i.p. injection of 0.5 mg *InVivoMAb*  
15  
16 437 anti-Tnfa (Clone XT3.11, Lot4653-1/0413, BioXCell, USA) or *InVivoMAb* rat IgG1 (Clone  
17  
18 438 HRPN, Lot 5339/1014, BioXCell, USA) <sup>73,74</sup>. Twenty-four hours after antibody application,  
19  
20 439 animals were sacrificed and plasma and organs were collected. ~~Unilateral ureteral~~  
21  
22 440 ~~ligation was performed in 6 weeks old C57/Bl6J mice purchased from Jackson laboratory~~  
23  
24 441 ~~(Bar Harbor, ME). After 14 days, animals were sacrificed and organs were collected.~~The  
25  
26 442 effect of TNF in wild-type mice was assessed by injecting ~~12~~<sup>13</sup> weeks old C57Bl/6J mice  
27  
28 443 on two consecutive days with 2 µg TNF. After ~~72~~<sup>48</sup> hours, plasma and organs were  
29  
30 444 collected.  
31  
32  
33 445 Nephropathy was induced in 10 to 12 weeks old C57Bl/6J mice. After 3 days of  
34  
35 446 adaptation with calcium-free diet (irradiated S7042-E005S, Sniff Spezialdiäten GmbH,  
36  
37 447 Germany), mice were fed for 10 days with either calcium free diet or 0.67% oxalate in  
38  
39 448 calcium-free diet (irradiated S7042-E010) followed by a 5-day recovery phase in standard  
40  
41 449 diet (3433, Kliba, Kaiseraugst, Switzerland). Forty-eight hours prior to sacrifice, mice  
42  
43 450 received a single i.p. injection of 0.5 mg anti-TNF or isotypic IgG1 control. Mice were  
44  
45 451 sacrificed and plasma and organs were collected.  
46  
47  
48 452 ~~H-10/10~~ deficient mice (~~H-10/10~~<sup>-/-</sup>) develop spontaneous colitis and were used as a non-  
49  
50 453 renal inflammatory disease model <sup>50</sup>. ~~H-10/10~~<sup>-/-</sup> mice between 12-14 weeks were  
51  
52 454 sacrificed to collect plasma and organs. ~~H-10/10~~<sup>-/-</sup> mice were treated with a single i.p.  
53  
54 455 injection of 0.5 mg *InVivoMAb* anti-Tnfa (Clone XT3.11, Lot4653-1/0413, BioXCell, USA)  
55  
56 456 or *InVivoMAb* rat IgG1 (Clone HRPN, Lot 5339/1014, BioXCell, USA) <sup>73,74</sup> 48 hours prior  
57  
58 457 to sacrifice and plasma and organs were collected. For some experiments, kidneys from  
59  
60 458 kidney-specific von-Hippel-Lindau deficient mice were used <sup>46</sup>. All animal studies were



performed according to protocols approved by the legal authority (Veterinary Office of the Canton of Zurich or the Committee on Animal Research, University of California San Francisco).

## Plasma and urine analysis

Blood and 24 hours urine were collected from *Pkd1<sup>fl/fl</sup>, cre+* and *Pkd1<sup>fl/fl</sup>, cre-* mice at 6 and 12 weeks after birth. Briefly, *Pkd1<sup>fl/fl</sup>, cre* mice were kept for three days in metabolic cages (Tecniplast, Italy) whereas the last day was used for 24 hours urine collection. Afterwards mice were anesthetized with isoflurane and blood was collected from the heart. Plasma and urine aliquots were rapidly frozen and stored at -80 °C until measurement. Urine and plasma laboratory analyses were performed on a UniCel DxC 800 Synchron (Beckman Coulter, Switzerland) by the Zurich Integrative Rodent Physiology (ZIRP) core facility. The ratio of the maximum rate of tubular phosphate reabsorption to the glomerular filtration rate (TmP/GFR) was calculated as follows:

$TmP/GFR \text{ in } mmol/L = P_P - [U_P \times P_{crea} / U_{crea}]^{75}$ . [The fractional excretion of phosphate](#)

[was calculated according to the following equation:  \$FE\_{P\_i} = \(U\_{P\_i} \times P\_{crea}\) / \(P\_{P\_i} \times U\_{crea}\) \times 100\$ .](#)

[where  \$P\_{P\_i}\$ ,  \$U\_{P\_i}\$ ,  \$P\_{crea}\$ , and  \$U\_{crea}\$  refer to the plasma and urinary concentration of phosphate and creatinine, respectively<sup>75</sup>.](#) The plasma concentration of intact FGF23 (Kainos

Laboratories, Japan or Immutopics International, USA), [cFGF23 \(Immutopics](#)

[International, USA\)](#), intact PTH (Immutopics International, USA) and TNF (Bio-Techne

AG, Switzerland) were measured by enzyme-linked immunosorbent assays according to

the manufacturers protocols.

## Cell culture

All cell culture reagents were from Life Technologies Europe B.V. (Switzerland) unless stated otherwise. Two to four month old *Pkd1<sup>fl/fl</sup>, cre* mice (4-6 mice per experiment, male and female mixed) were sacrificed with carbon dioxide. Tibias and femurs from the hindlegs were harvested. The epiphyses were cut and bones were flushed with Hank's

TNF stimulates FGF23

1  
2  
3  
4 485 Balanced Salt Solution (HBSS) containing 1% penicillin streptomycin (Pen Strep) to  
5  
6 486 remove the bone marrow. Bones were cut into small pieces of 1-2 mm<sup>2</sup>. Bone cell  
7  
8 487 extraction was performed according to established protocols <sup>39, 40</sup>. Briefly, small bone  
9  
10 488 pieces were repeatedly digested with either a solution containing 2 mg/ml collagenase  
11  
12 489 type II, 0.05% (w/v) soybean trypsin inhibitor (Sigma-Aldrich, Switzerland), 20 mM  
13  
14 490 HEPES, 1% Pen Strep in HBSS or 10 nM EDTA, 1% fetal bovine serum (FBS), 1% Pen  
15  
16 491 Strep in phosphate buffered saline (PBS) for 25 min at 37°C. Cells from digestion steps  
17  
18 492 6-9 or cells and bone pieces from digestion step >9 were cultured for 2 weeks in an  
19  
20 493 osteogenic medium (minimal essential medium  $\alpha$  (mem $\alpha$ ) containing 10% FBS, 1% Pen  
21  
22 494 Strep, 50  $\mu$ g/ml 2-phospho-L-ascorbic acid trisodium salt (Sigma-Aldrich, Switzerland),  
23  
24 495 and 1 mM  $\beta$ -glycerophosphate (Sigma-Aldrich, Switzerland)). After 2 weeks, cells were  
25  
26  
27 496 supplemented for 24 hours with either 10 nM 1,25(OH)<sub>2</sub>-~~vitamin-D~~<sub>3</sub>2D  
28  
29 497 (CaymanChemical, USA) or 10 ng/ml mouse TNF (R&D Systems, USA) and total mRNA  
30  
31 498 was extracted.  
32  
33  
34 499 MC3T3-E1 subclone 4 preostoblast cells (CRL-2593, Lot 59899932, ATCC France)  
35  
36 500 passage 17/4 were expanded for 4-5 days with MEM $\alpha$  medium supplemented with 10%  
37  
38 501 FBS and 1% PenStrep. After reaching 80-90% confluence, MC3T3-E1 cells were  
39  
40 502 trypsinized and plated in collagen coated 6-well plates (80'000 cells/well). Medium was  
41  
42 503 changed to osteogenic differentiation medium (MEM $\alpha$  supplemented with 10% FBS, 1%  
43  
44 504 PenStrep, 50 $\mu$ g/ml 2-phospho-L-ascorbic acid trisodium salt (Sigma-Aldrich,  
45  
46 505 Switzerland), and 1 mM beta glycerophosphate (Sigma-Aldrich, Switzerland)). After 2  
47  
48 506 weeks differentiation along the osteogenic lineage cells were supplemented for 24 or 48  
49  
50  
51 507 hours with either 10 nM 1,25(OH)<sub>2</sub>-~~vitamin-D~~<sub>3</sub>2D (CaymanChemical, USA) or an equal  
52  
53 508 amount of ethanol and incubated for 24 or 48 hours under hypoxic (0.2% O<sub>2</sub>) or normoxic  
54  
55 509 conditions. Hypoxia experiments were performed in a gas-controlled workstation  
56  
57 510 (InvivoO<sub>2</sub>, Baker Ruskinn, UK).

## 511 RNA extraction, reverse transcription and qPCR

512 Organs and scraped colonic mucosa were harvested and rapidly frozen in liquid nitrogen.  
513 Tissues were homogenized using either a Precellys homogenizer or a liquid nitrogen  
514 cooled mortar and pestle (bone). Total mRNA from bone as well as from cultured cells  
515 was extracted with TRIzol (Life Technologies Europe B.V., Switzerland) followed by  
516 purification with RNeasy Mini Kit (Qiagen, Switzerland) according to the manufacturers  
517 protocol. Total mRNA from kidney and colonic mucosa were extracted with RNeasy Mini  
518 Kit (Qiagen, Switzerland) according to the ~~manufacturers~~ manufacturer's protocol. DNase  
519 digestion was performed using the RNase-free DNAase Set (Qiagen, Switzerland). Total  
520 RNA extractions were analyzed for purity and concentration using the NanoDrop ND-  
521 1000 spectrophotometer (Wilmington, Germany). RNA samples were diluted to a final  
522 concentration of 100 ng/μl and cDNA was prepared using the TaqMan Reverse  
523 Transcriptase Reagent Kit (Applied Biosystems, Roche, Foster City, CA). In brief, in a  
524 reaction volume of 40 μl, 300 ng of RNA was used as template and mixed with the  
525 following final concentrations of RT buffer (1x): MgCl<sub>2</sub> (5.5 mmol/l), random hexamers  
526 (2.5 μmol/l), dNTP mix (500 μmol/l each), RNase inhibitor (0.4 U/μl), multiscribe reverse  
527 transcriptase (1.25 U/μl), and RNase-free water. Reverse transcription was performed  
528 with temperature conditions set at 25 °C for 10 min, 48 °C for 30 min, and 95 °C for 5  
529 min on a thermocycler (Biometra, Germany). Quantitative PCR (qPCR) was performed  
530 on the ABI PRISM 7700 Sequence Detection System (Applied Biosystems). Primers for  
531 genes of interest were designed using Primer 3 software. Primers were chosen to span  
532 exon - exon boundaries to exclude the amplification of contaminating genomic DNA  
533 (primer and probe sequence see Table S5). The specificity of all primers was tested and  
534 always resulted in a single product of the expected size (data not shown). Probes were  
535 labeled with the reporter dye FAM at the 5'-end and the quencher dye TAMRA at the 3'-  
536 end (Microsynth, Switzerland). qPCR reactions were performed using the KAPA PROBE  
537 FAST qPCR Kit (KappaBiosystems, USA) or PowerUp™ SYBR® Green Master Mix  
538 (Applied Biosystems, Switzerland).

TNF stimulates FGF23

### 539 **Protein extraction and Western blot analysis**

540 Organs were rapidly frozen in liquid nitrogen. Tissues were homogenized in  
541 homogenization buffer containing 0.27 M sucrose, 2 mM EDTA (pH8), 0.5% NP-40, 60  
542 mM KCl, 15 mM NaCl, 15 mM HEPES (pH7.5) (all Sigma-Aldrich, Switzerland) and  
543 complete protease inhibitor cocktail (Roche, Switzerland) using Precellys homogenizer.  
544 Nuclei were separated by a sucrose cushion and resuspended in a nuclear extraction  
545 buffer containing 20 mM HEPES (pH 7.5), 400 mM NaCl, 1 mM EDTA (pH 8), 1 mM DTT  
546 and 1 mM PMSF (all Sigma-Aldrich, Switzerland). [BBM vehicles were prepared using the](#)  
547 [Mg<sup>2+</sup> precipitation technique](#) <sup>76</sup>. After measurement of protein concentration (Bio-Rad,  
548 Hercules, CA, USA), 60 µg of nuclear proteins [or 20 µg of BBM proteins](#) were solubilized  
549 in loading buffer containing DTT and separated on a 10% polyacrylamide gel. For  
550 immunoblotting, proteins were transferred electrophoretically to polyvinylidene fluoride  
551 membranes (Immobilon-P, Millipore, Bedford, MA, USA). After blocking with 5% milk  
552 powder in Tris-buffered saline/0.1% Tween-20 or 5% bovine serum albumin (BSA) in  
553 Tris-buffered saline/0.1% Tween-20 for 60 min, blots were incubated with the primary  
554 antibodies: mouse monoclonal anti-phospho-NFκB p65 (Ser536)(7F1) (Cell Signaling  
555 Technology, USA; 1:1000) ~~or~~, rabbit monoclonal NFκB p65 (D14E12) (Cell Signaling  
556 Technology, USA; 1:1000), [rabbit polyclonal anti-NaPi-IIa](#) (<sup>77</sup>~~homemade~~; 1:3000) [or](#)  
557 [mouse monoclonal anti-β-actin](#) either for 2 h at room temperature or overnight at 4 °C.  
558 Membranes were then incubated for 1 h at room temperature with secondary goat anti-  
559 rabbit or donkey anti-mouse antibodies (1:5000) linked to alkaline phosphatase  
560 (Promega, USA) or HRP (Amersham, MA, USA or R&D Systems, USA). The protein  
561 signal was detected with the appropriate substrates using the DIANA III-  
562 chemiluminescence detection system (Raytest, Straubenhardt, Germany). All images  
563 were analyzed using the software Advanced Image Data Analyser AIDA, Raytest to  
564 calculate the ratio between phosphorylated protein to total protein.

## 565 Immunofluorescence staining

566 Mouse kidneys were perfused through the left heart ventricle with a fixative solution  
567 containing 3% paraformaldehyde in phosphate buffered saline (PBS). Kidneys were  
568 embedded in TissueTec and frozen in liquid nitrogen. Five  $\mu\text{m}$  cryosections were cut.  
569 Slides were rehydrated with PBS, treated for 5 min with 0.5% SDS in PBS followed by  
570 10 min treatment with 0.5% Triton-X-100 in PBS (Sigma-Aldrich, Switzerland). Unspecific  
571 sites were blocked with 1% bovine serum albumin (BSA) in PBS for 1 h at room  
572 temperature. Primary antibodies were diluted in 1% BSA in PBS (rat anti-FGF23 clone  
573 #283507 (R&D Systems, USA) 1:1000; rabbit anti-Nurr1 N-20 sc-991 (Santa-Cruz, USA)  
574 1:200) and kidney sections were incubated with the primary antibody overnight at 4 °C.  
575 After washing with PBS, sections were incubated with the corresponding secondary  
576 antibody (1:500) (anti-rabbit DyLight 594 (Jackson ImmunoResearch, Europe), anti-rat  
577 NL493 (R&D Systems, USA)), and DAPI (Life Technologies Europe B.V., Switzerland,  
578 1:1000) for 1 h at room temperature. Slides were washed twice with PBS before they  
579 were mounted with Dako glycergel mounting medium (Dako, Switzerland). Sections were  
580 visualized on a Leica DM 5500B fluorescence microscope and images processed with  
581 ImageJ.

## 582 Statistical analysis

583 Statistics were performed using unpaired Student's t-test, ANOVA, or Two-Way-ANOVA  
584 (GraphPad Prism version 7, GraphPad, San Diego, CA) and R programming  
585 environment including the nlme, [lme4](#), [visreg](#), [splines](#), [rmsdata.table](#), [car](#), [and-lmtest](#), and  
586 [forestplot](#) packages **Error! Reference source not found.Error! Reference source not**  
587 **found.Error! Reference source not found.Error! Reference source not found.Error!**  
588 **Reference source not found.** P < 0.05 was considered significant.

589 The identification of predictors for iFGF23 variation in the SKIPOGH population was  
590 performed using linear mixed models with random intercept. The distribution of all  
591 parameters was analyzed in histograms. Due to a heavily skewed distribution, IL-6, IL-

TNF stimulates FGF23

10, IFN $\gamma$  and IL1- $\beta$  were log-transformed. All parameters were centralized and then normalized by their standard deviations. Linear or nonlinear relationship of each variable with iFGF23 was assessed using a component residual plot. ~~A restricted cubic spline function with 4 knots was applied to 25 (OH)-vitamin D<sub>3</sub> and eGFR (CKD-EPI).~~ However, all parameters were considered linear. Assumptions on the within-group error were checked with plots of the standardized residuals versus fitted values and a Q-Q plot of the residuals. The assumptions on the random effects were checked with a Q-Q plot of the random effects. ~~The Wald test statistic was used to identify the predictors of iFGF23 in the linear mixed model.~~

### 601 **Author contributions**

602 Conceptualization, D. E-S., P.H.I.S., and C.A.W; Methodology, D. E-S., P.H.I.S., and  
603 C.A.W; Formal analysis, D. E-S. and P.H.I.S.; Investigation, D. E-S., P.H.I.S., B.G., N.G.,  
604 C.B., M.Z., D.S., M.R., D.A., B.P., M.P., A.L., V.B., and G.-M. F; Resources C.A.W., D.H.,  
605 F.K., I.F-W., G.R., M. B., F.P., M.F., F.L., R.H.W., S.H.B. and I.F.; Writing – Original  
606 Draft, D. E-S. Writing -Review & Editing, D. E-S., P.H.I.S., and C.A.W; Visualization, D.  
607 E-S. and P.H.I.S.; Supervision, C.A.W.; Funding Acquisition, C.A.W, all authors read,  
608 edited and approved the manuscript.

### 609 **Acknowledgments**

610 This study was supported by grants from the Swiss National Center for Competence in  
611 Research NCCR Kidney.CH to C. A. Wagner, the Novartis Foundation for medical-  
612 biological research to C. A. Wagner and D. Egli-Spichtig, the SNSF early postdoc mobility  
613 grant to D. Egli-Spichtig and the Deutsche Forschungsgemeinschaft to Michael Föller  
614 and Florian Lang (La315-15). P.H. Imenez Silva was recipient of a fellowship from the  
615 IKPP Kidney.CH under the European Union Seventh Framework Programme for  
616 Research, Technological Development and Demonstration under the grant agreement  
617 no 608847 and Conselho Nacional de Desenvolvimento Científico e Tecnológico (CNPq)  
618 grant number 205625/2014-2. The use of the ZIRP Core facility for Rodent Physiology is

1  
2  
3  
4 619 gratefully acknowledged. SKIPOGH was supported by a SPUM grant from the Swiss  
5  
6 620 National Center for Competence in Research (FN 33CM30-124087) and by intramural  
7  
8 621 support of Lausanne, Geneva, and Bern University Hospitals. cFGF23, PTH and vitamin  
9  
10 622 D measurements were supported by an unrestricted research grant from Abbvie (Daniel  
11  
12 623 Fuster and Nasser Dhayat) and by intramural support of Bern University Hospital. We  
13  
14 624 thank the study nurses Marie-Odile Levy, Guler Gök-Sogüt, Ulla Schüpbach, and  
15  
16 625 Dominique Siminski for their involvement and help with recruitment. We also thank  
17  
18 626 Sandrine Estoppey for her help in logistic and database management. SKIPOGH  
19  
20 627 investigators include Murielle Bochud (PI), Fred Paccaud and Michel Burnier, Lausanne  
21  
22 628 University Hospital, Lausanne; Pierre-Yves Martin and Antoinette Péchère-Bertschi,  
23  
24 629 Geneva University Hospitals, Geneva; Bruno Vogt, Inselspital, Bern and Olivier Devuyst,  
25  
26 630 University of Zürich, Zürich. SNFR-supported SKIPOGH-1 fellows include Daniel  
27  
28 631 Ackermann (Inselspital, Bern), Georg Ehret, Idris Guessous and Belen Ponte (Geneva  
29  
30 632 University Hospitals, Geneva) and Menno Pruijm (Lausanne University Hospital,  
31  
32 633 Lausanne).

### 634 **Conflict of interests**

35  
36  
37  
38 635 C.A. Wagner has been a member of an advisory board to Bayer Pharma AG, and  
39  
40 636 provided consultancy to Medice. No other financial interests are reported.

41  
42  
43 637  
44 638  
45 639

640 **Figure legends**641 **Figure 1**

642 ~~TNF is a predictor of plasma iFGF23 in a human cohort.~~ **Identification of plasma iFGF23**  
 643 **predictors in a human cohort.** (a) Forest plot showing the fixed effects calculated for  
 644 all predictors used in the mixed linear model for the subpopulation of 429 participants  
 645 after all the exclusion criteria applied. Fixed effect estimates ( $\beta$ ), standard error, ratio  
 646 between the estimates and their standard errors (t-value), and associated p-value from  
 647 a t-distribution. The parameters are ordered by fixed effect estimates. (b) Association  
 648 between plasma TNF and iFGF23 in the SKIPOGH cohort in a subpopulation of 429  
 649 participants after all the exclusion criteria applied. The regression line and confidence  
 650 band were obtained from the linear mixed model containing all the predictors.

651 **Figure 2**

652 **FGF23 and inflammation in the kidney of *Pkd1* KO mice.** Plasma FGF23 (a) and  
 653 ~~TmP/GFR~~ (b) as well as renal *Tnf* (aee) and renal *Tgfb* (bfd) mRNA expression relative  
 654 to 18SrRNA in *Pkd1<sup>fl/fl</sup>, cre-* (white squares) and *Pkd1<sup>fl/fl</sup>, cre+* (black squares) animals  
 655 after 6 and 12 weeks. Phosphorylation of NF $\kappa$ B p65 (ege) in the nuclear fraction of total  
 656 kidney protein homogenates in *Pkd1<sup>fl/fl</sup>, cre-* (white squares) and *Pkd1<sup>fl/fl</sup>, cre+* (black  
 657 squares) animals after 12 weeks. Renal (f) and bone (g) *Fgf23* mRNA expression relative  
 658 to 18SrRNA in *Pkd1<sup>fl/fl</sup>, cre-* (white squares) and *Pkd1<sup>fl/fl</sup>, cre+* (black squares) animals  
 659 after 12 weeks. ND = not detected. Two-way ANOVA with Bonferroni correction (a, b - d)  
 660 or unpaired t-test (ee - g), \* p<0.05.

661 **Figure 3**

662 **TNF neutralization lowers FGF23 in *Pkd1* KO mice.** Plasma TNF (a), iFGF23 (b),  
 663 phosphate (c), and plasma-urea (d) levels, bone (e) and renal (f) *Fgf23* (e), renal *Fgf23*  
 664 (f), renal *Tnf* (g), and renal *Tgfb* (h) mRNA expression relative to *Hprt*, as well as  
 665 abundance of NaPi-IIa (i) in the renal BBM relative to  $\beta$ -actin 24 hours after injection of  
 666 0.5mg isotypic IgG control or anti-TNF neutralizing antibodies in 11-12 weeks old *Pkd1<sup>fl/fl</sup>,*  
 667 *cre-* (white squares) and *Pkd1<sup>fl/fl</sup>, cre+* (black squares) animals. ND = not  
 668 detectable. Two-way ANOVA with Bonferroni correction \* p<0.05.

669 **Figure 4**

670 **TNF stimulates FGF23 *in vivo* and *in vitro*.** Plasma iFGF23 (a), TNF (b), phosphate  
 671 (bc), creatinine (e), and urea (d) levels and  $FE_{P_{-i}}$  (f) as well as bone (g), spleen (h)  
 672 thymus (i) and bone marrow (j) *Fgf23* mRNA expression relative to *Hprt* (g,h) or 18SrRNA  
 673 (i,j) 48 hours after two consecutive injections of vehicle or 2  $\mu$ g recombinant mouse TNF  
 674 in 12 weeks old wild type mice. Unpaired t-test \* p<0.05. Fold increase of *Fgf23* (ek),  
 675 *Dmp1* (fl), *Galnt3* (gm), and *Nurr1* (hn) mRNA expression compared to untreated control  
 676 in primary murine osteocytes after stimulation with 1,25(OH)<sub>2</sub>-vitamin-D<sub>3</sub>D (white  
 677 squares) or 10ng/ml TNF (black squares) for 24 hours. Single experiments were  
 678 normalized to their untreated control (dashed line = 1). Number of independent  
 679 experiments 9-10; One-way ANOVA with Bonferroni correction \* p<0.05 compared to  
 680 1,25(OH)<sub>2</sub>-vitamin-D<sub>3</sub>D treated cells, # p<0.05 compared to untreated cells.



681 **Figure 5**

682 **TNF neutralization lowers ~~also~~ plasma iFGF23 in mice with oxalate nephropathy.**  
683 Oxalate-nephropathy was induced in wild type mice. Plasma iFGF23 (a), plasma TNF  
684 (b), renal *Tnf* (c) mRNA expression relative to *Hprt*, plasma phosphate (d), urinary  
685 phosphate to creatinine ratio (e), plasma creatinine (e,f) and plasma urea (fg) 48 hours  
686 after injection of 0.5 mg isotypic IgG control or anti-TNF neutralizing antibodies in control  
687 diet (white squares) and oxalate nephropathy (black squares) induced mice. One-way  
688 ANOVA with Bonferroni correction \* p<0.05.

689 **Figure 6**

690 **Colonic inflammation increases plasma iFGF23 via TNF in *Il-10* KO mice.** Plasma  
691 iFGF23 (a) levels and colonic *Tnf* (b) mRNA expression relative to 18SrRNA in 14 weeks  
692 old *Il-10*<sup>+/+</sup> and *Il-10*<sup>-/-</sup> mice. Plasma iFGF23 (c), phosphate (d), creatinine (e), and urea  
693 (f) levels as well as abundance of NaPi-IIa at the renal BBM 48 hours after injection of  
694 0.5 mg isotypic IgG control or anti-TNF neutralizing antibodies in 12 weeks old *Il-10*<sup>-/-</sup>  
695 mice. Unpaired t-test \* p<0.05.

696

## 697 REFERENCES

- 698  
699 1. Isakova T, Wahl P, Vargas GS, *et al.* Fibroblast growth factor 23 is elevated before  
700 parathyroid hormone and phosphate in chronic kidney disease. *Kidney Int* 2011; **79**: 1370-  
701 1378.  
702
- 703 2. Block GA, Klassen PS, Lazarus JM, *et al.* Mineral metabolism, mortality, and morbidity  
704 in maintenance hemodialysis. *J Am Soc Nephrol* 2004; **15**: 2208-2218.  
705
- 706 3. Gutierrez OM. Fibroblast growth factor 23 and disordered vitamin D metabolism in  
707 chronic kidney disease: updating the "trade-off" hypothesis. *Clin J Am Soc Nephrol* 2010;  
708 **5**: 1710-1716.  
709
- 710 4. Gutierrez OM, Mannstadt M, Isakova T, *et al.* Fibroblast growth factor 23 and mortality  
711 among patients undergoing hemodialysis. *N Engl J Med* 2008; **359**: 584-592.  
712
- 713 5. Faul C, Amaral AP, Oskouei B, *et al.* FGF23 induces left ventricular hypertrophy. *J Clin*  
714 *Invest* 2011; **121**: 4393-4408.  
715
- 716 6. Souma N, Isakova T, Lipiszko D, *et al.* Fibroblast Growth Factor 23 and Cause-Specific  
717 Mortality in the General Population: The Northern Manhattan Study. *J Clin Endocrinol*  
718 *Metab* 2016; **101**: 3779-3786.  
719
- 720 7. Quarles LD. Skeletal secretion of FGF-23 regulates phosphate and vitamin D metabolism.  
721 *Nat Rev Endocrinol* 2012; **8**: 276-286.  
722
- 723 8. Hu MC, Shiizaki K, Kuro-o M, *et al.* Fibroblast growth factor 23 and Klotho: physiology  
724 and pathophysiology of an endocrine network of mineral metabolism. *Annu Rev Physiol*  
725 2013; **75**: 503-533.  
726
- 727 9. Urakawa I, Yamazaki Y, Shimada T, *et al.* Klotho converts canonical FGF receptor into  
728 a specific receptor for FGF23. *Nature* 2006; **444**: 770-774.  
729
- 730 10. Zhang B, Umbach AT, Chen H, *et al.* Up-regulation of FGF23 release by aldosterone.  
731 *Biochem Biophys Res Commun* 2016; **470**: 384-390.  
732
- 733 11. Daryadel A, Bettoni C, Haider T, *et al.* Erythropoietin stimulates Fibroblast Growth  
734 Factor 23 (FGF23) in mice and men. *Pflügers Arch* 2018; **470**: 1569-1582 *in press*.  
735
- 736 12. Bar L, Feger M, Fajol A, *et al.* Insulin suppresses the production of fibroblast growth  
737 factor 23 (FGF23). *Proc Natl Acad Sci U S A* 2018; **115**: 5804-5809.  
738
- 739 13. Kuro OM, Moe OW. FGF23-alphaKlotho as a paradigm for a kidney-bone network. *Bone*  
740 2017; **100**: 4-18.  
741
- 742 14. Mendoza JM, Isakova T, Ricardo AC, *et al.* Fibroblast Growth Factor 23 and  
743 Inflammation in CKD. *Clin J Am Soc Nephrol* 2012; **7**: 1155-1162.  
744
- 745 15. Wallquist C, Mansouri L, Norrback M, *et al.* Associations of Fibroblast Growth Factor  
746 23 with Markers of Inflammation and Leukocyte Transmigration in Chronic Kidney  
747 Disease. *Nephron* 2018; **138**: 287-295.  
748
- 749 16. Hanks LJ, Casazza K, Judd SE, *et al.* Associations of fibroblast growth factor-23 with  
750 markers of inflammation, insulin resistance and obesity in adults. *PLoS One* 2015; **10**:  
751 e0122885.

1  
2  
3  
4  
5  
6  
7  
8  
9  
10  
11  
12  
13  
14  
15  
16  
17  
18  
19  
20  
21  
22  
23  
24  
25  
26  
27  
28  
29  
30  
31  
32  
33  
34  
35  
36  
37  
38  
39  
40  
41  
42  
43  
44  
45  
46  
47  
48  
49  
50  
51  
52  
53  
54  
55  
56  
57  
58  
59  
60

- 752  
753 17. El-Hodhod MA, Hamdy AM, Abbas AA, *et al.* Fibroblast growth factor 23 contributes to  
754 diminished bone mineral density in childhood inflammatory bowel disease. *BMC*  
755 *Gastroenterol* 2012; **12**: 44.  
756
- 757 18. Iliopoulos D, Malizos KN, Oikonomou P, *et al.* Integrative microRNA and proteomic  
758 approaches identify novel osteoarthritis genes and their collaborative metabolic and  
759 inflammatory networks. *PLoS One* 2008; **3**: e3740.  
760
- 761 19. Dai B, David V, Martin A, *et al.* A comparative transcriptome analysis identifying FGF23  
762 regulated genes in the kidney of a mouse CKD model. *PLoS One* 2012; **7**: e44161.  
763
- 764 20. Farrow EG, Davis SI, Summers LJ, *et al.* Initial FGF23-mediated signaling occurs in the  
765 distal convoluted tubule. *J Am Soc Nephrol* 2009; **20**: 955-960.  
766
- 767 21. Clinkenbeard EL, Farrow EG, Summers LJ, *et al.* Neonatal iron deficiency causes  
768 abnormal phosphate metabolism by elevating FGF23 in normal and ADHR mice. *J Bone*  
769 *Miner Res* 2014; **29**: 361-369.  
770
- 771 22. Ito N, Wijenayaka AR, Prideaux M, *et al.* Regulation of FGF23 expression in IDG-SW3  
772 osteocytes and human bone by pro-inflammatory stimuli. *Mol Cell Endocrinol* 2015; **399**:  
773 208-218.  
774
- 775 23. Masuda Y, Ohta H, Morita Y, *et al.* Expression of Fgf23 in activated dendritic cells and  
776 macrophages in response to immunological stimuli in mice. *Biol Pharm Bull* 2015; **38**:  
777 687-693.  
778
- 779 24. David V, Martin A, Isakova T, *et al.* Inflammation and functional iron deficiency regulate  
780 fibroblast growth factor 23 production. *Kidney Int* 2016; **89**: 135-146.  
781
- 782 25. Feger M, Hase P, Zhang B, *et al.* The production of fibroblast growth factor 23 is  
783 controlled by TGF-beta2. *Sci Rep* 2017; **7**: 4982.  
784
- 785 26. Glosse P, Fajol A, Hirche F, *et al.* A high-fat diet stimulates fibroblast growth factor 23  
786 formation in mice through TNFalpha upregulation. *Nutr Diabetes* 2018; **8**: 36.  
787
- 788 27. Onal M, Carlson AH, Thostenson JD, *et al.* A Novel Distal Enhancer Mediates  
789 Inflammation-, PTH-, and Early Onset Murine Kidney Disease-Induced Expression of the  
790 Mouse Fgf23 Gene. *JBMR Plus* 2018; **2**: 32-47.  
791
- 792 28. Durlacher-Betzer K, Hassan A, Levi R, *et al.* Interleukin-6 contributes to the increase in  
793 fibroblast growth factor 23 expression in acute and chronic kidney disease. *Kidney Int*  
794 2018; **94**: 315-325.  
795
- 796 29. Alwan H, Pruijm M, Ponte B, *et al.* Epidemiology of masked and white-coat  
797 hypertension: the family-based SKIPOGH study. *PLoS One* 2014; **9**: e92522.  
798
- 799 30. Farrow EG, Yu X, Summers LJ, *et al.* Iron deficiency drives an autosomal dominant  
800 hypophosphatemic rickets (ADHR) phenotype in fibroblast growth factor-23 (Fgf23)  
801 knock-in mice. *Proc Natl Acad Sci U S A* 2011; **108**: E1146-1155.  
802
- 803 31. Amdur RL, Feldman HI, Gupta J, *et al.* Inflammation and Progression of CKD: The CRIC  
804 Study. *Clin J Am Soc Nephrol* 2016; **11**: 1546-56.  
805

- 1  
2  
3  
4 806 32. Feng YM, Thijs L, Zhang ZY, *et al.* Glomerular function in relation to circulating  
5 807 adhesion molecules and inflammation markers in a general population. *Nephrol Dial*  
6 808 *Transplant* 2018; **33**: 426-435.  
7 809
- 8 810 33. Piontek K, Menezes LF, Garcia-Gonzalez MA, *et al.* A critical developmental switch  
9 811 defines the kinetics of kidney cyst formation after loss of Pkd1. *Nat Med* 2007; **13**: 1490-  
10 812 1495.  
11 813
- 12 814 34. Mace ML, Gravesen E, Nordholm A, *et al.* Kidney fibroblast growth factor 23 does not  
13 815 contribute to elevation of its circulating levels in uremia. *Kidney Int* 2017; **92**: 165-178.  
14 816
- 15 817 35. Smith ER, Holt SG, Hewitson TD. FGF23 activates injury-primed renal fibroblasts via  
16 818 FGFR4-dependent signalling and enhancement of TGF-beta autoinduction. *Int J Biochem*  
17 819 *Cell Biol* 2017; **92**: 63-78.  
18 820
- 19 821 36. Smith ER, Tan SJ, Holt SG, *et al.* FGF23 is synthesised locally by renal tubules and  
20 822 activates injury-primed fibroblasts. *Sci Rep* 2017; **7**: 3345.  
21 823
- 22 824 37. Meir T, Durlacher K, Pan Z, *et al.* Parathyroid hormone activates the orphan nuclear  
23 825 receptor Nurr1 to induce FGF23 transcription. *Kidney Int* 2014; **86**: 1106-1115.  
24 826
- 25 827 38. McEvoy AN, Murphy EA, Ponnio T, *et al.* Activation of nuclear orphan receptor NURR1  
26 828 transcription by NF-kappa B and cyclic adenosine 5'-monophosphate response element-  
27 829 binding protein in rheumatoid arthritis synovial tissue. *J Immunol* 2002; **168**: 2979-2987.  
28 830
- 29 831 39. Bakker AD, Klein-Nulend J. Osteoblast isolation from murine calvaria and long bones.  
30 832 *Methods Mol Biol* 2012; **816**: 19-29.  
31 833
- 32 834 40. Stern AR, Stern MM, Van Dyke ME, *et al.* Isolation and culture of primary osteocytes  
33 835 from the long bones of skeletally mature and aged mice. *Biotechniques* 2012; **52**: 361-  
34 836 373.  
35 837
- 36 838 41. Feng JQ, Ward LM, Liu S, *et al.* Loss of DMP1 causes rickets and osteomalacia and  
37 839 identifies a role for osteocytes in mineral metabolism. *Nat Genet* 2006; **38**: 1310-1315.  
38 840
- 39 841 42. Topaz O, Shurman, D L, Bergman, R, Indelman, M, Ratajczak, P, Mizrachi, M,  
40 842 Khamaysi, Z, Behar, D, Petronius, D, Friedman, V, Zelikovic, I, Raimer, S, Metzker, A,  
41 843 Richard, G, Sprecher, E. Mutations in *GALNT3*, encoding a protein involved in O-linked  
42 844 glycosylation, cause familial tumoral calcinosis. *Nat Genet* 2004; **36**: 579-581.  
43 845
- 44 846 43. Kato K, Jeanneau, C, Tarp, M A, Benet-Pages, A, Lorenz-Depiereux, B, Bennett, E P,  
45 847 Mandel, U, Strom, T M, Clausen H. Polypeptide GalNAc-transferase T3 and familial  
46 848 tumoral calcinosis: secretion of FGF23 requires O-glycosylation. *J Biol Chem* 2006; **281**:  
47 849 18370-18377.  
48 850
- 49 851 44. Fine LG, Bandyopadhyay D, Norman JT. Is there a common mechanism for the  
50 852 progression of different types of renal diseases other than proteinuria? Towards the  
51 853 unifying theme of chronic hypoxia. *Kidney Int Suppl* 2000; **75**: S22-26.  
52 854
- 53 855 45. Eckardt KU, Bernhardt WM, Weidemann A, *et al.* Role of hypoxia in the pathogenesis of  
54 856 renal disease. *Kidney Int Suppl* 2005: S46-51.  
55 857
- 56 858 46. Frew IJ, Thoma CR, Georgiev S, *et al.* pVHL and PTEN tumour suppressor proteins  
57 859 cooperatively suppress kidney cyst formation. *EMBO J* 2008; **27**: 1747-1757.  
58 860  
59  
60

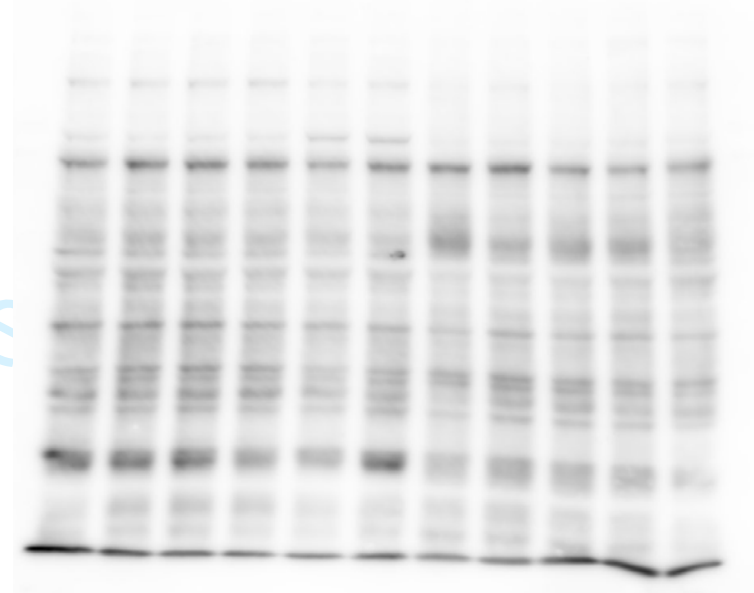
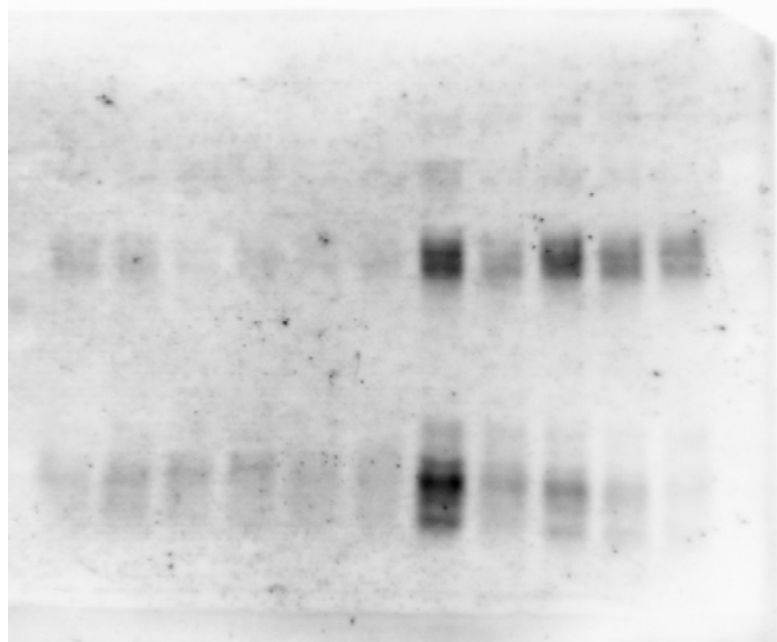
1  
2  
3  
4  
5  
6  
7  
8  
9  
10  
11  
12  
13  
14  
15  
16  
17  
18  
19  
20  
21  
22  
23  
24  
25  
26  
27  
28  
29  
30  
31  
32  
33  
34  
35  
36  
37  
38  
39  
40  
41  
42  
43  
44  
45  
46  
47  
48  
49  
50  
51  
52  
53  
54  
55  
56  
57  
58  
59  
60

- 861 47. Maxwell PH, Wiesener MS, Chang GW, *et al.* The tumour suppressor protein VHL  
862 targets hypoxia-inducible factors for oxygen-dependent proteolysis. *Nature* 1999; **399**:  
863 271-275.
- 864  
865 48. Schonberger D, Harlander S, Rajski M, *et al.* Formation of Renal Cysts and Tumors in  
866 Vhl/Trp53-Deficient Mice Requires HIF1alpha and HIF2alpha. *Cancer Res* 2016; **76**:  
867 2025-2036.
- 868  
869 49. Mulay SR, Eberhard JN, Pfann V, *et al.* Oxalate-induced chronic kidney disease with its  
870 uremic and cardiovascular complications in C57BL/6 mice. *Am J Physiol Renal Physiol*  
871 2016; **310**: F785-F795; [ajprenal.00488.02015](https://doi.org/10.1152/ajprenal.00488.02015).
- 872  
873 50. Kullberg MC, Rothfuchs AG, Jankovic D, *et al.* Helicobacter hepaticus-induced colitis in  
874 interleukin-10-deficient mice: cytokine requirements for the induction and maintenance  
875 of intestinal inflammation. *Infect Immun* 2001; **69**: 4232-4241.
- 876  
877 51. Dhayat NA, Ackermann D, Pruijm M, *et al.* Fibroblast growth factor 23 and markers of  
878 mineral metabolism in individuals with preserved renal function. *Kidney Int* 2016; **90**:  
879 648-657.
- 880  
881 52. Zeier M, Fehrenbach P, Geberth S, *et al.* Renal histology in polycystic kidney disease  
882 with incipient and advanced renal failure. *Kidney Int* 1992; **42**: 1259-1265.
- 883  
884 53. Li X, Magenheimer BS, Xia S, *et al.* A tumor necrosis factor-alpha-mediated pathway  
885 promoting autosomal dominant polycystic kidney disease. *Nat Med* 2008; **14**: 863-868.
- 886  
887 54. Mulay SR, Anders HJ. Crystallopathies. *N Engl J Med* 2016; **374**: 2465-2476.
- 888  
889 55. Spichtig D, Zhang H, Mohebbi N, *et al.* Renal expression of FGF23 and peripheral  
890 resistance to elevated FGF23 in rodent models of polycystic kidney disease. *Kidney Int*  
891 2014.
- 892  
893 56. Zanchi C, Locatelli M, Benigni A, *et al.* Renal Expression of FGF23 in Progressive Renal  
894 Disease of Diabetes and the Effect of Ace Inhibitor. *PLoS One* 2013; **8**: e70775.
- 895  
896 57. Zhang X, Guo K, Xia F, *et al.* FGF23(C-tail) improves diabetic nephropathy by  
897 attenuating renal fibrosis and inflammation. *BMC Biotechnol* 2018; **18**: 33.
- 898  
899 58. Stubbs JR, He N, Idiculla A, *et al.* Longitudinal evaluation of FGF23 changes and mineral  
900 metabolism abnormalities in a mouse model of chronic kidney disease. *J Bone Miner Res*  
901 2012; **27**: 38-46.
- 902  
903 59. Fernandez M, Triplitt C, Wajcberg E, *et al.* Addition of pioglitazone and ramipril to  
904 intensive insulin therapy in type 2 diabetic patients improves vascular dysfunction by  
905 different mechanisms. *Diabetes Care* 2008; **31**: 121-127.
- 906  
907 60. Liu N, Nguyen L, Chun RF, *et al.* Altered endocrine and autocrine metabolism of vitamin  
908 D in a mouse model of gastrointestinal inflammation. *Endocrinology* 2008; **149**: 4799-  
909 4808.
- 910  
911 61. Chen H, Xu H, Dong J, *et al.* Tumor necrosis factor-alpha impairs intestinal phosphate  
912 absorption in colitis. *Am J Physiol Gastrointest Liver Physiol* 2009; **296**: G775-781.
- 913  
914 62. Augustine MV, Leonard MB, Thayu M, *et al.* Changes in vitamin D-related mineral  
915 metabolism after induction with anti-tumor necrosis factor-alpha therapy in Crohn's  
916 disease. *J Clin Endocrinol Metab* 2014; **99**: E991-998.

## TNF stimulates FGF23

- 1  
2  
3  
4 917  
5 918 63. Agrawal M, Arora S, Li J, *et al.* Bone, inflammation, and inflammatory bowel disease.  
6 919 *Curr Osteoporos Rep* 2011; **9**: 251-257.  
7 920  
8 921 64. Martin A, David V, Li H, *et al.* Overexpression of the DMP1 C-terminal fragment  
9 922 stimulates FGF23 and exacerbates the hypophosphatemic rickets phenotype in Hyp mice.  
10 923 *Mol Endocrinol* 2012; **26**: 1883-1895.  
11 924  
12 925 65. Bellido T, Jilka RL, Boyce BF, *et al.* Regulation of interleukin-6, osteoclastogenesis, and  
13 926 bone mass by androgens. The role of the androgen receptor. *J Clin Invest* 1995; **95**: 2886-  
14 927 2895.  
15 928  
16 929 66. Wang C, Tian L, Zhang K, *et al.* Interleukin-6 gene knockout antagonizes high-fat-  
17 930 induced trabecular bone loss. *J Mol Endocrinol* 2016; **57**: 161-170.  
18 931  
19 932 67. Hellwig-Burgel T, Rutkowski K, Metzen E, *et al.* Interleukin-1beta and tumor necrosis  
20 933 factor-alpha stimulate DNA binding of hypoxia-inducible factor-1. *Blood* 1999; **94**: 1561-  
21 934 1567.  
22 935  
23 936 68. Clinkenbeard EL, Hanudel MR, Stayrook KR, *et al.* Erythropoietin stimulates murine and  
24 937 human fibroblast growth factor-23, revealing novel roles for bone and bone marrow.  
25 938 *Haematologica* 2017; **102**: e427-e430.  
26 939  
27 940 69. Flamme I, Ellinghaus P, Urrego D, *et al.* FGF23 expression in rodents is directly induced  
28 941 via erythropoietin after inhibition of hypoxia inducible factor proline hydroxylase. *PLoS*  
29 942 *One* 2017; **12**: e0186979.  
30 943  
31 944 70. Pruijm M, Ponte B, Ackermann D, *et al.* Heritability, determinants and reference values  
32 945 of renal length: a family-based population study. *Eur Radiol* 2013; **23**: 2899-2905.  
33 946  
34 947 71. Ponte B, Pruijm M, Ackermann D, *et al.* Reference values and factors associated with  
35 948 renal resistive index in a family-based population study. *Hypertension* 2014; **63**: 136-142.  
36 949  
37 950 72. Piontek KB, Huso DL, Grinberg A, *et al.* A functional floxed allele of Pkd1 that can be  
38 951 conditionally inactivated in vivo. *J Am Soc Nephrol* 2004; **15**: 3035-3043.  
39 952  
40 953 73. Grinberg-Bleyer Y, Saadoun D, Baeyens A, *et al.* Pathogenic T cells have a paradoxical  
41 954 protective effect in murine autoimmune diabetes by boosting Tregs. *J Clin Invest* 2010;  
42 955 **120**: 4558-4568.  
43 956  
44 957 74. Carlson MJ, West ML, Coghil JM, *et al.* In vitro-differentiated TH17 cells mediate lethal  
45 958 acute graft-versus-host disease with severe cutaneous and pulmonary pathologic  
46 959 manifestations. *Blood* 2009; **113**: 1365-1374.  
47 960  
48 961 75. Brodehl J, Krause A, Hoyer PF. Assessment of maximal tubular phosphate reabsorption:  
49 962 comparison of direct measurement with the nomogram of Bijvoet. *Pediatr Nephrol* 1988;  
50 963 **2**: 183-189.  
51 964  
52 965 76. Biber J, Stieger B, Stange G, *et al.* Isolation of renal proximal tubular brush-border  
53 966 membranes. *Nat Protoc* 2007; **2**: 1356-1359.  
54 967  
55 968 77. Custer M, Lötscher, M, Biber, J, Murer, H, Kaissling, B. Expression of Na-P<sub>i</sub> cotransport  
56 969 in rat kidney: localization by RT-PCR and immunohistochemistry. *Am J Physiol* 1994; **266**: F767-  
57 970 774..  
58 971

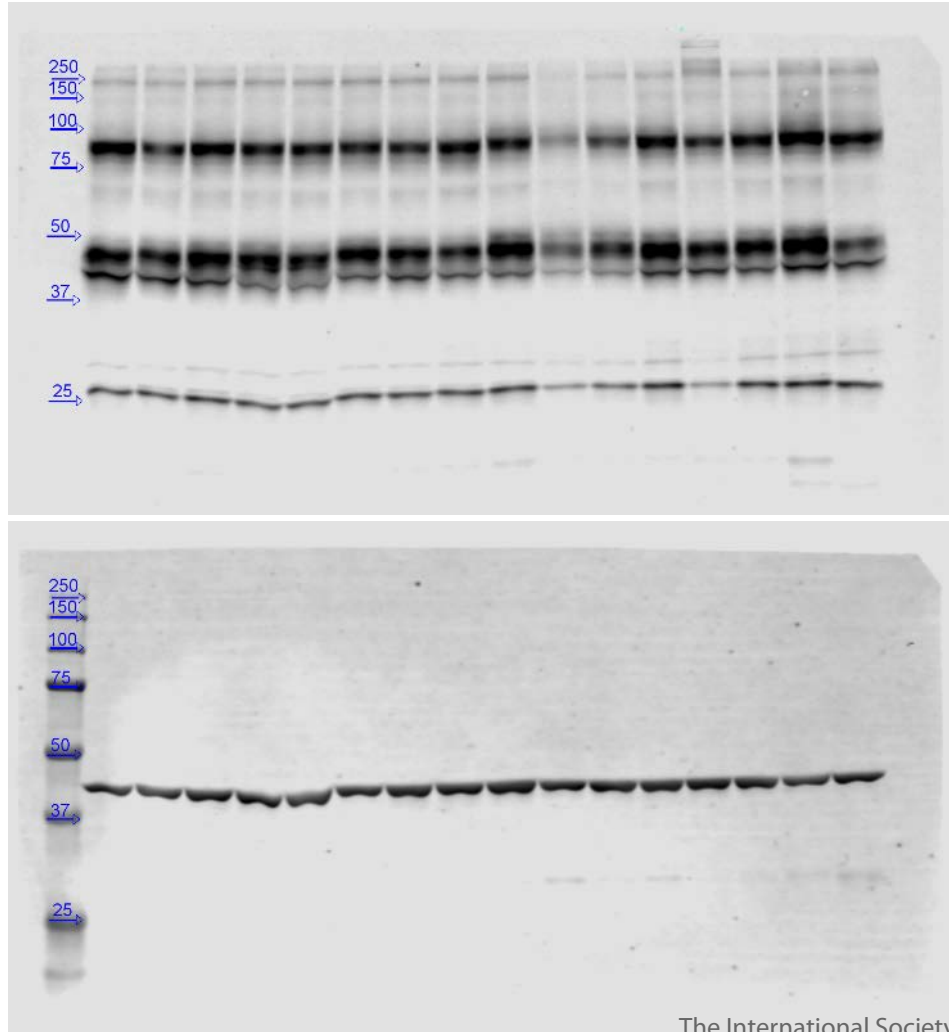
# Figure 2



er Review

1  
2  
3  
4  
5  
6  
7  
8  
9  
10  
11  
12  
13  
14  
15  
16  
17  
18  
19  
20  
21  
22  
23  
24  
25  
26  
27  
28  
29  
30  
31  
32  
33  
34  
35  
36  
37  
38  
39  
40  
41

# Figure 3



1  
2  
3  
4  
5  
6  
7  
8  
9  
10  
11  
12  
13  
14  
15  
16  
17  
18  
19  
20  
21  
22  
23  
24  
25  
26  
27  
28  
29  
30  
31  
32  
33  
34  
35  
36  
37  
38  
39  
40  
41



# Figure 6

